Innovative antimicrobial blue light (aBL) strategies for the elimination of antibiotic resistant bacteria (ARB) in wastewater from ARB hotspots

Zur Erlangung des akademischen Grades einer

DOKTORIN DER NATURWISSENSCHAFTEN (DR. RER. NAT.)

von der KIT-Fakultät für Chemieingenieurwesen und Verfahrenstechnik des Karlsruher Instituts für Technologie (KIT)
genehmigte

DISSERTATION

Von

M.Sc. Xiaoyu Cong

aus Liaoning

Tag der mündlichen Prüfung: 05.12.2025

Erstgutachter: Prof. Dr. Harald Horn
Zweitgutachter: Prof. Dr.-Ing. Matthias Franzreb
KIT Associate Fellow: Prof. Dr. Thomas Schwartz

Abstract

The widespread presence of antibiotic resistant bacteria (ARB) and antibiotic resistance genes (ARGs) in wastewater from antimicrobial resistance (AMR) hotspots (such as nursing homes and slaughterhouses) poses significant global health risks. This is especially true for the clinically important ESKAPE pathogens listed by the World Health Organization (WHO). This study quantified facultative pathogenic bacteria (FPB) within the ESKAPE group and clinically significant ARGs in raw wastewater (RWW) from these sources using molecular biology methods and were also cultured on selective medium. The primary objective was to assess and improve treatment efficiency through the use of innovative, decentralized disinfection technologies.

Although conventional biological treatments and advanced oxidative processes reduced the concentration of FPB and ARGs, they did not achieve complete elimination. To overcome this limitation, antimicrobial blue light (aBL), a novel disinfection technology for treating wastewater, was explored, both alone and in combination with photosensitizers. The study employed broad-spectrum LED-based blue light irradiation (applied in both static and continuous-flow reactors) in combination with the porphyrin-based photosensitizer TMPyP (10^{-6} M) and the oxidative agent hydrogen peroxide (H_2O_2, 1 mM). Further analysis with real wastewater effluents from slaughterhouse and from treatment plants demonstrated variable susceptibilities among different FPBs and ARGs to the aBL-based treatments. The combination treatments showed significantly enhanced bacterial inactivation and ARG removal compared to aBL irradiation alone. aBL combined with TMPyP notably improved the biocidal effects against previously less-sensitive bacteria.

A static photoreactor was employed to validate the hypothesis that different bacterial species exhibit varying susceptibility to aBL treatment due to differences in endogenous photosensitizer content, an observation that was also confirmed in this study. An upgraded continuous-flow aBL photoreactor was employed to assess its effectiveness in removing various FPB and ARGs. Among all the target genes and bacterial groups analyzed, enterococci emerged as highly sensitive FPBs, and ARGs including *erm*B, *tet*M, *sul*1, and bla_{VIM} exhibited notable reductions.

Across all treatments applied in this study, aBL combined with TMPyP was confirmed to be the most effective. Reactive oxygen species (ROS) analysis confirmed singlet oxygen and hydrogen peroxide as primary reactive agents responsible for microbial inactivation when aBL was applied in combination with TMPyP. This treatment also induced

substantial DNA damage, with up to 13 lesions per 10 kilobases, effectively impairing DNA repair mechanisms and preventing bacterial regrowth. Molecular investigations indicated that aBL irradiation, particularly when supplemented with TMPyP, induced oxidative stress responses in bacteria. The impact of oxidative stress response was reflected by significant gene expression changes: *sod*A, *rec*A, *oxy*R, and *tol*C were strongly upregulated, highlighting activated oxidative stress defense mechanisms. In contrast, *omp*F was downregulated, suggesting adaptive membrane permeability reduction.

These findings highlight the strong disinfection potential and mechanistic advantages of aBL combined with porphyrin-based photosensitizers or oxidative agents for the decentralized disinfection of ARB and ARGs- contaminated wastewater. This innovative approach provides a promising solution to mitigate antimicrobial resistance hotspots by effectively targeting clinically relevant pathogens and their associated resistance determinants.

Zusammenfassung

Das weltweit verbreitete Auftreten von antibiotikaresistenten Bakterien (ARB) und Antibiotikaresistenzgenen (ARGs) in Abwässern aus Hotspots des Auftretens dieser Antibiotikaresistenzen (wie Pflegeheimen und Schlachthöfen) stellt ein erhebliches globales Gesundheitsrisiko dar. Dies gilt insbesondere für die von der Weltgesundheitsorganisation (WHO) gelisteten klinisch wichtigen ESKAPE-Erreger. In dieser Studie wurden fakultativ pathogene Bakterien (FPB) innerhalb der ESKAPE-Gruppe und klinisch signifikante ARGs in Rohabwässern (RWW) aus diesen Quellen mithilfe molekularbiologischer Methoden quantifiziert und über selektive Medien auch kultiviert. Das primäre Ziel bestand darin, die Behandlungseffizienz durch den Einsatz innovativer, dezentraler Desinfektionstechnologien zu bewerten und zu verbessern.

Obwohl herkömmliche biologische Behandlungsverfahren und fortschrittliche oxidative Prozesse die Konzentration von FPB und ARGs reduzierten, konnten sie diese nicht vollständig eliminieren. Um diese Einschränkung zu überwinden, wurde antimikrobielles blaues Licht (aBL), eine neuartige Desinfektionstechnologie für Abwässer, sowohl allein als auch in Kombination mit Photoverstärker untersucht. Die Studie verwendete eine breitbandige LED-basierte Blaulichtbestrahlung (angewendet sowohl in statischen als auch in Durchflussreaktoren) auch in Kombination mit dem porphyrinbasierten Photoverstärkern TMPyP (10^{-6} M) und dem Oxidationsmittel Wasserstoffperoxid (H_2O_2, 1 mM). Analysen mit realen Abwässern aus Schlachthausabwässern und Kläranlagen zeigten unterschiedliche Empfindlichkeiten verschiedener FPBs und ARGs gegenüber den aBL-basierten Behandlungen. Die Kombinationsbehandlungen zeigten im Vergleich zur alleinigen aBL-Bestrahlung eine deutlich verbesserte Inaktivierung der Bakterien und Entfernung der ARGs. aBL in Kombination mit TMPyP verbesserte die biozide Wirkung gegen weniger empfindliche Bakterien deutlich.

Ein statischer Photoreaktor wurde verwendet, um die Hypothese zu validieren, dass verschiedene Bakterienarten aufgrund unterschiedlicher Gehalte an endogene Photoverstärker-Molekülen eine unterschiedliche Empfindlichkeit gegenüber der aBL-Behandlung aufweisen. Diese Beobachtung wurde auch in dieser Studie bestätigt. Alternativ wurde ein Durchfluss Photoreaktor für die Blaulicht Bestrahlung eingesetzt, um seine Wirksamkeit bei der Entfernung verschiedener FPBs und ARGs zu bewerten. Unter allen analysierten Zielgenen und Bakteriengruppen erwiesen sich Enterokokken als

hochsensible FPBs, und ARGs wie *erm*B, *tet*M, *sul*1 und bla_{VIM} zeigten eine deutliche Reduktion.

Bei allen angewandten Behandlungen in dieser Studie erwies sich aBL in Kombination mit TMPyP als die wirksamste. Die Analyse reaktiver Sauerstoffspezies (ROS) bestätigte, dass Singulett-Sauerstoff und Wasserstoffperoxid die primären endogenen reaktiven Agenzien sind, die für die Inaktivierung von Mikroorganismen verantwortlich sind, wenn aBL in Kombination mit TMPyP angewendet wird. Diese Behandlung führte auch zu erheblichen DNA-Schäden mit bis zu 13 Läsionen pro 10 Kilobasen, wodurch die DNA-Reparaturmechanismen wirksam beeinträchtigt und das erneute Wachstum von Bakterien verhindert wurden. Molekulare Untersuchungen zeigten, dass die aBL-Bestrahlung, insbesondere in Kombination mit TMPyP, oxidative Stressreaktionen in Bakterien auslöste. Die Auswirkungen der oxidativen Stressreaktion spiegelten sich in signifikanten Veränderungen der Genexpression wider: *sod*A, *rec*A, *oxy*R und *tol*C waren hochreguliert, was auf aktivierte oxidative Stressabwehrmechanismen hindeutet. Im Gegensatz dazu war die Expression von *omp*F herunterreguliert, was auf eine adaptive Verringerung der Membranpermeabilität hindeutet.

Diese Ergebnisse unterstreichen das starke Desinfektionspotenzial und die mechanistischen Vorteile von aBL in Kombination mit porphyrinbasierten Photoverstärkern oder oxidativen Wirkstoffen für die mögliche dezentrale Desinfektion von ARB und ARGs in kontaminiertem Abwasser. Dieser innovative Ansatz bietet eine vielversprechende Lösung zur Eindämmung von Hotspots der Antibiotikaresistenz, indem er klinisch relevante Krankheitserreger und die damit verbundenen Resistenzdeterminanten wirksam bekämpft.

Table of Contents

List of Tables

List of Figures

1 Introduction and theoretical background

Over the last few decades antibiotics have become less effective as pathogens have developed resistance against them, resulting in multi-resistant bacteria (Aminov, 2009). Microbial communities are metabolically diverse and possess a strong ability to mount defensive strategies to resist selective forces like those imposed by exposure to antibiotics. These selective pressures have, in turn, induced the mobilization and horizontal transfer of an extensive range of ARGs among different bacterial species (Larsson & Flach, 2022).

AMR is considered to be one of the most pressing health issues of the 21st century and was declared a global priority by the WHO. The dissemination of ARGs and ARB has been directly linked to increased morbidity and mortality due to infections caused by high-priority pathogens that are difficult to treat. In the European Union (EU) alone, nosocomial infections due to these organisms result in nearly 25,000 deaths per year (ECDC/EMEA Joint Working Group 2009). However, AMR is not limited to hospitals and clinics. Environmental pathways, especially wastewater discharge, agricultural runoff and pharmaceutical industry effluence, represent significant reservoir and extended pathways for the transmission of ARGs. Human activities such as excessive and inappropriate use of antibiotics in medicine, aquaculture and livestock rearing have increasingly contributed to the selection and spread of resistant strains and residues into the environment (Kumar & Pal, 2018; Larsson & Flach, 2022).

This study focuses on AMR as a continued and serious public health challenge at the global level and highlights current actions and initiatives to address and reduce this "silent pandemic". To deal with this increasing threat, several innovative technological approaches are being assessed and applied. More sophisticated wastewater treatment technologies are required to reduce the proliferation of resistance genes through the environment, in addition to enhanced antibiotic stewardship and surveillance. Conventional treatment processes are generally inadequate for the complete elimination of ARGs and ARB. Therefore, new and advanced methods such as ozonation, UV irradiation, advanced oxidation processes (AOPs), membrane filtration and aBL have been proposed and assessed for their capability to eradicate or at least dramatically reduce microbial pollutants and as well as resistance determinants. In addition, advances in metagenomics and molecular diagnostics provide new opportunities for the precise monitoring of the prevalence of resistance genes in complex environmental samples,

facilitating the evidence-based management of risk and the implementation of mitigation strategies.

1.1 Properties and use of antibiotic-consumption, effects

1.1.1 The era of antibiotics

Antibiotics have been among the most successful chemotherapeutic agents in medical history, saving millions of lives and effectively treating the overwhelming number of infectious diseases (Aminov, 2009). Their widespread use is essential not only in human medicine, but also in veterinary medicine, where they are highly involved in preventative treatment and disease therapy.

The discovery of the first serious antibiotic, penicillin, in the 1920s and its introduction into clinical use in the 1940s represented a paradigm shift in dealing with bacterial infections. It has continued to revolutionize infection control, showcasing the capacity to combat bacterial pathogenesis (White and Cox, 2016).

The golden age of antibiotic therapy began in the 1940s and lasted until the early 1960s, when the first wave of natural resistance started to emerge (Lewis, 2020). During that era, a number of the antibiotic classes now in use, including the tetracyclines, sulphonamides, and broad-spectrum penicillins were first discovered and used. During this period antibiotics caused mortality from bacterial infections to plummet, earning them the name miracle drugs.

However, this era also saw the dawn of AMR, as bacteria started to develop natural defenses against these drugs. Currently, the challenges have been exacerbated by the burgeoning of the global demand for antibiotics, due to population growth, increased access to healthcare, and agriculture (X. Liu et al., 2019). While the benefits of antibiotics are undeniable, their future effectiveness depends on how wisely and cautiously they are managed.

1.1.2 Global consumption trend

More recently, Boeckel et al., (2014) noticed 35% increase in global antibiotics use from 2000 to 2010 (52.06 to 70.44 billion standard unit). It is expected that this trend will persist as Klein et al., (2018) also predicting that global demand could reach 200% based on 2015 level by 2030. It is interesting to note that 76% of this last increase is accounted for by just five developing countries- Brazil, Russia, India, China and South Africa. Seasonal

variations in antibiotic utilization have also been reported in several countries and might be related to respiratory infections and prescribing practices.

Particularly concerning is the steep incline in the consumption of the 'last resort antibiotics'; carbapenem consumption increased by 45% and polymyxin by 13% over the study period. The spike underscores the rise of these important medications as resistance to primary drugs grows. Amoxicillin is in the lead by weight (80 tons), followed by other β-lactams (35 tons) and fluoroquinolones (25 tons), as a mere 15% is applied in hospital wards (GERMAP, 2016). Global antibiotic consumption declined during the COVID-19 pandemic but rebounded in the subsequent years. From 2016 to 2023, total consumption increased from 29.5 to 34.3 billion defined daily doses (DDDs), representing a 16.3% rise. Over the same period, the consumption rate per 1,000 people per day grew by 10.6% (Klein et al., 2024). Despite the disparity between outpatient and inpatient settings, both environments exert substantial selective pressure that drives resistance.

Antibiotics have also been applied extensively in veterinary medicine since the first clinically available antibiotic, penicillin, was developed for treatment of human infections (McLain et al., 2016). As Regulation (EU) 2019/6 stresses, resistance on farm animals constitutes an even more complex problem than in humans, requiring more careful and responsible use of antibiotics at the level of veterinary practices. The most frequently used classes of antibiotic in animal health (including food-producing, companion, or exotic species) are quinolones (in particular fluoroquinolones), aminopenicillins (with or without β-lactamase inhibitors), first and second generation cephalosporins, tetracyclines, and sulfonamides (alone or in combination with potentiators). Furthermore, the usage of (i) third- and fourth-generation cephalosporins, macrolides, and glycopeptides termed highest priority critically important antibiotics (HPCIAs) is worrisome because of their importance in human medicine (Broens & Geijlswijk, 2018). According to The State of the World's Antibiotics 2015, roughly 65,000 of the 100,000 tons of antibiotics produced annually worldwide are used in farming. This is supplemented by the fact that worldwide usage in bovine, poultry, and porcine species was calculated at 93,309 tons in 2017 (Gelband et al., 2015). A more recent study conducted with ovine animals as well showed antibiotic use of 99,502 tons in 2020 and it is projected that this would increase to 107,472 tons by 2030 if current patterns continue (Mulchandani et al., 2023).

These results highlight the growing necessity to reconsider how antibiotics are used in all aspects of healthcare. Increasing dependence on broad-spectrum and last resort antibiotics suggests a loss of a broader 'arsenal' of effective drugs such that resistance

management becomes not simply a clinical concern but a global environmental and public health priority.

1.1.3 Key antibiotic classes and mechanism of action

There are many types of antibiotics that vary in the chemical structure, the mechanism of action, and the range of organisms that they are active against which has resulted in numerous classification schemes based on one of these aspects. Chemical structure of antibiotics is often divided into β-lactam and non β-lactam (Haddad et al., 2024). The most active members of the β-lactam family include penicillins, cephalosporins, monobactams and carbapenems (Etebu & Arikekpar, 2016). In addition to β-lactam, other mainly groups of antibiotics includes macrolides, tetracyclines, quinolones, aminoglycosides, sulphonamides, glycopeptides and oxazolidinones (Etebu & Arikekpar, 2016; van Hoek et al., 2011). The antibiotic modes of action can be categorized into the following groups, according to the cellular processes they interfere with: (1) Blockage of cell wall formation, (2) disruption of cell membrane functions, (3) interference with ribosome function, (4) inhibition of nucleic acid synthesis, and (5) blocking of folate metabolism (Dowling et al., 2017). Table 1.1 categorizes clinically important antibiotic families, outlines the bacterial processes or structures they target, and provides representative peer-reviewed references detailing each mechanism of action.

Peptidoglycan is an essential polymer for the bacterial cell wall, which contributes to rigidity and protection. Its synthesis is the site of action of many antibiotics, including β-lactams (Y. Liu & Breukink, 2016). β-Lactams antibiotics are characterized by their four-membered β-lactam ring structure required for their antibacterial action. They act by inhibiting penicillin binding proteins (PBPs), which are responsible for cross-linking the peptidoglycan chains. By binding to PBPs, β-lactams disrupt cell wall assembly, leading to osmotic instability and cell lysis (Dowling et al., 2017). Resistance to β-lactams is predominantly mediated by *bla* genes that encode β-lactamases (e.g., bla_{TEM}, bla_{SHV}, $bla_{CTX\text{-}M}$, and bla_{OXA}) hydrolyzing the β-lactam ring and thus inactivating the antibiotics.

Cationic Antimicrobial Peptides (CAMPs) are a second class of antibiotics targeting bacterial membranes. These peptides are positively charged at neutral pH, and they interact with negatively charged structures like lipopolysaccharides (LPS) in Gram-negative and teichoic acids in Gram-positive bacteria. Their amphiphilic nature enables them to integrate into the membrane and disrupt its integrity, leading to leakage of cellular contents and eventual cell death (E. Huang & Yousef, 2014).

Bacterial protein biosynthesis takes on the ribosome, which consists of 30S and 50S components. Specifically, these subunits are targets for antibiotics (aminoglycosides, tetracyclines, macrolides) that induce translational inhibition. The class of antibiotics that disrupts nutrient element scavenge each target different stages, binding of tetracyclines to the 30S subunit, aminoglycosides to cause the misread of mRNA, and macrolides to inhibit peptide elongation in the 50S subunit (Arenz & Wilson, 2016).

Nucleic acids (DNA and RNA) are central to bacterial replication and survival. Fluoroquinolones disrupt DNA synthesis by inhibiting DNA gyrase and topoisomerase IV, enzymes crucial for supercoiling and replication of bacterial DNA. These antibiotics are effective against both Gram-positive and Gram-negative pathogens and are considered broad-spectrum agents (Drlica & Zhao, 1997).

There are even antibiotics that work by attacking the metabolism of the bacteria. For example, folic acid synthesis, an important nucleotide synthesis pathway, is blocked by the sulfonamides. These agents are structural analogs of para-aminobenzoic acid (PABA), an intermediate of folate biosynthesis, and competitively inhibit the enzyme dihydropteroate synthase, which results in growth inhibition of bacteria (J. Chen & Xie, 2018).

Table 1.1: Overview of major antibiotic classes, their cellular mechanisms of action and key literature references.

Antibiotic Class	Mechanism of Action	References
Beta lactams: Carbapenem, Cephalosporins, Monobactams, Penicillin	Inhibit cell wall synthesis	Bush & Bradford, 2016; Prescott & Hardefeldt, 2024; Vilvanathan, 2021
Lipopeptides	Depolarize cell membrane	Bionda et al., 2013
Aminoglycosides, Tetracyclines, Macrolides	Inhibit protein synthesis by binding to 30S ribosomal unit and 50S ribosomal unit	Allen, 2002; Anandabaskar, 2021; Katz & Ashley, 2005
Quinolones	Inhibit nucleic acid synthesis	Aldred et al., 2014; Spencer & Panda, 2023
Sulfonamides	Inhibit metabolic pathways	J. Chen & Xie, 2018

1.2 Evolution and mechanism of antimicrobial resistance

An increasing number of studies have revealed that bacteria employ phenotypic and genetic mechanisms to apply a natural defense to antibiotics, which diminished treatments for bacterial infections in human and animals (Urban-Chmiel et al., 2022). Resistance may develop as intrinsic, attributed to the organism's genetic make-up, or as acquired, predominantly through the process of horizontal gene transfer (HGT), that confer abilities to cope when exposed to antibiotics (Darby et al., 2023). Aquatic systems are increasingly acknowledged as reservoirs for the rise and spread of AMR. Under these conditions, bacteria can develop resistance either via spontaneous genetic mutations or by taking up ARGs from their local environments (Amarasiri et al., 2020). The major resistance mechanisms are displayed in Figure 1.1, striated as (1) decrease of permeability of membrane, or active efflux for intracellular drug concentration; (2) modification the site of target antibiotic; (3) chemical degradation, or enzymatic modification of the drug; and (4) metabolic bypass of the intracellular pathway inhibited (Darby et al., 2023; Santajit & Indrawattana, 2016).

1.2.1 Intrinsic resistance

The natural resistance, also known as the core resistome, refers to the natural resistance shared by all bacterial species. The constitutive resistance is mediated by intrinsic structural and functional characteristics that impede the action of antimicrobials.

One common mode is reduced permeability of the outer membrane, especially in Gram negative organisms. These Gram negatives' outer membrane acts as a selective permeability barrier, porin proteins prevent the entry of large or hydrophobic antibiotic molecules (Nikaido, 1994; Saxena et al., 2023). Differences in porin contents and pore sizes in bacteria may account for the different susceptibilities toward individual antibiotics.

Another important mechanism is the constitutive expression of efflux pumps that actively transport a variety of toxic compounds, including antibiotics, out of the cell, (Van Bambeke et al., 2000). Such pumps also include those which may have a relatively narrow or wide substrate specificity. For example, efflux mechanisms contribute to the innate resistance of *Escherichia coli* and *Pseudomonas aeruginosa* to linezolid and several other antibiotics (Piddock, 2006; Randall et al., 2013).

Another type of intrinsic resistance is due to the lack of suitable targets for antibiotics. For example, species of Mycoplasma do not even have a peptidoglycan cell wall, so they are intrinsically resistant to β-lactam antibiotics that target the cell wall during synthesis. Last,

but not least, some bacteria produce constitutive detoxifying enzymes that deactivate antibiotics by enzymatic degradation or chemical modification. By contrast, these enzymes are frequently expressed irrespective of antibiotic exposure, facilitating pre-emptive resistance (Murugaiyan et al., 2022; Safitri, 2025).

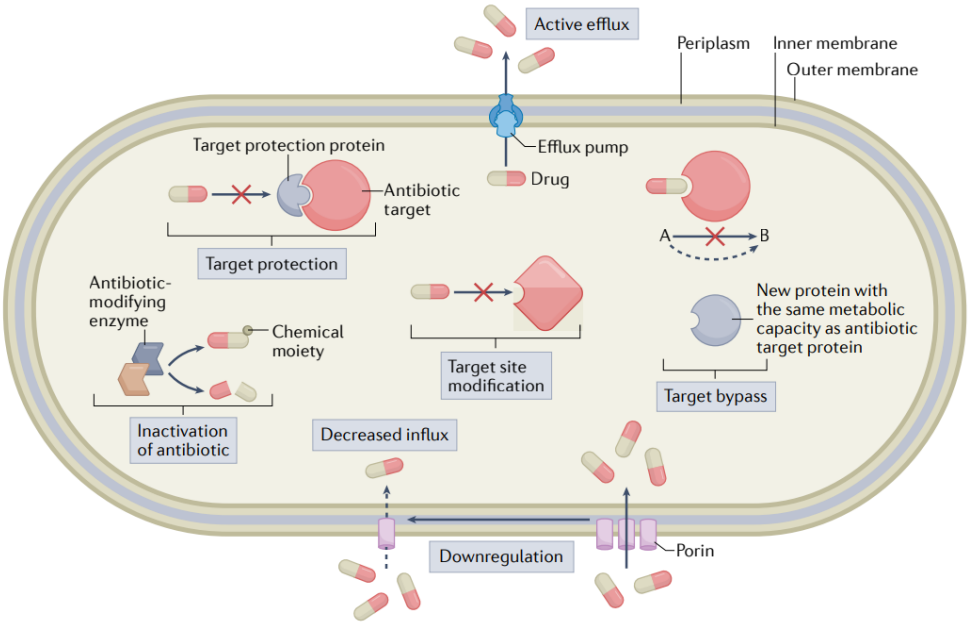

Figure 1.1: Overview of the molecular mechanisms of antimicrobial resistance. This schematic illustrates six primary strategies by which bacteria evade antibiotic action:1) inactivation of antibiotics; 2) Target site modification; 3) Target protection; 4) Target bypass; 5) Decreased influx; 6) Active efflux. Adapted from Darby et al. (2023).

1.2.2 Acquired resistance

The two main mechanisms by which bacteria gain resistance to antibiotics are: i) Spontaneous chromosomal mutations, and ii) HGT (Li & Zhang, 2022). Mutant-mediated resistance is generally manifested in form of alterations of chromosomal genes or, less frequently, by extrachromosomal plasmids. These mutations may change target areas so as to render the drug ineffective, decrease the uptake of drugs, or increase drug extrusion, and are inherited by the progeny through vertical gene transfer (VGT). Vulnerable bacteria may become resistant to antimicrobial agents by chance chromosomal mutations that occur under selective pressure. Different mechanisms may be involved in the acquisition of resistance due to such genetic alterations. Mutations can occur in genes coding for the direct targets of antimicrobials, in regulatory elements, or even efflux pump constituents.

Once transmitted, these genetic changes are inherited by subsequent generations, spreading the resistant traits within bacterial population.

In contrast to VGT, HGT between species and genera permits bacteria to rapidly distribute their resistance traits. The three predominant HGT methods include transduction, transformation and conjugation (as shown in Figure 1.2) (Aminov, 2011; S. Li et al., 2021; Marraffini & Sontheimer, 2008).

Transduction is the phage-mediated movement of genetic material from a donor to a recipient bacterium in the absence of cellular contact (J. Chen et al., 2018). During generalized transduction, random pieces of bacterial chromosomal DNA are sometimes mistakenly packaged into phage capsids during phage production. Such transducing particles can adsorb to a new host cell, and deliver the encapsidated bacterial DNA, so that upon homologous recombination with the genome of the recipient, stable gene transfer occurs (Lerminiaux & Cameron, 2019). This mechanism has also been suggested to contribute to the dissemination of resistance genes in the environment: e.g., Zhang et al. (2019a) reported several extended-spectrum β-lactamase (ESBL) genes bla_{TEM}, $bla_{CTX\text{-}M}$, $bla_{CMY\text{-}2}$, bla_{KPC}, $bla_{OXA\text{-}48}$, bla_{PSE} genes were found in bacteriophage DNA extracted from canal water, sewage, and river samples.

Transformation refers to the acquisition of free DNA molecules from the extracellular medium, mainly by the uptake of free DNA into the cell, via a process in which the plasma membrane is made competent, i.e. momentarily more permeable to DNA (Li & Zhang, 2022). This phenomenon is likely to occur in most (if not all) of the aquatic bacteria tested since natural competence has been reported for many aquatic bacteria (Davison, 1999), and surface waters are a possible reservoir of resistance genes.

Conjugation occurs when a donor cell adheres to a recipient via a conjugative pilus, after which a single strand of self-replicating plasmid DNA is transferred into the recipient (Davison, 1999). This process also translocates a range of MGEs (plasmids, transposons, integrons, IS, ISCR elements, genomic islands and ICE) from donor to recipient (Marti et al., 2014). One of the most emblematic cases of HGT-mediated resistance is the horizontal transfer of β-lactamase genes, which are harbored by conjugative plasmids that spread by both inter- and intraspecies transfer in the Enterobacteriaceae and *Acinetobacter spp.* (Mathers et al., 2011; Valenzuela et al., 2007).

HGT is a form of adaptation employed by bacteria to quickly respond to environmental stresses such as antibiotics. This allows bacteria to acquire traits that were not part of their ancestral line such as AMR, virulence or an improved metabolism, via the acquisition of new genetic material (Acar Kirit et al., 2022). This gene stealing ability is the key to

microbial evolution and is also highly important for public health and environmental protection.

Bacteria have developed various complex defense strategies against environmental stress as well as antibiotics (Murugaiyan et al., 2022). These survival strategies include intrinsic resistance mechanisms and acquire responses like efflux pumps, enzyme synthesis, target modification, and biofilm production. A more thorough comprehension of these mechanisms is not only critical for devising strategies to overcome current AMR but also provides new candidates for the design of future antimicrobial agents.

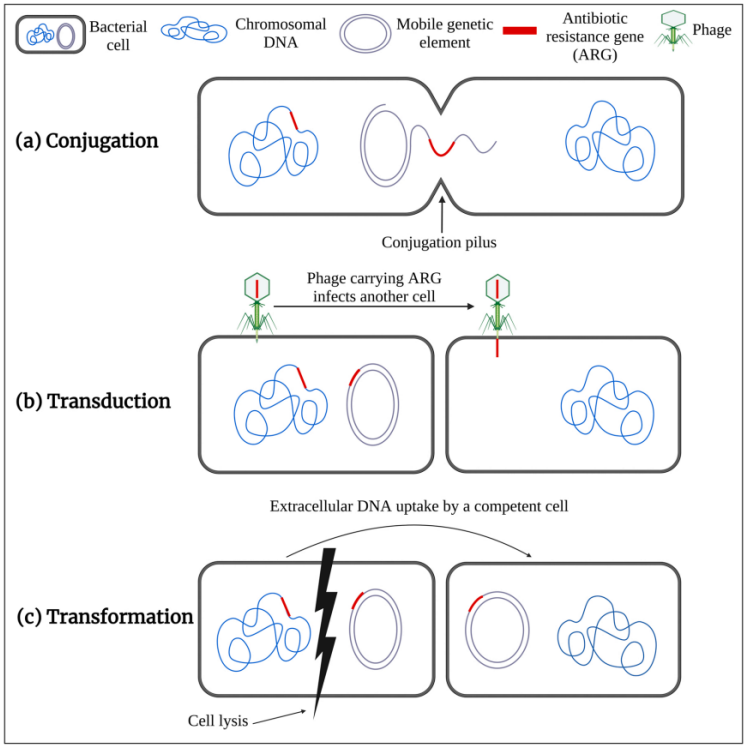

Figure 1.2: Major mechanisms of horizontal transfer of ARGs: a) Conjugation, b) Transduction, c) Transformation (Nnorom et al., 2023).

1.2.3 Mobile genetic elements

Mobilizable genetic elements (MGEs) are the main drivers in the dissemination of antibiotics resistance through HGT among bacteria. These MGEs such as insertion sequences (IS), integrons, transposons, and plasmids, facilitate the capture, accumulation, and mobilization of ARGs, ultimately contributing to the rapid evolution of bacterial genomes (Noel et al., 2022; Partridge et al., 2018).

IS are some of the most basic (simplest) MGE, typically around 1 kb in size, containing the inverted repeats (IRs) and one or two open reading frames that act as transposase genes. This enzyme recognizes the repeats and catalyzes the excision and re-integration of the element into a new position in the genome (Hickman & Dyda, 2015). In *Acinetobacter spp.*, carbapenem and cephalosporin resistance has been largely attributed to ISAba elements, the majority of which carry an efficient outward facing promoter system that increases the expression level of a β-lactamase gene to a clinically relevant degree (Noel et al., 2022).

Transposons resemble insertion sequences but also include additional cargo genes, often encoding AMR, and can “jump” between genomic locations, transferring one or more resistance determinants (Noel et al., 2022; Popa et al., 2018). Transposons are further classified into two main groups: retrotransposons, which transpose via an RNA intermediate and are predominantly found in eukaryotes, and DNA transposons, which move as DNA and occur in both eukaryotes and prokaryotes (Babakhani & Oloomi, 2018). In bacteria, DNA transposons are classified into four types: IS, composite transposons, non-composite transposons (e.g., the Tn3 family), and Mu-type transposable phages, all of which are frequently implicated in clinically relevant resistance among Enterobacteriaceae (Babakhani & Oloomi, 2018; Hegstad et al., 2010).

Integrons served as gene capture or expression systems of ARGs, particularly in Gram-negative bacteria. They are made up of a stable scaffold which contains the integrase gene (intI), a recombination site (attI) and promoter (Pc) for expression of inserted gene cassettes (Gillings, 2017). Integrons have played a major role in the evolution of multidrug resistance, often being the focal points for the accumulation of ARGs over decades (Rowe-Magnus & Mazel, 2002).

Plasmids (extrachromosomal circles of DNA) are also key vehicles of resistance genes. They are able to duplicate autonomously and to be transmitted vertically during cell division and horizontally while conjugating (Partridge et al., 2018). Plasmids are in many respects HGT vectors for other MGEs, such as IS elements and transposons, which extend the reach of their resistance dissemination (Helinski, 2022). Carbapenem resistance in *A. baumannii*, for example, has been found to be due to the gene $bla_{\text{OXA-23}}$ on a conjugative plasmid (Huang et al., 2012).

The reciprocity of these MGEs generates a fluid and highly malleable genetic environment which permits bacteria to easily adapt to antibiotic selective pressures in the clinic, environment and also in agriculture. This emphasizes the immediate requirement for the combined surveillance and molecular dissection of resistance mechanisms beyond traditional culture-based diagnostics.

1.2.4 Infections with resistant bacteria

By 2050, antimicrobial resistant bacteria are expected to cause over 33,000 deaths in the European Union (European Centre for Disease Prevention and Control, 2019; O'Neill, 2016). These unfavorable consequences include both the clinical parameters such as death and treatment failure and an economic burden. Treatment failures and mortality are a lot higher (about twice as high) for infections due to resistant strains than to susceptible strains (Eliopoulos et al., 2003).

A root cause of this crisis is the dissemination of multidrug-resistant (MDR) bacteria, both Gram positive and Gram negative, that are responsible for infections increasingly difficult or even impossible to treat with traditional drugs. Most such infections have been associated with a category of multidrug-resistant pathogens, the so-called ESKAPE group (*Enterococcus faecium*, *Staphylococcus aureus*, *Klebsiella pneumoniae*, *Acinetobacter baumannii*, *Pseudomonas aeruginosa* and *Enterobacter spp*). These organisms contribute to a considerable number of hospital-acquired infections and have been targeted by the WHO as displaying potential to resist the activity of most antibiotics (Tacconelli et al., 2018). One of the ESKAPE's key mechanisms of survival includes producing resistance enzymes, such as β-lactamases and aminoglycoside-modifying enzymes, wherein the enzymes transform and inactivate antibiotic (Santajit & Indrawattana, 2016). These mechanisms are prevalent in *K. pneumoniae*, *A. baumannii*, and *P. aeruginosa* and have made infections with these organisms some of the hardest to manage.

In 2017, in order to respond to the increasing threat of AMR, the WHO released a list of antibiotic-resistant pathogens, classified in three priority levels, medium, high and critical (Tacconelli et al., 2018). ESKAPE pathogens have been classified by the WHO as resistant to three and more antibiotic classes, and posed a threat to life-threatening, hospital-acquired infections, which are estimated to be a leading global cause of morbidity and mortality (Denissen et al., 2022). The increasing clinical impact of these organisms is demonstrated by hospital surveillance studies. Arbune et al. (2021) investigated 4,293 clinical isolates and reported that 97% of the collection consisted of ESKAPE organisms. *Escherichia coli* (38.3%) and *Staphylococcus aureus* (26%) were the most prevalent among these and underlining their association with nosocomial infections. In addition to this, human activities have further spread ESKAPE species into the environment, which has been shown to have a highly active role in their propagation, raising concerns that this development must be managed and combated.

Some ESKAPE species have become especially worrisome. Of the ESKAPE pathogens, *Enterococcus faecium* and other *Enterococcus* are Gram positive, facultatively anaerobic

genus of enormous clinical relevance. Ampicillin- and vancomycin-resistant enterococcal infections have increased dramatically in the last two decades. For example, the number of cases of ampicillin-resistant enterococcal infections in university hospitals rose from some 10 per hospital in 1999, to around 50 per hospital by 2005 (Top et al., 2008). A similar worrying development is being observed for *Staphylococcus aureus*.

Methicillin resistance *S. aureus* (MRSA) was recorded for the first time in 1961, due to the widespread use of penicillin (De Oliveira et al., 2020). Subsequent to this breakthrough, vancomycin has remained the preferred choice for treating MRSA, although occurrences of at least intermediate resistance have been raised (Chambers & DeLeo, 2009). These infections impose considerable challenges to the healthcare systems, given higher morbidity, extended hospitalizations, and additional treatment costs, all which make them an ongoing public health concern (Santajit & Indrawattana, 2016).

Carbapenem-resistant *K. pneumoniae* infections have high mortality rates among Gram negative pathogens such as *Acinetobacter baumannii*, *P. aeruginosa*, and *K. pneumoniae* (Tzouvelekis et al., 2012). In *A. baumannii* imipenem-hydrolyzing metallo-β-lactamases (e.g., bla_{IMP} and bla_{OXA}) have been reported (Vila et al., 2007). On the other hand, *P. aeruginosa* exhibits inherent low susceptibility to various types of antibiotics. Furthermore, the presence of ESBLs in Enterobacteriaceae is linked to high rates of failure for therapy and death in patients with bacteremia, compared with those infected by non ESBL-producing isolates (Melzer & Petersen, 2007). Altogether, the widespread distribution and adaptability of these organisms highlight the need for surveillance on a global scale, better antimicrobial stewardship, and discovery for new treatment options.

1.3 Environmental dissemination of ARGs and ARB

1.3.1 ARGs and ARB in the environments

The environment is significantly contributing as source and vehicle for the appearance and spread of ARBs and corresponding ARGs (Bengtsson-Palme et al., 2018). Most resistance genes that are identified in clinical isolates are believed to be acquired from the environment and their spread into human-pathogenic microorganisms is highly facilitated by anthropogenic activities. Human-mediated pollution, through clinical, agricultural, and aquacultural activities, has released very large numbers of resistant bacteria and genetic elements to natural ecosystems (Czatzkowska et al., 2022; Amábile-Cuevas, 2021).

In crops and livestock systems, veterinary drugs are introduced to the environment mostly through manure. Manure is extensively used of a soil fertilizer, from which they can be

transferred into the food web and represent a health hazard for the public (Han et al., 2018; Martin et al., 2015). For example, Hu et al. (2016) also showed that cattle manure amendment in 140-day microcosm experiment could enrich soil-derived β-lactam resistance genes and decrease soil bacterial community structure. ARB have also been detected in wildlife and their habitats, and relatively mobile species, such as migratory birds and fish, have been considered as major vehicles for ARGs' translocation around the world (Y.-M. Chen et al., 2020; Greig et al., 2015). For instance, the ARGs β-lactam and tetracycline have been introduced to aquatic birds through contaminated waters (Martiny et al., 2011).

Another very important source is livestock keeping. Antibiotics are widely used in animal farming and various ARGs are frequently observed in the waste of livestock worldwide (He et al., 2020). The majority of these agents are used non-therapeutically, occurring for growth promotion and prophylaxis, and they persist in the gastrointestinal tract at low, sub-lethal concentrations, which can selectively impact susceptible bacteria (Woolhouse & Ward, 2013). The major ARG classes in the livestock waste are *tet*, *sul*, *erm*, *fca* and *bla* genes, and the *tet* and *sul* genes are among the most abundant regardless of surveys (He et al., 2020). Moreover, Multidrug-resistant *P. aeruginosa* and *A. baumannii* have been recovered from swine, poultry and cattle, emphasizing cross-species threat (Al Bayssari et al., 2015).

Landfills are also an often-neglected hotspot for the enhancement of resistance. Inadequate elimination of expired and unused antibiotics is causing continuous environmental contamination and selective pressure (Czatzkowska et al., 2022; R. Zhang et al., 2022). The landfill has also been well described since the last decade to be a hotspot for AMR. L. Li et al., (2020) recovered 41 $bla_{\text{TEM-1}}$ bearing resistant isolates in a municipal solid waste. More recent research by Gao et al. (2025) found 1,403 ARG subtypes from 29 resistance classes in landfill samples and emphasized the huge repository of resistance determinants in these environments.

1.3.2 ARGs and ARB in the aquantic settings

Aquatic systems are emerging important reservoirs for the transmission of ARGs and ARB, and numerous routes contribute to their transmission. These include (but are not limited to) municipal wastewater treatment plants (WWTPs), agricultural runoff, terrestrial and aquatic animal reservoirs, livestock effluents, and landfill leachates (Cerqueira et al., 2019; Y.-M. Chen et al., 2020; Harnisz et al., 2020; He et al., 2020; Wang et al., 2020a). As shown in Figure 1.3, ARB and ARGs originating from activities such as aquaculture,

livestock wastewater, and agricultural runoff are released into the environment, spread through aquatic and terrestrial ecosystems, and ultimately reach humans via drinking water, recreational exposure, and consumption of contaminated crops and fish.

WWTP effluent, agricultural runoff, and other human inputs that contribute to elevated levels of ARGs and ARB and contribute to their spread, are commonly introduced into aquatic systems, such as lakes and rivers (Michael et al., 2013). ARGs and ARB were detected in groundwater as well as in drinking water sources (Mackie et al., 2006; Servais & Passerat, 2009; Su et al., 2018). Stoll et al. (2012) tested surface water samples from Germany and Australia for 24 ARGs related to the following eight antibiotic families (penicillins, aminoglycosides, glycopeptides, chloramphenicol, tetracyclines, macrolides, trimethoprim, and sulfonamides). Moreover, Xi et al. (2009) identified and quantified ARGs and ARB in source waters and finished and tap drinking water, supporting the finding that drug resistance is an issue along water distribution systems. More recently, Lei et al. (2024) found 45 ARGs, mainly against aminoglycosides, sulfonamides, tetracyclines, in groundwater contaminated after surface pollution.

WWTPs are presently identified as key hotspots for the retention and dissemination of antibiotics, ARGs and ARB (Biswal et al., 2014; Michael et al., 2013; Niestępski et al., 2020; Wang et al., 2020b). WWTPs are found to be a source of these contaminants, which are present in human and animal feces that contain untransformed antibiotics when they are excreted from urine and feces (Rizzo et al., 2013a). WWTP is designed to eliminate chemical contaminants and degradable organics, however, it is generally ineffective for the removal of ARGs and ARB. Worldwide overviews of antibiotic, ARGs and ARB occurrences and fates in WWTPs have been conducted and emphasize the risks of these pollutants for receiving aquatic systems (Y. Wang et al., 2022).

Traditional WWTPs work in the phases of primary, secondary and tertiary treatment to eliminate conventional pollutants (Bouki et al., 2013). Mechanical operations (e.g., screening, grit removal, sedimentation, etc.) remove coarse solids, oils and greases in the preliminary stage. But no antibiotic or resistance engines are considered in this phase (H. Chen & Zhang, 2013; Pei et al., 2019). The secondary treatment includes biological and chemical methods, such as aeration, oxidation and biofiltration, to degrade organic pollutants, but can generally achieve only around 1 log reduction in ARGs and ARB (P. Gao et al., 2012; Pei et al., 2019). Tertiary treatment consists of advanced filtration (namely membrane filtration, MF), UV disinfection, ozonation, or constructed wetlands, all of which are aimed at recalcitrant compounds, pathogens, and nutrients (Pei et al., 2019).

Considering that primary and secondary treatments are ineffective at removing ARGs/ARB, tertiary processes are becoming more critical in eliminating these pollutants.

With the advent of the mid-2000s, the presence of ARGs in WWTPs has attracted increasing attention, as demonstrated by accumulating investigations of their distributions and levels (Wang et al., 2020b). In the literatures, a variety of ARGs have been reported in influent, effluent and sludge. Historically, the ARGs in WWTPs most reported include β-lactamases gene (e.g. bla_{CTX-M}, bla_{TEM}, bla_{OXA}), quinolone (*qnr*S, *qnr*C), sulfonamide (*sul*1, *sul*2), tetracycline (*tet*A, *tet*B, *tet*M, *tet*Q), macrolide (*erm*B, *ere*A) and class 1 integron (*intl*1) (H. Chen & Zhang, 2013; P. Gao et al., 2012; Laht et al., 2014; Pärnänen et al., 2019).

Clinically relevant pathogens in WWTPs have continued to be identified in surveys. Nishiyama et al. (2021) identified laboratories for WWTPs involving ESKAPE group ARB-carbapenemase producing Enterobacteriaceae (CPE), ESBL and ampC producing Enterobacteriaceae (ESBL, APE), MDR *Acinetobacter*, MDR *P. aeruginosa*, MRSA, and Vancomycin resistant *Enterococcus faecalis* (VRE). Likewise, Korzeniewska et al. (2013) reported the *E. coli* isolates resistant to cefotaxime, ceftazidime, cefpodoxime, gentamicin, amikacin and trimethoprim from 10.6 to 94.7% in influent and from 25.9 to 100% in effluent. In addition, (Pärnänen et al., 2019) described the occurrence of ARGs in 12 WWTPs across Europe, detecting widely distributed bla_{GES}, bla_{OXA}, bla_{VEB}, *ere*A, *erm*F, *sul*1, *tet*M, *tet*Q, *aad*A, and *str*B genes direct in both influent and effluent fraction, and also identified integrase, transposase, and multidrug-resistance markers, and *qac*H genes direct in both influent and effluent. Yao et al. (2021) have also emphasized that hospital influents to WWTPs are characterized by an especially high abundance of ARGs which emphasizes the importance of point-source contributions. Overall, these results support the use of advanced treatment processes and source control strategies for protecting natural aquatic environments from WWTPs discharge of ARGs and ARB.

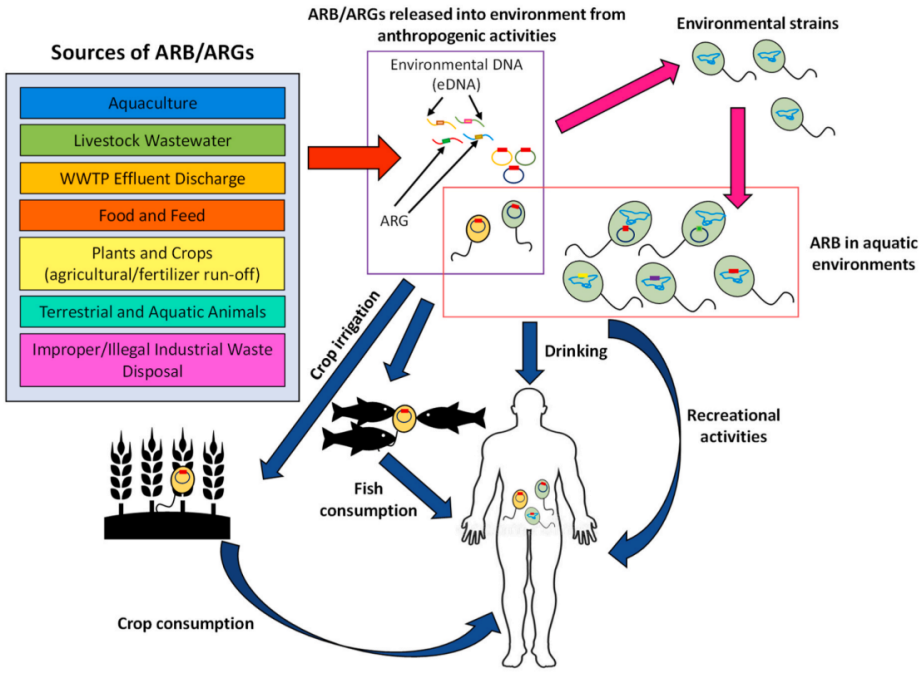

Figure 1.3: Envrionmental transmission pathways of antibiotic resistant bacteria and genes from anthropogenic sources to human exposure (Adapted from Amarasiri et al., 2020).

1.4 Treatment strategies

1.4.1 Technologies for Disinfection

It is known that all over the world, chlorination is used frequently as a disinfectant, because it is very strong oxidant which affect the microorganism nucleic acids and the membrane permeability (Anastasi et al., 2013). Although some investigations observed a complete inactivation of ARB by chlorination (J.-J. Huang et al., 2011), there have been studies that revealed unsatisfactory results, even for the same bacterial strains (P. Gao et al., 2012; Yuan et al., 2015). For instance, Karumathil et al. (2014) reported that the majority of *A. baumannii* isolates survived exposure to chlorine and the expression of some of the ARGs was also found to be enhanced. Shi et al., (2013) also observed that the chlorination process led to an increase in the relative abundances of multiple ARG genes, while it decreased the relative abundance of *sul*1. The disinfection rate of chlorine has a positive correlation with its dose and the contact time, however, the composition of the WWTP effluent, e.g. the content of organic substances can also cause the efficacy of ARG removal to change (Y. Zhang et al., 2015).

Ozonation received much interest as an efficient disinfection method because of its high spectrum of activity and collateral benefits such as color, odor and trace organic

contaminants removal (Foroughi et al., 2022). In aqueous media, the ozone in air dissolves and undergoes relatively fast auto-decomposition into superoxide, hydroperoxyl, and hydroxyl radicals ($OH^{\bullet}$), which non-selectively attack the bacterial cell wall and oxidize polyunsaturated fatty acids and amino acid residues in peptides and amino acid and peptides in enzymes and proteins, unfurling the cellular contents (Pei et al., 2019). Ozone doses of more than 0.5 gO_3 /gDOC were found to be efficient in the bacterial inactivation (Slipko et al., 2022). Overall, ozonation was widely shown to consistently decrease ARB, that tend to be in the order of magnitude more resistant for Enterobacteriaceae than for *Pseudomonas aeruginosa* (Alexander et al., 2016; Sousa et al., 2017). As for reduction ranging from (Foroughi et al., 2022), log-scale reductions between 0.02 and more than 5 have been observed. The infiltration of cell membranes and the destruction of proteins were faster by ozone (than with chlorination and UV), but to achieve complete degradation of ARGs, extended retention times were required (Pei et al., 2019).

Ultraviolet (UV-C) light (usually in the range of 250-270 nm) has been extensively used in wastewater treatment, offering the advantages of rapid inactivation of microbes with minimum generation of disinfection by-products and short contact times (Percival et al., 2014). Pyrimidine dimer formation and DNA strand breaks are ongoing damage mechanisms that lead to microbial death and loss of replication and functionality (Rizzo et al., 2013b). But its potential in terms of the ARGs wanted to be removed is modest. For instance, Zhang et al. (2015) demonstrated only a 0.1–0.23 log decrease for the ARGs content of wastewater at a UV dose of 62.4 mJ/cm^2, while Zheng et al. (2017) also found that, although low UVC fluences increased the ratio of tetracycline- and sulfamethoxazole-resistant species, selectivity for those resistant strains occurred. This could be due to UV induced DNA damage can be repaired by Photoreactivation and dark repair mechanisms. However, UV is still effective at decreasing the overall microbial count even of resistant strains. In one published study, the reduction of tetracycline resistant bacteria from around 10^2-10^3 copies/mL to 10^1-10^2 copies/mL was achieved with UV exposure (Kim et al., 2010).

1.4.2 Membrane filtration

Membrane separation is widely applied in wastewater reuse and includes microfiltration (MF), ultrafiltration (UF), nanofiltration (NF) and reverse osmosis (RO) according to its membrane cutoffs (Y. Guo, 2021; Kalli et al., 2023). Of these, MF is still the most common and economical membrane technology in wastewater treatment where the pore size is generally greater than 0.1 µm and the pores effectively retain suspended solid particles and bacteria with that diameter (0.1-10 µm) (Abid et al., 2012).

MF has been also shown to remove the ARGs and ARB. For example. Lu et al. (2020) that MF decreased *tet*B, *tet*G, *tet*X, *erm*F, and *qnr*S in one to two log cycles, while *erm*T, *qnr*A, and *qnr*B did not change significantly. Hiller et al. (2022) confirmed these observations, and they highlighted that ARG removal by membrane processes highly depends on which genes are being targeted.

A key drawback of membrane filtration is the production of a concentrate (retentate) stream that accumulates high level of ARGs and ARB. This concentrated by-product not only poses an environmental challenge by potentially promoting further selection of resistant strains, but also creates a sencondary waste stream that requires additional treatment. In fact, Hembach et al. (2019) found that 6–7 log units of ARGs were removed from the permeate by ultrafiltration, while the level in the retentate was increased by about 2 log units, which might promote the enhancement of HGT between microbial communities. Therefore, even if membrane filtration has strong potentials to manage AMR in treated wastewater, it requires additional strategies for managing its concentrated waste streams.

1.4.3 Advanced oxidation processes

Disinfection could not remove ARB, ARGs and pathogens thoroughly, and therefore, the traditional treatment methods should be combined with oxidative processes for that (Kalli et al., 2023). AOPs are also a process that has generally been used in the elimination of ARGs and ARB via on-site production of ROS (Gmurek et al., 2022). $OH^{\bullet}$ radicals have nonselective reactivity and high oxidative potential (Eo = O2.73 V) compared with other ROS (Sonntag, 2006) and are a main ROS species responsible for contaminant oxidation, along with O_3, $O_2^{\bullet-}$, and H_2O_2, which also contribute significantly to contaminant degradation (Kutuzova et al., 2021).

Conventional AOPs use the oxidants like O_3, UV light, H_2O_2 or combinations of the same in the hybrid systems like H_2O_2/O_3, O_3/UV and H_2O_2/UV, etc. Other sophisticated methods are based on (titanium dioxide) TiO_2 photocatalysis and the Fenton reaction (Kalli et al., 2023; Y. Yoon et al., 2017).

UV (AOPs) are attractive due to the low-energy requirements and reduce by-product formation and environmental load. Usual UV-based photochemical AOPs may include UV/H_2O_2, UV/chlorine, and UV/persulfate which have shown greater ARB and ARG removal efficiency over the use of UV alone in wastewater (Kalli et al., 2023; Y. Zhang et al., 2022). For example, at an acidic pH 3.5, the UV/H_2O_2 with 0.01 M of H_2O_2 and 30 min UV could result in the inactivation of 2.8-3.5 $\log_{10}$ units of the ARGs abundance (Y. Zhang

et al., 2016). Similarly, Beretsou et al. (2020) reported UV disinfection and 40 mg/L H_2O_2 as an effective strategy for deactivating Water contaminated with fecal coliforms, total heterotrophs and Enterococcus, along with Pseudomonas isolates resistant to trimethoprim, erythromycin and ofloxacin at doses of 0.1-1J/cm^2. UV/chlorine photolysis mainly produces $OH^{\bullet}$ and reactive chlorine species (RCS), which are dominant in ARGs degradation (Zhang et al., 2019b). For example, >5 log inactivation of antibiotic-resistant *E. coli* was performed while both intracellular and extracellular ARGs (*tet*A, *sul*1, *sul*2 and *erm*B) were removed efficiently using the UV/Cl_2 process (Y. Zhang et al., 2024). Sulfate radicals ($SO_4^{\bullet-}$) produced by the UV/persulfate process destroy cell membranes and components, while also restraining cell divisions, thus facilitating ARB and ARG removal more efficiently than UV irradiation alone, which mainly inactivates bacteria by damaging DNA (Xiao et al., 2020).

As to the UV-catalyzed AOPs, photocatalytic oxidation (PCO) has achieved a great performance to eliminate AMR in lab-feasibility tests. Typical semiconductor photocatalysts are TiO_2, zinc sulfide (ZnS), tungsten trioxide (WO_3) and tin dioxide (SnO_2) (J. Wang & Zhuan, 2020). In particular, TiO_2 is a promising option; P25, a commercially available mixture of anatase and rutile photons biocatalyst is known to have enhanced photocatalytic capability under UV illumination (Awitor et al., 2008). Photocatalytic oxidation is capable of successfully eliminating ARGs and ARB, such as, the decrease of *mec*A and *amp*C under UV254 irradiation (120 mJ/cm^2) in the existence of TiO_2 is as high as 4.7-5.8 $\log_{10}$ units (C. Guo et al., 2017) In another study, Tsai et al. (2010) employed TiO_2 activated with UV-A exposure to inactivate three clinically important antibody resistant pathogens, namely MRSA, Multidrug resistant *A. baumannii* (MDRAB) and VRE in an aqueous suspension.

Collectively, AOPs, particularly the combination of UV with an oxidative agent or a catalyst, provide a promising and efficient scheme to reducing ARG dissemination into environment.

1.4.4 Novelty of antimicrobial blue light

Novel strategies to combat AMR In recent years, there has been an increased search for new non-antibiotic strategies to combat the growing problem of AMR. aBL therapy is one of these new modalities receiving great interest. The operating wavelength range of aBL is from 400 up to 480 nm, aBL exhibits non-specific antimicrobial efficacy (Y. Wang et al., 2017) on a range of bacteria pathogens. Currently, one of the most accepted hypotheses about the mechanism of action of aBL as an antimicrobial is that it acts by photoexcitation of endogenous chromophores, such as porphyrins and flavins, inducing the production of

ROS. When irradiated with blue light, same autoendogenous photosensitizers are excited from their ground state to either a short-lived (singlet state) or a long-lived (triplet state) excited state. In a toxicological context, in the presence of molecular oxygen, such excited states may follow two alternative photochemical pathways: type I mechanism involves an electron transfer process and results in ROS generation (i.e., H_2O_2, superoxide anions ($O_2^{\bullet-}$), or $OH^{\bullet}$, while the type II one is based on an energy transfer that leads to the long-lived, but cytotoxic form of molecular oxygen called singlet oxygen ($^1O_2$) (X. Hu et al., 2018). Such ROS trigger oxidative harm to cellular structures such as lipid and protein ultimately leading to cell death (Chu et al., 2019).

Bauer et al. (2021) reported the applicability of 405 nm aBL to reduce the colony forming units (CFUs) of all the ESKAPE pathogens, with the exception of *Enterococcus faecium* under viable but non-culturable (VBNC), leaving no significant cytotoxicities. Similarly, Hoenes et al. (2021) and Cong et al. (2023) verified the effectiveness of aBL at wavelength of 405 to 450 nm for inactivation of ESKAPE bacteria, they re-invigorate the prospect of aBL as a non-antibiotic alternative for combating MD-resistant pathogens. More recently, Cong et al. (2025) demonstrated that different FPB and ARGs exhibit variable susceptibility to aBL-mediated irradiation. Among the tested FPB, Enterococcus species were the most sensitive to blue light exposure. In terms of resistance genes, bacteria harboring *erm*B, *tet*M, *sul*1, and bla_{VIM} showed the highest reduction rates, indicating that aBL may preferentially target certain resistance determinants and associated bacterial hosts.

1.5 Analytical methods for antimicrobial resistance detection

The detection of AMR in environmental samples is usually based on two main methodological strategies, i.e. microbiological and molecular. For the microbiological (phenotypic) approach, it is based on finding facultatively pathogenic bacteria and AMR using observable traits including growth in the presence of selected antibiotics. Although this approach permits detecting resistant bacteria, it does not provide information on the resistance mechanisms involved. In most instances, strain-level classification (including resistance profiles and taxonomies) typically necessitate supplementary testing. In contrast, in genotypic, molecular techniques, resistance genes can be directly detected in DNA extracted from environmental samples. These processes allow the detection of culturable and non-culturable bacteria with high sensitivity and specificity. There are some reports on the development of molecular tools including qPCR, digital PCR, and metagenomic sequencing for ARGs absolute quantification and detailed knowledge of the

resistome, and these tools are considered very useful for environmental surveillance and risk assessment linked to ARGs and ARB.

1.5.1 Methods Based on Cultivation

Culture-based methods are routinely used to detect and enumerate viable bacteria but are dependent on laboratory apparatus and time consuming. Typically, these methods consist of collection of samples, serial dilution, inoculation on to selective or differential media and growth to allow for the development of colonies. Vegetative colonies become visible in 18–24 h for most of the waterborne bacterial pathogens, and a few bacterial strains may dearth 72 h for incubation process (Hameed et al., 2018). Results are usually expressed in the units of CFUs, which represent the population size of only the cells that can grow under the laboratory conditions (for example, the nutrient medium used, the temperature, incubation time and the amount of oxygen, if any) (Davis, 2014). A routine method is the spread inoculation of a preset quantity of sample on an agar plate supplemented with an appropriate nutritive and incubation at 37°C for human isolates or 42°C for environmental samples.

Culture-dependent methods involve the isolation of bacteria on nutrient media followed by antibiotic susceptibility testing, typically using minimum inhibitory concentration (MIC) assays (Manaia et al., 2016; Rodloff et al., 2008). In these approaches, bacterial isolates are cultivated on carefully formulated media containing protein extracts, inorganic salts, and suitable carbon sources under controlled laboratory conditions. MIC testing is then used to determine the lowest concentration of an antibiotic that inhibits visible bacterial growth, allowing classification of isolates as “susceptible,” “intermediate,” or “resistant” based on established clinical breakpoints.

To improve the specificity of detection, selective media are frequently employed. These media apply selection pressures, such as the inclusion of specific antibiotics or essential growth factors, to enrich for bacteria with particular resistance traits. In many cases, combinatorial selection criteria are used to enhance targeting precision and suppress non-target organisms.

A major advantage of this culture-based approach is the ability to isolate and maintain pure bacterial colonies. These isolates can be subjected to further biochemical characterization, AMR profiling, or molecular-level investigations (e.g., sequencing), which provides valuable insights into the mechanisms and dissemination of resistance. While useful for identifying antibiotic-resistant strains and understanding phenotypic resistance,

these approaches have significant limitations. Many environmental bacteria, especially those that are stressed, dormant, or nutritionally fastidious, fail to grow under standard laboratory conditions. As a result, culture-dependent methods tend to underestimate both microbial diversity and the true scope of environmental resistance (Jäger et al., 2018).

1.5.2 Culture-independent methods

Culture-independent molecular methods have greatly improved both qualitative and quantitative analyses of antibiotic-resistance genes, enabling simultaneous targeting of multiple genes and delivering greater specificity and sensitivity (Nguyen et al., 2021; Yamin et al., 2023). These methods are particularly useful in the area of aquatic and environmental microbiology because most microorganisms are uncultivable with conventional laboratory practices and community composition meaningfully changed during the treatment process.

Polymerase chain reaction (PCR)-based techniques, such as conventional PCR, quantitative PCR (qPCR), high-throughput qPCR (HT-qPCR), and digital PCR (dPCR), are frequently used to detect ARGs and ARB from environmental samples. Within the repertoire, quantitative PCR (qPCR) is a very popular tool for the specific and direct quantification of targeted genes. qPCR is based on the same principles as conventional PCR, with the addition of fluorescent dyes or probes, so that the DNA amplification can be monitored in real time. The higher the number of synthesized DNA the more intense is the fluorescence, from which the initial target concentration can be accurately determined (Kralik & Ricchi, 2017).

In the typical qPCR assay, the reaction mix is composed of template DNA, gene-specific primers, and a polymerase master mix (Kralik & Ricchi, 2017). The thermal cycle regime is characterised by a denaturization, an annealing, and an extension phase, and data are analysed based on the cycle threshold (Ct), the cycle at which fluorescence is increasing above background (McCall et al., 2014). Calibration using standard curves (checking for slope, y-intercept and correlation coefficient) guarantees the robustness of the quantification, and melting curve analysis confirms product specificity. For further enumeration of detection, propidium monoazide (PMA) treatment is commonly employed to differentiate the DNA of viable and nonviable cells. PMA enter the cells with the damaged cell membrane and, once light excitation, PMA cross-links to repress the amplification of DNA. This ensures that only DNA of viable bacteria was included in the results (Wagner et al., 2008).

Reliable gene expression analysis in bacteria using RT-qPCR relies heavily on the use of RT-qPCR, that employs fluorescent DNA-binding dyes, known as the gold standard method. The method transforms mRNA to cDNA by reverse transcriptase and then amplifies and real-time detects the target sequence with fluorescence detection. This procedure permits quantification of relative gene expression under the specific experimental conditions. Usually, expression levels are estimated using the relative Ct (cycle threshold) method ($2^{-\Delta\Delta Ct}$ method). This analytic strategy is based on the normalization of the target gene expression to a stably expressed internal reference gene, which serves as an internal standard and compensates for variabilities in RNA input and reverse transcription reaction. Different reference genes were tested during validation work and the 16S rRNA gene has been considered as the most extensively used and validated reference gene because expression is relatively stable among numerous bacterial taxa (Rocha et al., 2015). Recent technological breakthroughs have also broadened the applications of RT-qPCR by allowing high-resolution gene expression profiling, even in single cells. This development makes it possible to study cell-to-cell heterogeneity and dynamics of microbial responses with extremely high resolution.

1.6 Research hypotheses and study aim

Conventional WWTPs are inefficient in the elimination of ARGs and ARB. Accordingly, specific wastewater sources such as slaughterhouses, hospital effluents or pharmaceutical industry emissions have been reported as front nodes of AMR propagation (Rozman et al., 2020). Meanwhile, even though the pollutants have been treated, the effluent measure still remain the ARGs and ARB, which will be finally discharged into natural surface water body and has significant environmental and public health risks. This highlights the desperate need for point source localized treatment technologies which can act on these sources to minimize AMR spread into larger ecosystems. The main objective of this project is to develop and test a modular light-based Advanced Oxidation Technology (aBL) for cost-effective, decentralized wastewater treatment of select AMR hotspots. This gives rise to several hypotheses:

Hypothesis of the dissertation study

- **Hypothesis 1**: Combined aBL strategies employing a broad blue-light spectrum in a static photoreactor can achieve substantial removal of ESKAPE bacteria as well as the natural bacterial population present in slaughterhouse wastewater.

- **Hypothesis 2**: Using a small-scale continuous flow aBL photoreactor, both ARGs and ARB can be effectively removed from municipal WWTP effluent with the integration of qPCR analyses.
- **Hypothesis 3**: Specific cellular targets can be identified to provide deeper insight into the functional responses induced by aBL irradiation in bacteria.

2 Antibiotic resistances from slaughterhouse effluents and enhanced antimicrobial blue light technology for wastewater decontamionation

Published as: *Cong, X., Krolla, P., Khan, U. Z., Savin, M., & Schwartz, T. (2023). Antibiotic resistances from slaughterhouse effluents and enhanced antimicrobial blue light technology for wastewater decontamionation. Environmental Science and Pollution Research, 30(50), 109315-109330*.

2.1 Introduction

AMR is one of the greatest health challenges of our time and has significant economic consequences for society (WHO, 2017; 2019; 2020). The WHO documented worldwide that about 700,000 deaths per year are caused by ARB (WHO 2019). Furthermore, it is predicted that their number will increase to nearly 10 million in 2050 (Kraker et al., 2016).

The global spread of AMR is mainly due to the emission of ARB, ARGs, FPB, and AMR-causing substances in human and animal waste into the environment. In this context, it is also important to mention the selective pressure via antibiotic misuse and overuse, which is an important aspect for the evolution and spread of ARB. Recently, much effort has been devoted to deciphering the sources, transmission pathways and sinks of AMR in a series of AMR screening studies around the world (Cacace et al., 2019; Marano et al., 2020; Pärnänen et al., 2019). Major hotspots of anthropogenic AMR include (i) point sources, e.g. hospitals, nursing homes, private households, pharmaceutical industries, animal husbandries and slaughterhouses (Savin et al., 2020; Voigt et al., 2020);(ii) urban WWTPs (Alexander et al., 2020); and (iii) other diffuse sources (Alexander et al., 2020; Amos et al.,2014a; Amos et al., 2014b; Hembach et al., 2022; Paulus et al., 2019; Schwermer et al., 2017).

Wastewater from AMR hotspots is mostly discharged into the public sewerage system, which plays an important role as a recipient of potentially harmful and AMR-promoting substances as well as ARBs and ARGs (Alexander et al., 2022). Therefore, it acts not only as an incubator for the emergence of AMR, but also as a pathway for the transfer of ARBs and ARGs from their sources to WWTP. Currently, the global widespread use of antibiotics in animal husbandry has sped up the prevalence and occurrence of AMR and posed massive issues for global human health (He et al., 2020; Hembach et al., 2022). Over 80%

of the meat consumption per person in Germany is comprised of pork and poultry. Furthermore, these two animal species receive nearly 80% of all antibiotics used in the livestock industry in Germany (Hembach et al., 2022; Schwaiger et al., 2012; Schwarz & Chaslus-Dancla, 2001; ZMP, 2003). The wastewater from slaughterhouses is believed to contain ARB and ARGs of clinical relevance that cannot be totally eliminated by means of conventional treatment techniques (Savin et al., 2020). As a result, different clinically relevant AMR may be present in municipal sewer systems and subsequently in the effluent of WWTPs reaching the aquatic environment. Through HGT, ARB and ARGs can spread swiftly throughout the environment indigenous bacteria, which have a detrimental effect on human health in case of transfer to hygienically relevant bacteria. It is unknown whether resistance-causing bacteria enter sewer systems more frequently at the point of slaughter compared to municipal or clinical emitters.

Different clusters, occurring in different (commonly, intermediately, and rarely) abundancies of ARGs were previously identified in wastewater, but also in anthropogenically influenced surface waters (Hembach et al., 2019). Here, the commonly occurring resistance gene cluster with *erm*B, *tet*M, bla_{TEM}, and *sul*1 directed against macrolids, tetracylines, β-lactams, and sulfonamide antibiotics are listed. The cluster with the intermediately occurring resistance genes $bla_{CTX\text{-}M}$, $bla_{CTX\text{-}M\text{-}32}$, $bla_{OXA\text{-}48}$, and $bla_{CMY\text{-}2}$ coding for cephalosporine (2nd generation), and carbapeneme antibiotic resistances. The most critical cluster contains rarely occurring resistance genes against reserve antibiotics used in human therapies (bla_{VIM}, *van*A, *mec*A, *mcr*-1, bla_{NDM}), i.e. against carbapenems (e.g. imipenem), gycopeptides (e.g. vancomycin), methicilline (MRSA), and cyclic peptides (e.g. colistin) (Alexander et al., 2020; Hembach et al., 2019).

The effect of blue light as an antimicrobial active driver, referred to as „antimicrobial blue light-aBL“, has been known for some time, but remained largely unexploited (Leanse et al., 2022; Y. Wang et al., 2017). Most of the studies are linked with hospital settings for the decontamination of wounds or other biotic and abiotic surfaces (Hamblin & Hasan, 2004; Wainwright, 1998). In addition, aBL treatment is also used in the food industry and in multiple barriers technologies in conditioning processes (Hadi et al., 2020). The blue light was shown in many studies to inactivate a wide range of pathogenic bacteria, regardless of their antibiotic resistance profile, Gram behavior or other physiological specificities (Maclean et al., 2009). Inactivation has been demonstrated on biofilms in addition to planktonic life forms (Ferrer-Espada et al., 2019, 2020). Based on these facts, the use of a broad blue spectrum emitting light source has been selected to excite the different photo-sensitive structures, leading to a non-specific and sustained killing effect on bacterial cells, especially of the ESKAPE group (Hoenes et al., 2019). Different targets in bacterial cells

like DNA, proteins, lipids, and the cell membranes are impacted by aBL (dos Anjos et al., 2023). So far, less is known about results of an irradiation of a broad aBL spectrum to bacterial cells and an evaluation of inactivation effects especially in industrial wastewater systems. In current publications, only light of a certain wavelength or a narrow wavelength range, mainly emitted from LED light sources, is used as aBL for irradiation (Maclean et al., 2009). Frequently, aBL with emission wavelengths around 405 nm or 415 nm is used to excite endogenous porphyrin-containing molecules. Wavelengths around 450 nm are also known to excite the cytochromes of the P450 complex. These cytochromes consist of porphyrin-containing molecular clusters, mostly photo-sensitive porphyrinogenic precursors. P450 classes catalyze the terminal reduction of oxygen of the Electron Transfer Chain (ETC) as oxidoreductases. Their function can be disturbed by light in the 450 nm range, leading to the death of bacterial organisms. In addition, wavelengths of 410 - 435 nm are still used as antibacterially effective, based on flavin-containing proteins and molecules of different oxidation states (Plavskii et al., 2018).

Blue light with co-applied exogenously administrations of photosensitizer such as prophyrin derivatives are already in use in medical photo-dynamic therapies (PDT). Such systems are used clinically in the field of wound healing and cancer therapy, where they also show great success in combating bacterial infections (Leanse et al., 2022; Maclean et al., 2008; Y. Wang et al., 2017). Beside the antibacterial impact, effective LED-based broad-spectrum antiviral treatments in combination with light-stimulated photo-sensitizers were demonstrated by Heffron et al. (2021). The reason for the antibacterial effect of blue light is it´s interaction with endogenous, photo-sensitive molecules (heme proteins, cytochromes, flavoproteins, oxygenases etc.). These photo-sensitive molecules react under light absorption with an energy or electron transfer to other molecules in the direct vicinity. The formation of so-called ROS, such as $^1O_2$, $O_2^{\bullet-}$, the highly toxic $OH^{\bullet}$ affect negatively vital structures of bacterial cells (i.e. membranes, protein structures of the electron transfer chain (ETC), or antioxidative protective systems (Hamblin & Hasan, 2004; Wainwright, 1998).

It is believed that the wastewaters from slaughterhouses contain bacteria and genes with the ability to spread zoonotic and human health relevant diseases (Savin et al., 2020). To prevent and decrease serious health issues caused by the dissemination of ARB and ARGs, the current investigations examined the prevalences of ESKAPE-group bacteria, various classes of clinically significant ARGs, and how exposure to both conventional treatment methods and ozone affected the abundance of each gene target. Therefore, one objective of this study is the determination of the occurrence and abundances of 21 gene targets in the wastewater samples collected from poultry and pig slaughterhouses on

various sampling days and sampling locations. We are focusing on the occurrence of Gram-negative and Gram-positive members of the ESKAPE bacteria (WHO, 2017). ESKAPE is an acronym comprising the scientific names of six highly virulent and antibiotic resistant bacterial facultative pathogens including: *Enterococcus faecium*, *Staphylococcus aureus*, *Klebsiella pneumoniae*, *Acinetobacter baumannii*, *Pseudomonas aeruginosa*, and *Enterobacter spp.* Due to their heightened resistance to frequently used antibiotics, these FPB pose an additional threat to the safety of the general population (Mulani et al., 2019). The second objective of this study is the impact of broad-spectrum LED bluelight on these FPB of the ESKAPE group. Here, the sensitivity of these bacteria is studied with and without photo-sensitizer application. The impact of high and low nutrient media on the aB inactivation especially on bacteria from different growth phases are analyzed. Especially, blue light insensitive reference bacteria and native slaughterhouse wastewater samples were treated with aBL together with porphyrin-based photo-sensitizer molecules for an inactivation of health critical bacteria.

2.2 Material and methods

2.2.1 Sampling and sample preparation

The wastewater samples were collected twice from a German poultry slaughterhouse on different days in summertime. Six samples were collected for each monitoring date: two samples from the RWW that is the influent of an integrated and conventional wastewater treatment plant (WWTP), two samples from the effluent that is released from the conventional WWTP, and two samples from the effluent that has subsequently undergone an ozone treatment (75 g ozone/m^3). The daily wastewater volume of the poultry slaughterhouse was about 3,600 m^3. The average slaughter rate is >100,000 chicken per day.

In case of a German pig slaughterhouse the sample acquisition was conducted in two independent campaigns. Four samples were taken for each monitoring date: two from the RWW that is the influent of an integrated physical-chemical treatment and 2 sample from the effluent that is release from the physical-chemical facility containing a flotation and precipitation treatment of particulate matter. The slaughterhouse exhibits a slaughtering capacity >10,000 pigs per day. Daily wastewater volume of about 2,100 m^3 are treated by a physical-chemical and biological WWTP using flotation and precipitation (flocculation).

After these on-site pre-treatments, the conditioned wastewater of pig slaughterhouse is released into a municipal WWTP via public sewer systems and the wastewater from the poultry slaughterhouse is discharged into a river receiving body.

The samples from poultry and pig slaughterhouses were transported to the laboratory via Express service at 4 - 7°C for max. 24 hours before being further processed. Following that, vacuum filtration was used to separate the wastewater liquids from suspended cellular matter including bacteria. Polycarbonate membranes (Ø 47mm, pore size 0.2µm, Whatman Nucleopore Track-Etched Membranes, Sigma-Aldrich, Munich, Germany) were used together with a sterilized filtration unit. Since the filtration volume depends on the turbidity, the volumes of each sample were 100 mL after conventional treatment, 200 mL for the effluent (poultry) after ozonation, 100 mL for the effluent (pig) after biological treatment and 30 mL for the RWW being the influent from WWTPs (i.e. RWW).

2.2.2 Live/dead discrimination using Propidium monoazide

PMA treatment can be utilized to distinguish intact bacteria from dead or injured bacteria (Jäger et al., 2018). Damaged bacteria membranes are penetrated by PMA, where it intercalates with internal cellular DNA and is irreversibly crosslinked by a photo-activation step with light. This crosslink reaction effectively inhibits any subsequent PCR amplification (Nocker et al., 2007a, 2007b). After vacuum filtration, the filter membranes were treated with 25 µM PMA solution (Biotium, Haywards, California, USA). The polycarbonate membranes were submerged in 2 mL colorless tubes (SafeSeal tubes, Carl Roth, Karlsruhe, Germany) containing the mixture of PMA and DNA-free water. Following a 5-minute incubation period in the dark, PMA-treated samples were subjected to the PhAST Blue Photo-Activation System (GenIUL, Barcelona, Spain) at 100% intensity for 15 minutes to enhance the PMA crosslinking with DNA.

2.2.3 DNA extraction for molecular biology analysis

DNA was extracted by using the FastDNA™ Spin Kit for Soil (MP Biomedicals, Santa Ana, USA) and FASTPREP® instrument (MP Biomedicals, Santa Ana, USA). For mechanical cell disruption, the filtrated membranes were put in the Lysing Matrix E tube. Proteins were then separated by centrifugation and precipitation, and the DNA was finally purified by attaching to a silica matrix. The concentration of the extracted DNA was measured by NanoDrop (ND-1000, PEQLAB Biotechnologie GmbH, Germany) and the Quant-iT™ PicoGreen® dsDNA Assay Kit (Thermo Fisher Scientific, Nidderau, Germany).

2.2.4 Quantitative PCR analysis

SYBR Green qPCR tests were performed using a Bio-Rad Cycle CFX96 (CFX96 TouchTM Deep Well Real-Time PCR Detection System, Bio-Rad, Munich, Germany), and the analysis was done using the manufacturer's software (Bio-Rad CFX Manager Software). Reactions were run in volumes of 20 µL, containing 10 µL Maxima SYBR Green/ROX qPCR Master Mix (2×) (Thermo Scientific Nidderau, Germany), 7.4 µL nuclease-free water (Ambion, Life technologies, Karlsbad, Germany), 0.8 µL of Primer FW (10 µm), 0.8 µL of Primer Rev (10 µm), and 1 µL of template DNA. The denaturation phase converts double-stranded DNA into single strands by heating up to a high temperature (about 95 °C) for 10 minutes. This was followed by 40 cycles of 15 s at 95 °C and 60 s at 60 °C. Melting curves were recorded by raising the temperature from 60 °C to 95 °C (1 °C every 10 s) to assess the specificity of the application. For each target either FPB or specific antibiotic resistance gene, the primer sequences used are listed in Table SA1. Information about the characteristics and quality of the qPCR systems used for the taxonomic genes as well as ARGs are given in Table SA1. For the quantitative evaluation of an unknown sample, the Ct value measured in the qPCR is assigned to the number of cell equivalents with the help of the previously generated calibration line using reference bacteria. The number of cell equivalents of the dilution series is determined on the basis of the researched genome sizes and the measured DNA concentrations using the URL Genomics & Sequencing Center tool (http://cels.uri.edu/gsc/cndna.html). Different gene clusters for antibiotic resistances categorize the analysed ARGs in frequently, intermediate, and rarely abundant gene targets and based on previous experiences published in Hembach et al (2017, 2022) and Alexander et al (2020, 2022). The clinical relevance of the investigated ARGs and FPB and their percentage share in clinical infections is given in Table 2.1. All qPCR data are listed in Table SA2 and Table SA3 in Supporting Information section.

Table 2.1: Clinically relevant of the investigated antibiotic resistance genes and facultative pathogenic bacteria and their percentage share in clinical infections in 2016 according to data from the National Reference Centre for Surveillance of Nosocomial infections (Aghdassi et al., 2016).

Antibiotic resistance genes	**Antibiotic classes concerned**
*erm*B	Macrolide antibiotic, Erythromycin
*int*I1	Integron Type 1 mobile genetic element (MGE)
*tet*M	Tetracycline antibiotic
bla_{TEM}	Penicilline antibiotic
*sul*1	Sulfonamide antibiotic
bla_{CTX-M}	Cephalosporin of 2. generation
$bla_{CTX-M-32}$	Cephalosporin of 2. generation
bla_{OXA-48}	Carbapeneme β-Lactame antibiotics
bla_{CMY-2}	Cephalosporin of 2. generation
bla_{VIM}	Carbapeneme, Imipenem (reserve antibiotic)
*van*A	Glykopeptide, Vancomycin (reserve antibiotic)
*mec*A	Penicilline, Methicillin resistance (multi-resistance in *S. aureus*)
mcr-1	Cyclic peptide antibiotic, Colistin (reserve antibiotic)
bla_{NDM}	Resistance against multiple β-Lactame antibiotics, Carbapeneme

Facultative pathogenic bacteria	**Clinical relevance**
Enterococci spp. (23S rDNA)	14,3 % of clinical infections
E. faecalis (dll gene)	6,9 % of clinical infections
P. aeruginosa (*ecfX* gene)	5,8 % of clinical infections
K. pneumoniae (*glt*A gene)	4,5 % of clinical infections
A. baumannii (*sec*E gene)	5 % of clinical infections
E. coli (*ycc*T gene)	16,6 % of clinical infections

2.2.5 Cultivation of ESKAPE facultative pathogenic bacteria for aBL irradiation

Bacterial strains were initially cultivated overnight in 40 mL high nutrient medium LB-Medium (Luria-Bertani, Sigma-Aldrich, Darmstadt, Germany) at 37 °C (stationary phase). In a second approach, freshly grown on the day of use bacterial suspensions from the exponential growth phase were used for aBL irradiation. Bacteria were washed three times with PBS solution (phosphate buffered saline) including centrifugation and resuspension steps. The washed bacterial pellets were resuspended in 20 mL PBS solution to an optical density of about $OD_{(600\ nm)}$: 0.1 (Hitachi Photometer, Hitachi-High-Tech Cooperation, Tokyo, Japan) which corresponds to about $5.0x10^8$ CFU / mL. Alternatively, low nutrient mineral medium BM2 (i.e. 100 mL 10x BM2, 10 mL glucose (40 % w/v), 10 mL $MgSO_4$ (200 mM), 1 mL $FeSO_4$ (10 mM) in 1 L sterile dH_2O; freshly prepared before use) was used to study the bacteria inactivation during aBL application. Both, bacterial suspensions from stationary as well as exponential growth phases were treated and analysed.

2.2.6 Experimental setup for aBL and photo-sensitizer treatment

For aBL illumination experiments sterile 20 mL glass vials together with a sterilized magnetic stirrer bar (Ø 2 mm * 5 mm) were used for a 5 mL volume approach. Therefore, 0.5 mL of the freshly washed bacterial suspension of $OD_{(600\ nm)}$ ~ 0.1 was pipetted to 4.5 mL PBS solution, resulting in a 10-fold dilution step with a final CFU of about $5.0x10^7$ per mL. Dark control experiments were performed in parallel by covering the vials tightly with a foil.

For the illumination of the bacterial suspensions 4 conventional 8 W LED bars (SolarStinger, SunStrip, DeepBlue, Econlux, Germany) were used. Equipped with a repeating sequence of 4 different LED types (Figure SA1) emitting wavelengths of 400 nm, 420 nm, 440 nm, and 460 nm, these LED bars were emitting an entire spectrum of blue light (Figure SA1). Due to the predetermined light source composition, a modulation of specific aBL emitting LED types was not possible. Sample vials were centre placed on a multi position magnetic strirrer (2Mag MixDrive60; Munich, Germany) and 1000 rpm were adjusted. The vials were located between two light source units in a refrigerated incubator at 30°C for the entire exposure time (Thermo MaxQ 4000; Thermo-Fischer Scientific, Darmstadt, Germany). As temperature control a separate vial containg liquid medium linked with a temperature sensor was run in parallel. The refrigerator setup helped to avoid any temperature mediated impact on bacteria during blue light exposition. Radiant intensity data were collected with a calibrated Spectrophotometer (FLAME-S-XR1-ES,

with optical fibre QP400-2-SR-BX; OceanInsight, Ostfildern, Germany) for the LED light source inside the incubator. As measurements inside a reaction vial in liquid could not be performed, the radiant intensity was measured at the vials position in air. Due to the fixed light emission of the LEDs, different light intensities, high and low, were performed by changing the light source and reaction vial distance. The conversion of the radiant intensity in W/cm^2 used into energy intensity in $J/s *cm^2$ is given for the applied high and low intensity in Table SA4. Here you will also find the energy densities calculated for the time dependent irradiations (1 - 4h).

Irradiation measurement values at 245 and 543 W/m^2 were chosen for aBL irradiation experiments. The photosensitizer 5, 10, 15, 20-Tetrakis-(N-Methyl-4-pyridyl) 21, 23-porphyrin tetratosylat (TMPyP; CAS: 36951-72-1) was purchased from Sigma-Aldrich (Darmstadt, Germany). A $1x10^{-3}$ M stock suspension of TMPyP photosensitizer was prepared with PBS and stored at 4 °C. The base structure of the planar organized, poly cationic TMPyP molecule is a porphyrin ring. Porphyrin molecules adsorb light at a specific spectrum. The so called Soret-band indicates the wavelength range of maximum adsorbtion, which is about 422 nm for TMPyP suspended in PBS. The TMPyP photosensitizer was premixed together with the bacterial test suspensions, followed by a 30 min preincubation step in dark before aBL irradiation.

A defined aliquot was taken out of the treated bacterial suspensions. Subsequently up to six ten-fold dilution steps were performed. From each dilution sample, 5 x 10 µL aliquots (droplets) were pipetted onto LB plates. The incubation time was 24 h and the temperature was adjusted to 37°C depending on the used reference bacteria. After incubation the numbers of colonies grown on the agar plates were counted and statistically analyzed to CFU per mL.

2.2.7 Slaughterhouse raw wastewater treated with aBL and porphyrin photosensitizer

A total of four RWW samples from a poultry slaughterhouse were studied. The RWW samples were directly collected from the influent to the slaughterhouses on-site WWTP and had not undergone any chemical or conventional treatment.

The RWW were centrifuged at 1500 rpm for one minute (Eppendorf 5810R refrigerated centrifuge) to sediment the rough particles. The optical density (OD) of the samples was then determined at 600 nm using a spectrophotometer (Hitachi U-5100). The OD_{600} values of the undiluted samples was about 1.8 for the chicken and 1.9 for the pig slaughterhouse

samples. Therefore, the samples were then diluted 1:10 in PBS (Phosphate buffer saline, pH 7.4). The OD values were about 0.3 after dilution. The diluted samples were added to 5 mL glass vials with a 5 mm magnet and sealed with a suitable glass lid. The glass vials were then placed on a magnetic stirrer (25 Mag Emotion, Mixdrive 60) in an incubator at a temperature of 37°C (Thermo MaxQ 4000). The glass vials with the diluted raw water samples were placed between 4 blue light bars on a magnetic stirrer. The magnet inside the glass vial rotated continuously to ensure a continuous movement of liquid in the glass vials and prevent a sedimentation of the bacterial cells. The samples were treated with blue light up to 4 hours (for dose calculation see Table SA4).

2.3 Results

2.3.1 Abundances of facultative pathogenic bacteria and ARGs in wastewaters from poultry slaughterhouse

Following PMA treatment of the samples, the ESKAPE group bacteria were measured using species-specific gene markers and the results are presented in Figure 2.1A. The most prevalent target species in the RWW were *E. coli*, followed by *Enterococcus spp*. and *A. baumannii*, with abundances of 1.8×10^8, 9.3×10^6, and 1.4×10^7 gene copies/100 mL, respectively. The lowest concentration with 2.6×10^3 gene copies/100 mL was quantified for *K. pneumoniae*. The abundances of *P. aeruginosa* and *E. faecalis* were 1×10^4 and 1.3×10^5 gene copies/100 mL, respectively.

K. pneumoniae and *E. faecalis* were reduced below the limit of detection (LOD) after the biological sludge treatment and subsequent ozonation, while *Enterococcus* spp., *P. aeruginosa, A. baumannii,* and *E. coli* were reduced in several $\log_{10}$ units by 6.5, 2.1, 4.2, and 4.2, respectively. Following the subsequent ozonation, *E. coli* and *Enterococcus spp.* demonstrated a lower decrease, whereas *P. aeruginosa* and *A. baumannii* exhibited a significant decrease below the LOD.

With the exception of the gene bla_{VIM}, almost all ARG targets were present in the raw water coming directly from the poultry slaughterhouse. In the raw sewage (i.e. influent of the on-site WWTP), among all “commonly occurring resistance genes” (Figure 2.1B), bla_{TEM} and *sul*1 exhibited the highest abundance of 3.8×10^8 and 3.6×10^8 gene copies/100 mL, respectively, followed by Integron-specific gene *intI*1 (1.1×10^8) being involved in HGT, *tet*M (9.1×10^7), and *erm*B (2.1×10^7). All regularly occurring ARGs decreased by several log units after using conventional biological treatment technologies; the most notable decline was 6 log units in case of *erm*B. The ARGs *tet*M and bla_{TEM} were reduced by 4.6 and 3.7 $\log_{10}$ units, respectively. Similarly, *sul*1 and *IntI*1 gene targets were removed by 2 $\log_{10}$

units. The subsequent ozonation reduced the *erm*B gene target below the detection limit. The *sul*1 gene was reduced up to 2 $\log_{10}$ units, followed by *tet*M (1 $\log_{10}$ unit), *intI*1 (1.3 $\log_{10}$ units), and bla_{TEM} (0.7 $\log_{10}$ unit).

The abundance of intermediate abundant ARGs in the analyzed samples is shown in Figure 2.1C. In raw water samples, bla_{OXA-48} (1.5×10^5 gene copies/100 mL), bla_{CMY--2} (1.2×10^6 gene copies/100 mL), $bla_{CTX-M32}$ (7.8×10^6 gene copies/100 mL), and bla_{CTX-M} (7.3×10^5 gene copies/100 mL) were present in relatively high concentrations.

Regarding the samples from the biological treatment on site, each gene concentration decreased to varying degrees. The bla_{CMY-2} gene concentration was found with the strong reduction, with 4.1 $\log_{10}$ units, followed by bla_{CTX-M} (3.6 $\log_{10}$ unit), bla_{OXA-48} (3.3 $\log_{10}$ unit), and $bla_{CTX-M32}$ (3 $\log_{10}$ unit). After ozonation of the previous biologically treated wastewater on site eliminated the bla_{OXA-48} gene below the LOD, whereas for the bla_{CMY-2} gene no significant reduction was observed. In addition, bla_{CTX-M} and $bla_{CTX-M32}$ were both decreased by 1.2 $\log_{10}$ and 1 $\log_{10}$ units after ozonation, respectively.

Most of the rarely occurring clinically relevant ARGs were not detected in pre-treated poultry wastewaters after ozonation (Figure 2.1D). The ARGs *mcr*-1, *mec*A, *van*A, and bla_{NDM} were detected in RWW samples released by poultry slaughterhouse with comparable concentrations of 2.6×10^5, 1.9×10^5, 1.1×10^5, and 2.6×10^5 gene copies/100 mL. These results indicated the presence of clinically important ARGs released by the RWW. The conventional biological treatment technologies decreased gene concentrations of bla_{NDM} and *mec*A by 1.5 and 2.3 $\log_{10}$ units, respectively, and other targets were measured below the detection limits. Most of the ARG targets of this category were found to be below the detection limits after ozone treatment. Only bla_{NDM} that was still detectable but was further reduced by 0.2 $\log_{10}$ units after ozonation.

Notably, high concentration of facultative pathogenic bacteria and different categories of ARGs are released via wastewater from poultry slaughterhouses. Despite the fact that these cell equivalent values decreased during on-site biological treatment and subsequent ozonation, the dissemination of hygienically relevant bacteria and ARGs continues to be serious issues and contribute to the spread of ARB. This applies especially to slaughterhouses that do not have effective wastewater treatment facilities. Here, insufficiently treated wastewater is discharged directly into the receiving waters or pollutes the municipal sewage treatment plants.

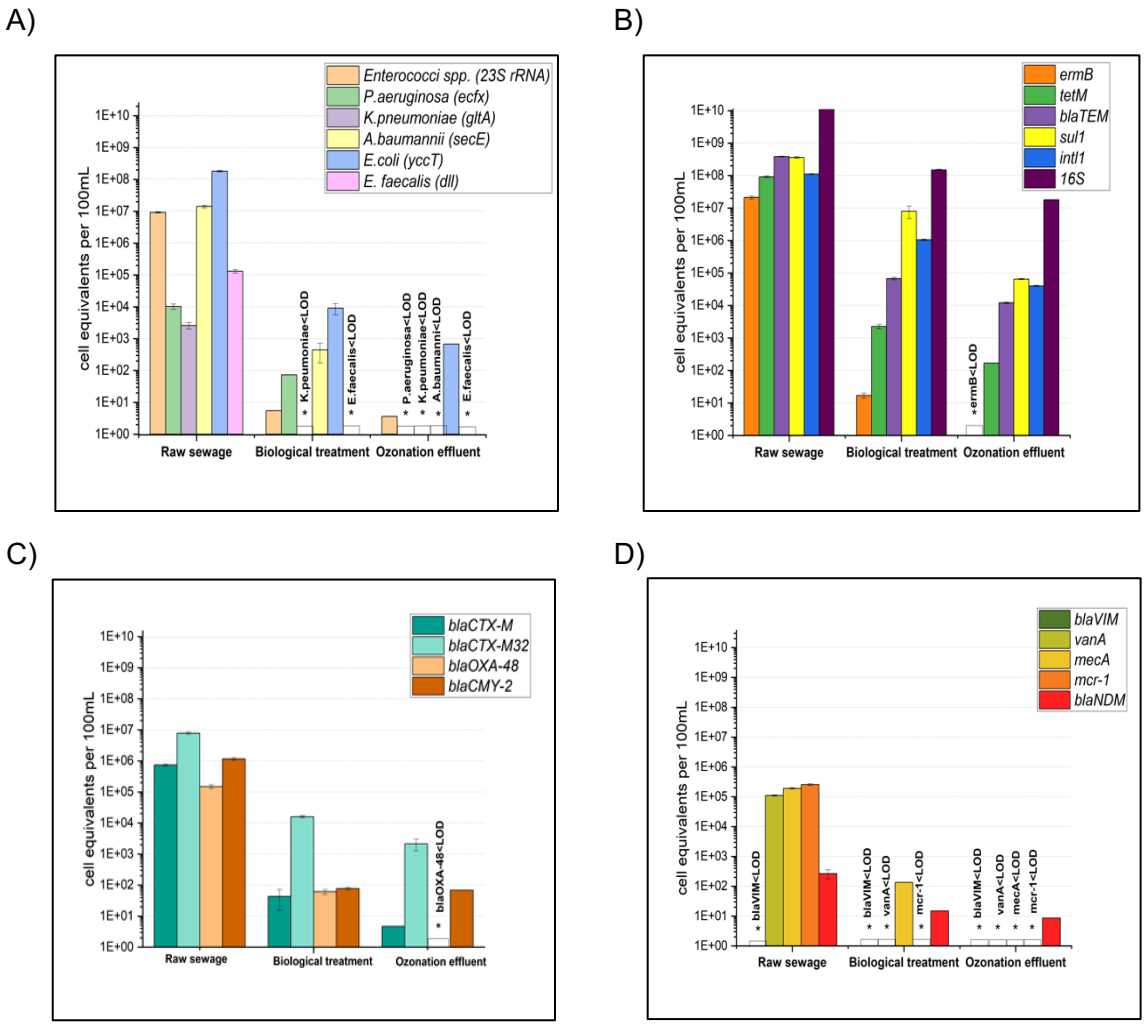

Figure 2.1: Water sample getting from poultry slaughterhouse. Abundance of facultative pathogenic bacteria (A), abundance of "commonly occurring resistance genes" (B), abundance of "intermediately occurring resistance genes" (C), and abundance of "rarely occurring resistance genes" (D). Gene targets for bacteria and antibiotic resistance genes were quantified by qPCR in raw wastewaters before and after on-site biological conventional wastewater treatments and ozone treatment. LOD: below limit of detection. The data from each sampling campaign are listed in Table SA2.

2.3.2 Abundances of facultative pathogenic bacteria and ARGs in wastewaters from pig slaughterhouse

As seen in Figure 2.2A, *E. coli* (3.8×10^8 gene copies per 100 mL) was the most abundant FPB, followed by *Enterococcus* spp. (7.8×10^6 gene copies/100 mL), *A. baumannii* (4.4×10^6 gene copies/100 mL). *P. aeruginosa,* and *E. faecalis* had roughly equal relative abundances with 1.0×10^4 and 1.1×10^4 gene copies/100 mL, respectively. *K. pneumoniae* had the lowest concentration, measuring 9.3×10^2 genecopies/100 mL. *P. aeruginosa, K.*

pneumoniae, and *E. faecalis* were reduced after advanced treatment below the LOD, whereas *Enterococcus* spp., *A. baumannii*, and *E. coli* were all reduced in several log_{10} units by about 4.

Regarding the different clusters of ARGs (Figure 2.2B, C, and D), *tet*M (8×10^8 gene copies/100 mL) and *sul*1 (8.4×10^8 gene copies/100 mL) genes demonstrated high concentrations among commonly occurring resistance genes. The relative abundances of bla_{TEM} and integron *Intl*1 were approximately the same with 2.1×10^8 and 1.9×10^8 gene copies/100 mL, respectively. The gene *ermB* exhibited the lowest gene copy value in the RWW, but showed the greatest reduction by 5.5 log_{10} units after biological treatment. Additionally, after being exposed to biological treatment, the eubacterial 16S rRNA gene marker was diminished by 3.5 log_{10} units from its initial concentration of 9.4×10^{11} gene copies per 100 mL. The ARGs *tet*M, bla_{TEM}, *sul*1, and *Intl*1 also showed reductions of 4.5, 3, 2, and 1.5 log_{10} units, respectively.

Among intermediate occurring ARGs (Figure 2.2C) consist of $bla_{CTX\text{-}M}$ (1.0×10^5 gene copies/100 mL), $bla_{CTX\text{-}M32}$ (1.3×10^6 gene copies/100 mL), $bla_{OXA\text{-}48}$ (4×10^7 gene copies/100 mL) and $bla_{CMY\text{-}2}$ (4.2×10^5 gene copies/100 mL). The ARG $bla_{CTX\text{-}M}$ was found to be the most affected ARG by the biological treatment in this group due to the largest drop in its cell equivalent value, which is by 3.8 log_{10} units, followed by $bla_{OXA\text{-}48}$ (3.1 log_{10} units), $bla_{CTX\text{-}M32}$ (2.5 log_{10} units), and $bla_{CMY\text{-}2}$ (1 log_{10} unit).

The final category consists of ARGs that were thought to be rare or to have only been detected in trace amounts in RWW or WWTP influent (Alexander et al, 2020; Hembach et al. 2017). Since this subset of ARGs was directed against last-resort antibiotics, we thought that these ARGs were the most critical among the targets being evaluated. These ARGs include *bla*VIM (lower than detection limit), *van*A (3×10^4 gene copies/100 mL), *mec*A (4.7×10^3 gene copies/100 mL), *mcr*-1 (1.2×10^5 gene copies/100 mL), and bla_{NDM} (1.7×10^3 gene copies/100 mL), which fall into the category of infrequently occurring resistance genes. Nevertheless, these gene targets together with their carrying bacteria can reach the aquatic environment in case of inproper removal treatments at slaughterhouses. Hence, the dissemination of these resistance genes could become a serious public and environmental threat, when people are colonized with these ARG carriers. In fact, the concentration of the colistin resistance gene *mcr*-1 was up to 1.2×10^5 gene copies/100 mL, indicating that the raw water samples were strongly contaminated as mentioned by other studies (Hembach et al, 2017; Savin et al., 2020; Alexander et al., 2020). The majority of the ARG targets (*van*A, *mec*A, and *mcr*-1) in this category were found to be below detection limits after biological treatment, and the cell equivalent number

of the gene *bla*$_{NDM}$ was decreased by 1.5 log_{10} units. Hence, the dissemination of these particulary critical resistance genes against reserve antibiotics (e, g. Vancomycin, Colistin, Imipenem) is inhibited or completly reduced.

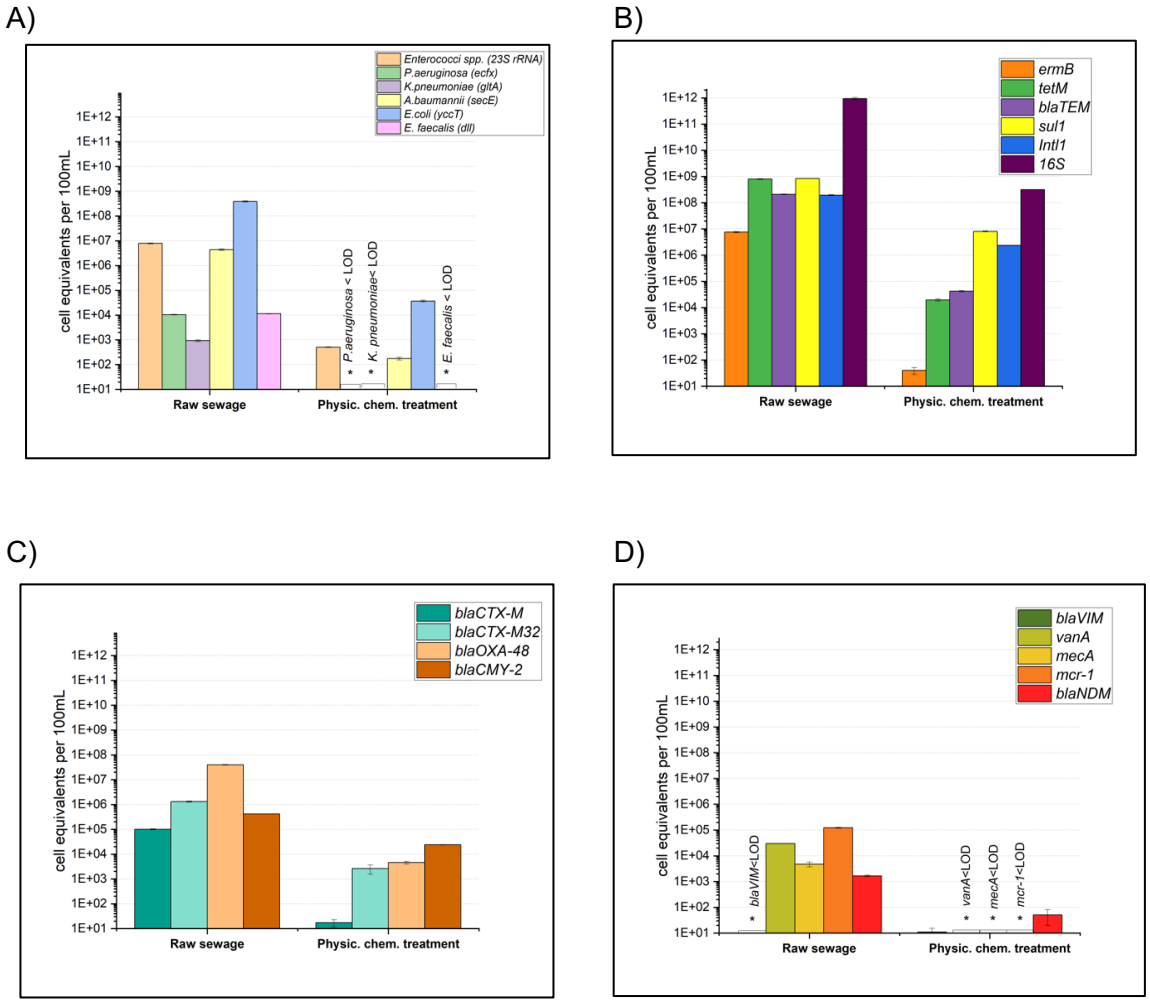

Figure 2.2: Water sample getting from pig slaughterhouse. Abundance of ESKAPE group bacteria (A), abundance of "commonly occurring resistance genes" (B), abundance of "intermediately occurring resistance genes" (C), and abundance of "rarely occurring resistance genes" (D). Gene targets for bacteria and antibiotic resistance genes were quantified by qPCR in raw wastewaters before and after on-site biological treatment. LOD: below limit of detection. The data from each sampling campaign are listed in Table SA3.

As mentioned before, it became obvious that raw sewage from poultry and pig slaughterhouses are highly contaminated with facultative pathogenic bacteria of the ESKAPE-group, but also with different clusters of clinically relevant ARGs. It is obvious

that all gene targets became less concentrated after physicochemical and biological treatments, and their abundances even significantly decreased after subsequent ozonation in case of the poultry slaughterhouse wastewater treatment. Hence, the implementation of treatment processes for an effective reduction of hygienically relevant bacteria and clinically important ARGs is recommended for slaughterhouses. The presented results did also show that combinatory technologies like biological treatment followed by ozonation are most successful aiming on a strong reduction of these microbiological parameters.

2.3.3 Inactivation of ESKAPE-group reference bacteria

The selected reference strains of the ESKAPE-group were irradiated with broad spectrum aBL (245 W/m^2; Figure 2.3). and the antibacterial efficiency was investigated by determination of bacterial concentrations (cfu/mL). Figure 2.3 describes the different inactivation dynamics of reference bacteria exposed to aBL treatment in a time dependent manner. Since the focus of this study is on wastewater treatment with aBL, bacterial suspensions were used that were comparable to the 16S rDNA qPCR results from real slaughterhouse wastewater (Figure 2.1 and Figure 2.2). In addition, increased cell numbers were necessary to evaluate the $\log_{10}$ reduction potential of the applied aBL irradiation. Taxon-specific differences became visible, when high density bacterial suspensions were used. It became obvious that after 6 h of irradiation the impact of aBL on the bacterial reference strains offer various sensitivities. Whereas cfu values of *E. faecium and K. pneumoniae* persisted at a high level similar or close to initial untreated sample (0 h), all other strains (i.e. *E. coli, S. aureus, P. aeruginosa*, and *A. baumannii*) were much stronger affected by the blue light. Here, the $\log_{10}$ unit's reduction ranged up to 8 $\log_{10}$ units in maximum (Figure 2.3).

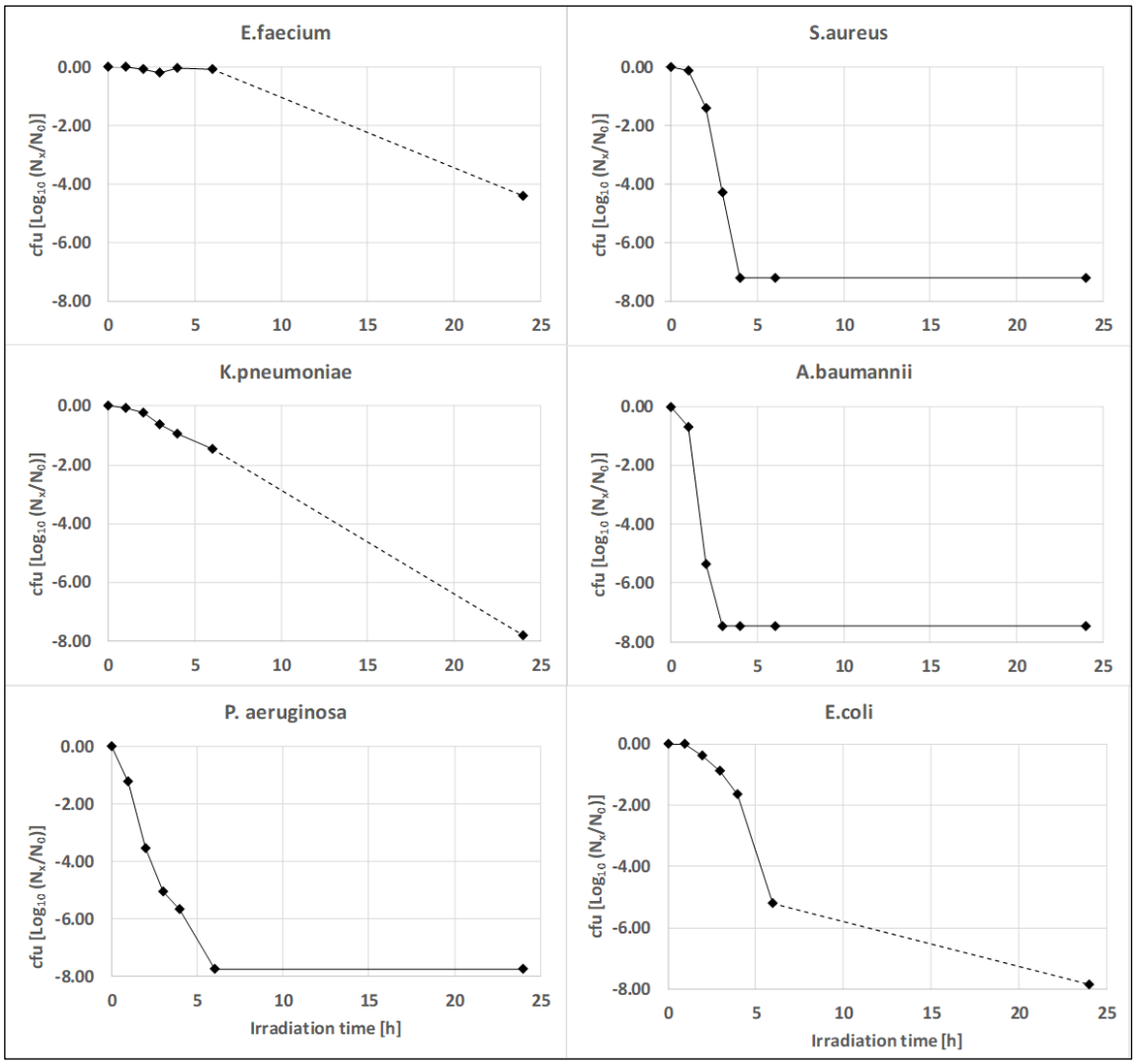

Figure 2.3: Log_{10}-reduction rate of facultative pathogenic bacteria after different hours of irradiation with broad range bue light (380-500 nm). The reduction rates were calculated by cultivation of serial dilutions of each reference bacterium at different time points. Broken lines represent exposure times without any distinct cultivation experiments assuming values above total reduction rate. Solid lines represent the continuous measured reduction rates of the different reference bacteria reaching the point of total reduction before the long term aBL irradiation (24 h).

The reference strains of *A. baumannii, P. aeruginosa,* and *S. aureus* showed a reduction of > 7 log_{10} units within the first 6 h of irradiation. In addition, the reduction for *E. coli* was about more than 5 log_{10} units. Similar to *K. pneumoniae, E. faecium* was less sensitive to blue light and no distinct reduction by aBL became visible. In consequence, it is possible to categorise the used different bacterial reference strains of the ESKAPE-group in 1) highly sensitive with *S. aureus, A. baumannii, and P. aeruginosa,* 2) sensitive with *E. coli*

as are presentative bacterium of the large group of *Enterobacteriacae*, and 3) resistant or less sensitive against aBL with *E. faecium* and *K. pneumoniae.*

To test the possible dependence of inactivation by aBL on growth phases and nutrient availability, the aBL insensitive reference bacterium *K. pneumoniae* was grown in a high nutrient medium (LB - Luria-Broth) and in a mineral medium (BM2 – Basal-Medium 2) with glucose as single carbon-hydrate source. Overnight cultures (stationary growth phase) and bacteria from the exponential growth phase in high and low nutrient growth media were used for aBL irradiation experiments (543 W/m^2; 30°C) (Figure 2.4). The late stationary phase cultures showed a less sensitivity to aBL during 4 h of irradiation in contrast to cultures harvested from the exponential growth phase. In both experimental approaches the starting cell count was analysed with about 8.0 log_{10} units cfu/mL. Here, the aBL impact on the *K. pneumoniae* suspensions were comparable in case of high and low nutrient cultivation conditions. The cell numbers were found to be about $1.0x10^7$ cfu/mL in both culture experiments. The maximal reduction capacities were found with a maximum of only 1 log_{10} units after 4 h illumination.

Reduction values gained from the exponentially growing bacteria offered slightly more antibacterial impacts especially when cultivated in high nutrient LB-medium with about 3 log_{10} units which corresponded to about $1.0x10^5$ cfu/mL. The antibacterial impact of blue light on exponentially growing cultures in low nutrient BM2 medium was much lower with about 1 log_{10} unit after 4 h of irradiation. Finally, it could be shown that the different growth phases and the better nutrient supply have an influence on the inactivation by aBL in *K. pneumoniae*, which might result from an increased metabolic activity.

A comprehensive elimination of the bacteria from the ESKAPE-group should be the goal of inactivation in various water matrices. To achieve this, it is necessary to integrate innovative approaches that optimise aBL treatment in order to inactivate aBL insensitive bacteria.

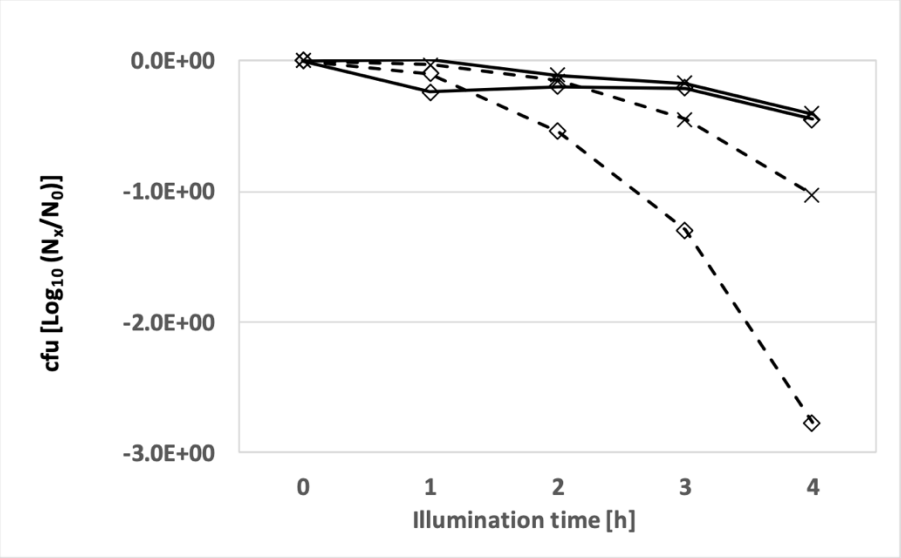

Figure 2.4: Effects of various culture growth media and growth phases of the aBL robust K. pneumoniae reference strain. High nutrient LB medium (diamond) and mineral medium BM2 (cross) were used. Different cultivation experiments were evaluated using overnight cultures representing stationary growth phase (solid lines), as well as cultured from freshly prepared exponentially growing bacteria culture (broken lines). Colony forming unit determination were run from 0 h (initial control) to 4 h of aBL irradiation. Results are means of three independant experiments.

Both insensitive reference bacteria *E. faecium* and *K. pneumoniae* were selected for photo-sensitizer experiments enhancing antibacterial efficiency of aBL. Here, strong additional effects of aBL treatment were detected already from 1 hour of irradiation in presence of the photo-sensitizer concentration of $1.0x10^{-6}$ M solution (approx. 1.35 mg/L) (Figure 2.5). Control experiments in dark showed the non-bacterial toxicity of the TMPyP photo-sensitizer (data not shown).

During an irradiation time of 4 hours the control suspensions without TMPyP confirmed the insensitivity of both *K. pneumoniae* and *E. faecium,* which showed no decrease of CFU per mL over time (Figure 2.5A). But, a $1.0x10^{-6}$ M addition of TMPyP to the bacterial suspensions showed strong reduction impacts almost after 1 h of aBL treatment. For *K. pneumoniae* a decreased colony counts with > 4 $\log_{10}$ units was measured, whereas no colonies were detectable for *E. faecium* (Figure 2.5B). In case of longer incubation times > 1h working with $1.0x10^{-6}$ M TMPyP and aBL no cfu was measured indicating the elimination of these both aBL insensitive bacterial strains (Figure 2.5B). The application of $1.0x10^{-7}$ M or $1.0x10^{-8}$ M TMPyP approaches together with aBL showed weaker reduction capacities for both reference bacteria *K. pneumoniae* and *E. faecium* (Figure 2.5C and D).

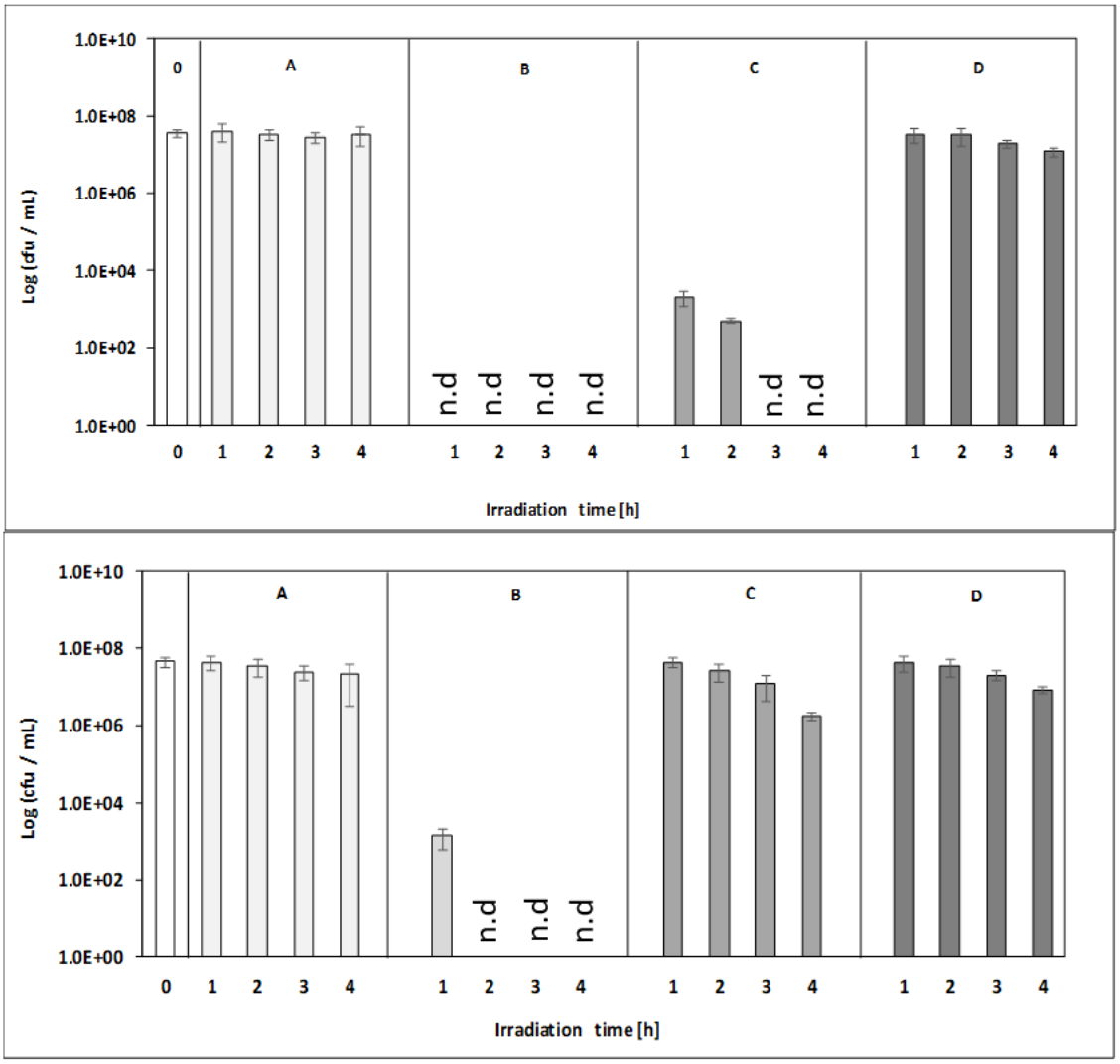

Figure 2.5: Bacterial suspension of aBL robust K. pneumoniae (top) and E. faecium (bottom) (both early stationary growth phase cultures for 1 to 4 h irradiation): (0) initial sample, (A) aBL without TMPyP, (B) aBL with TMPyP ($1.0x10^{-6}$M); (C) aBL plus TMPyP ($1.0x10^{-7}$ M); (D) aBL plus TMPyP ($1.0x10^{-8}$M). The aBL irradiation was performed using 543 W/m^2. The data are the means of different dilution steps calculated to CFU/mL. n.d: not detected.

2.3.4 Combinatory inactivation strategy with raw sewage from slaughterhouses

The application of this combinatorial inactivation strategy against entire bacterial populations was tested on a real raw sewage from a poultry slaughterhouse (Figure 2.6). Firstly, the impact of aBL on the total population of raw sewage was tested by preparing 1:10 dilutions of raw sewage due to the high turbidity of the samples. After 4 h, it was found

that the aBL irradiation without TMPyP treatment of the total population resulted in a weak reduction of about 1 log_{10} unit (data not shown). But, the presence of the photosensitizer TMPyP ($1.0x10^{-7}$ M) together with an aBL irradiations could decrease the bacterial concentration of the total population of diluted raw sewage to no detection during 4 h of treatment. More successfully, the photo-sensitizer concentration of $1.0x10^{-6}$ M TMPyP reduced the colony counts to no detection already after 0.5 h of treatment (Figure 2.6). Again, combinatorial approaches reducing unwanted bacterial contaminations were shown to be highly effective. However, wastewater parameters such as turbidity due to organic or abiotic loads must be taken into accounts. Therefore, in the data shown with RWW, only diluted approaches could be used. However, it must also be emphasised that these are small-volume laboratory experiments in a static approach. It remains to be seen to what extent these combinatory strategies can be applied in modified up-scaled flow reactors.

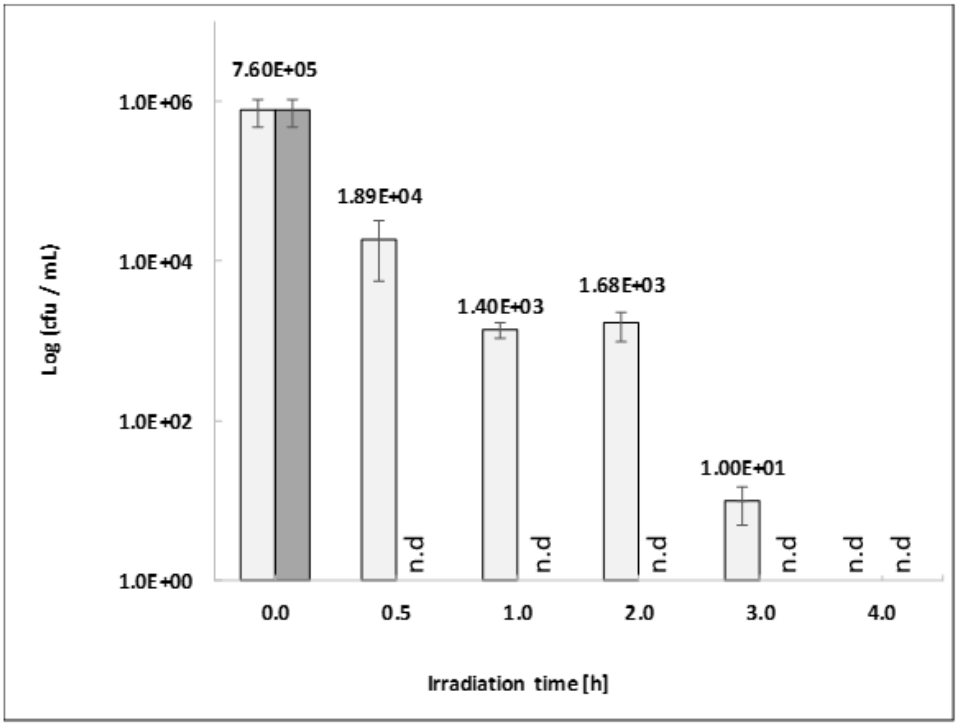

Figure 2.6: Native slaughterhouse raw sewage treated with aBL (543 W/m²) in addition with $1.0x10^{-6}$ M (dark bar) or $1.0x10^{-7}$ M TMPyP (light bar) for 0.5, 1.0, 2.0, 3.0, and 4.0 h. The initial cell count cultivated on LB medium derived from the same initial sewage sample. n.d: not detected.

2.4 Discussion

Wastewater from poultry and pig slaughterhouses is a hotspot for antibiotic resistances and FPB. Nowadays, the slaughterhouse technologies used have been adapted to the new circumstances, where so-called slaughter lines are now used for one animal species and can achieve enormous throughputs. For pigs, the slaughter capacity can reach over 20,000 animals per day; for chickens, the largest plants slaughter several hundred thousand animals per day. Due to food safety and hygiene requirements, savings in energy and water consumption are limited to a certain degree. The wastewater from slaughterhouses is organically highly contaminated and demonstrates high chemical oxygen demand (COD) values. Therefore, such industries usually have wastewater pre-treatment at their plant before conditioned wastewater are released to municipal sewer systems. This was also the case of our studies, where different wastewaters were analysed for FPB and thus also ARGs emitted from large slaughterhouses.

The concentrations of six different FPB based on the WHO priority list of the ESKAPE group (WHO 2019a), which are also known to be carriers of clinically relevant resistances, were quantified by molecular biology approaches in the effluent of poultry and pig slaughterhouses that carry out large-scale slaughtering. In addition, a total of 14 ARGs of different priorities for human medicine were selected, whose concentrations were also quantified. Only living, intact FPB or ARGs from living bacteria were quantified by qPCR in order to show reduction efficiencies of existing and innovative technologies. In comparison with other studies, who identified hotspots of antibiotic resistance dissemination (e.g. Alexander et al., 2022; Paulus et al., 2019; Voigt et al., 2020), we have also demonstrated that raw sewage from poultry and pig slaughterhouses is highly contaminated with FPB, but also with various categories of clinically relevant ARGs, including ARGs against the group of reserve antibiotics. Conventional biological or advanced (oxidative) treatments significantly decreased the concentration of the different gene targets by several $\log_{10}$ units depending on the bacterial target, after but were not eliminated. Therefore, the application of treatment procedures for a more effective reduction of hygienically relevant bacteria and clinically important ARGs, aiming at a stronger reduction/elimination of these microbiological parameters, is recommended.

The overall aim should be to minimize the spread of ARB and ARGs from hotspots disseminated into the public wastewater network and subsequent into the environment. Targeted and innovative light-based on-site measures relieve downstream wastewater areas of AMR contamination, reducing their release into the environment (Mulani et al., 2019). On the one hand, this concerns municipal central WWTPs, but on the other hand also receiving waters that take in the treated wastewater directly. Especially in times of

climate change with rising temperatures and dry periods, the percentage of treated wastewater in receiving waters can increase. This is associated with an increase in the concentrations of AMB and ARGs in these surface waters. Increased water temperature can then also enhance the persistence of these bacteria in the aquatic environment. The risk of contamination for humans is particularly present when protected assets in the type of water usages are affected. These are, for example, bathing waters, recreational areas, drinking water reservoirs, and agricultural areas that are irrigated with re-used waters. But increasingly frequent heavy rainfall events also lead to run-off of ARB, especially from agricultural land fertilised with manure from livestock farms. Hembach et al. (2022) already showed the contamination of liquid manure with ARGs.

As a proof of principle investigation, we demonstrated with the help of a laboratory pilot system the destruction of ARB/ARGs in contaminated wastewater from slaughterhouse with a blue light-based technology in combination with the photosensitizer TMPyP porphyrin molecule. It was discussed that different wavelengths are responsible for activation of diverse photo-sensitive molecules involved in bactericidal activities (Hessling et al., 2017; Hoenes et al., 2020). Whereas short blue-light of 405 nm is known to activate porphyrins, longer wavelengths up to 450 nm have a stronger interaction with endogenous flavins as photo-sensitizers (Hoenes et al., 2020; Plavskii et al., 2018). However, it also must be said that it is currently not clear how different bacterial genera react to visible light of the same wavelength (Tomb et al., 2018).

In connection with aBL irradiation, a comparison with the widely used ultraviolet (UV) light, as an applied photo-based antimicrobial technology is appropriate in order to look at the advantages and disadvantages of both methods. Especially UV-C (100 – 289 nm) mainly has germicidal effects. These effects are caused by the DNA and RNA as well as proteins absorbing irradiation at the respective wavelength. The absorption curve of DNA reaches its maximum at a wavelength of 260 nm and it´s local absorption minimum close to 280 nm. As a consequence, the germicidal effect for microbes is achieved at a wavelength of 260 nm (Jungfer et al., 2007; Süß et al., 2009). The effectiveness of UV light in the biological inactivation primarily results from the fact that DNA molecules absorb UV photons with peak absorption at 265 nm. In case of lethal damages, the DNA replication is blocked due to DNA alterations, mainly thymine dimers, which ultimately result in reproductive cell death. During evolution, bacteria generally possess molecular mechanisms, such as photo-reactivation and dark repair systems, to restore such DNA lesions. All mechanisms are regulated by the expression of the *rec*A gene, the key gene in this system (Jungfer et al., 2007; Sinha & Häder, 2002).

In contrast to UV inactivation, the aBL photo-based irradiation is activating the ROS in the bacterial cells. These reactive oxygen molecules are targeting different cellular structures inducing lethal impacts on the microorganisms. Hence, in case UV irradiation the nucleic acid alterations are the main underlying mechanism, where DNA directed repair mechanisms were developed in bacteria during evolution. In difference, up to now no repair mechanisms are known to repair the manifold target structures impaired by aBL irradiation (Hadi et al., 2020). Hence, a more sustainable application of aBL in combination with porphyrin photosensitizer is hypothesized. In principle, the use of LED-based photo-reactors is significantly more cost-saving than conventional lamp designs such as those used for UV-C irradiation. The UV medium-pressure radiation source with 1000-Watt power input generates a radiation flux of approx. 21.2 Watt in the range of 405 nm. A commercially available LED generates a radiation flux of 46 Watt at a power input of 100 Watt. If we increase this value by a factor of 10 to a LED spotlight with a power input of 1000 Watt, we will arrive at 460 Watt. Roughly speaking, an LED radiation source is 21.7 times more efficient in the 405 nm range than a classic medium-pressure radiation source with the same energy input and with the advantage that no undesired side reactions occur (personal communication with light industry company).

However, a direct comparison of the presented LED-based blue light system would only make sense once an up-scaling for a flow reactor with appropriately adapted LED light sources has been tested. Here, the energy inputs for the inactivation of critical bacteria (see Table SA4) refer exclusively to the stagnation reactor used for small-volume laboratory experiments.

The recent studies have shown that FPB of the ESKAPE group demonstrated a diverse susceptibility for the broad range of aBL (405 -450 nm wavelength). This phenomenon was independent from the Gram properities of the reference bacteria. *E. faecium* and *K. pneumoniae* demonstrated a strong insensitivity against aBL compared to the the other reference bacteria. But, the application of the porphyrin TMPyP enhanced the inactivation capacity of aBL in a similar range like the aBL sensitive strains. This enhancement is aBL dependent, since control experiments demonstrated no inactivation of the reference bacteria without previous blue light irradiation (dark exposure) as well as the non-toxicity of the photo-sensitizer molecule TMPyP (data not shown). It must be mentioned that aBL impact might also be influenced by components and ingredients of the raw sewage increasing the turbidity and transparency of the water matrix. Due to the high turbidity we needed to dilute the RWW samples released from slaughterhouses for aBL irradiation. No transmission of the blue light was possible in case of undiluted samples. In that concern, a previous filtration step could benefit the reduction performance for FPB and ARGs,

especially in case RWW. Since we have initially used a stagnation approach with a low sample volume, the inactivation capacities of an up-scaled flow aBL reactors has to be analysed designed for a modular implementation in sewer systems.

Actually, aBL treatment as a single inactivation approach demonstrated an apparently insufficient reduction capacity in real slaughterhouse sewage systems. Hence, aBL treatment was linked with the photosensitizer TMPyP application. Similar to the previous experiment with reference bacteria of the ESKAPE-group, the TMPyP photo-sensitizer addition increased the reduction using native slaughterhouse wastewater in a concentration depended manner. At present, it is still unclear why the effect of the photosensitizer TMPyP is restricted to such a limited concentration range when working with these aBL insensitive reference bacteria *K. pneumoniae* or *E. faecium*, and native wastewater samples. In principle, the results showed that it is possible to combine antimicrobial strategies to inactivate a potentially wide range of hygienically critical bacteria including insensitive bacteria.

It is hypothesized that the application of a specific concentration of TMPyP increase the target molecule amount responsible for the generation of reactive oxygen substances being the causative agent for bacterial killing rates impacts. Furthermore, threshold values of endogenous porphyrin amounts are a critical issue, since most effective concentration of photosensitizer TMPyP were detected to be 10^{-6} M.

However, it should be noted that not the harmless, native water flora is of hygienic relevance, but FPB with ARGs are of clinical relevance and should be inactivated. The inactivation effect on wastewater-borne active viruses or protozoa with hygienic relevance is also still unclear. These microbes are not considered in this study. Finally, these findings demonstrate a promising starting point of an alternative strategy to effectively eliminate a broad spectrum of (pathogenic) bacteria from wastewater by using aBL, especially in combination with additional inactivation approaches. As a near future perspective, modular designs of this aBL based technology should allow installation at hazardous critical hotspots in process lines.

2.5 Conclusion

Poultry and pig slaughterhouses produce wastewater with high concentrations of clinically relevant bacteria of the ESKAPE group and ARGs. Different clusters of critical ARGs are detectable in slaughterhouse RWW and show different reduction behaviour by conventional treatment processes. On-site treatments by biological wastewater treatment

and ozonation showed certain reduction capacities, which were not effective enough for all investigated ARGs and FPB. In this respect, it has not yet been possible by national and international authorities to define threshold values at which specific hygienically treatment of wastewaters should be implemented. In general, the occurrence of resistances to reserve antibiotics is described as a particularly critical issue and it´s dissemination should be avoided. Hence, the application of aBL LED irradiation demonstrated differences in the killing efficiency across the selected representatives of the ESKAPE group microorganisms. The reference organisms could be categorized to highly sensitive, sensitive, and insensitive for aBL inactivation. aBL in interaction with porphyrin photo-sensitizer TMPyP (10^{-6} M) allowed a reduction/elimination of reference bacteria and also bacteria in native slaughterhouse wastewater. Hence, combinatorial methods are more successful in protecting downstream areas of the aquatic use pathway.

Table SA 1: Primer sequences, calibaration line equation, efficiency values, detection limits, and correlation coefficientvalue of the calibration lines, amplicon sizes, references. The table clustered he qPCR systems used for the quantification of pathogenic bacteria and antibiotic resistence genes according to Hembach et al. (2017, 2022) and Alexander et al. (2020; 2022).

Target	Primer sequence	Equation of the calibration curve	Amplicon size	efficiency	R^2	LOD	Control strain	reference
Facultative pathogenic bacteria								
Enterococcus spp.	Fwd: AGAAATTCCAAACGAACTTG Rev: CAGTGCTCTACCTCCATCATT	F(x)= -3.585x+35.283	93 bp	90.1 %	1.000	65	*E. faecium* DSM20477	(Xi et al., 2009)
E. faecalis	Fwd: CACCTGAAGAAACAGGC Rev: ATGGCTACTTCAATTTCACG	F(x)= -3.472x+35.447	475 bp	94.1 %	0.999	6	*E. faecalis* ATCC51299	(Depardieu et al., 2004)
P. aeruginosa	Fwd: AGCGTTCGTCCTGCACAAGT Rev: TCCACCATGCTCAGGGAGAT	F(x)= -3.282x+35.276	81 bp	10.,7 %	0.999	3	*P. aeruginosa* DSM1117	(Clifford et al., 2012)
K. pneumoniae	Fwd: ACGGCCGAATATGACGAATTC Rev: AGAGTGATCTGCTCATGAA	F(x)= -3.387x+38.844	68 bp	97.4 %	0.998	18	*K. pneumoniae* DSM30104	(Clifford et al. 2012)
A. baumannii	Fwd: GTTGTGGCTTTAGGTTTATTATACG Rev: AAGTTACTCGACGCAATTCG	F(x)= -3.380x+35.679	94 bp	97.6 %	1.000	31	*A. baumannii* DSM30007	(Clifford et al. 2012)
E. coli	Fwd: GCATCGTGACCACCTTGA Rev: CAGCGTGGTGGCAAAA	F(x)= -3.361x+35.797	59 bp	98.4 %	0.994	4	*E. coli* DSM1103	(Clifford et al. 2012)
Antibiotic resistance genes								
*erm*B	Fwd: TGAATCGAGACTTGAGTGTGCAA Rev: GGATTCTACAAGCGTACCTT	F(x)=-3.328x+35.901	71 bp	100 %	1.000	16	*S. hyointestinalis* DSM20770	(Alexander et al., 2015)

Target	Primer sequence	Equation of the calibration curve	Amplicon size	efficiency	R^2	LOD	Control strain	reference
*Intl*1	Fwd: GCCTTGATGTTACCCGAGAG Rev: GATCGGTCGAATGCGTGT	F(x)= -3.472x+34.720	196 bp	94.1 %	1.000	126	*E. coli* pNORM	(Rocha et al. 2018)
*tet*M	Fwd: GGTTTCTCTTGGATACTTAAATCAATC Rev: CCAACCATAAATCCTTGTTCRC	F(x)=-3.424x+38.747	88 bp	95.9 %	0.998	4	*E. coli* DH5α	(Peak et al. 2007)
*bla*TEM	Fwd: TTCCTGTTTTTGCTCACCCAG Rev: CTCAAGGATCTTACCGCTGTTG	F(x)=-3.303x+38.559	112 bp	100.8 %	0.999	80	*E. coli* pNORM	(Rocha et al. 2018)
*sul*1	Fwd: CGCACCGGAAACATCGCTGCAC Rev: TGAAGTTCCGCCGCAAGGCTCG	F(x) -3,.87x+39.802	161 bp	97.6 %	0.999	80	*E. coli* pNORM	(Rocha et al. 2018)
*bla*CTX-M	Fwd: CGCTTTGCGATGTGCAG Rev: ACCGCGATATCGTTGGT	F(x)= -3.504x+34.255	551 bp	92.9 %	1.000	93	*E. coli* pNORM	(Rocha et al. 2018)
*bla*CTX-M-32	Fwd: CGTCACGCTGTTGTTAGGAA Rev: CGCTCATCAGCACGATAAAG	F(x)= -3.517x+37.800	155 bp	92.5 %	1.000	235	*E. coli* pNORM	(Rocha et al. 2018)
*bla*OXA-48	Fwd: TGTTTTTGGTGGCATCGAT Rev: GTAAMRATGCTTGGTTCGC	F(x)= -3.540x+36.913	177 bp	91.6 %	0.998	92	*K. pneumoniae* TGH Isolate 2	(Monteiro et al. 2012)
*van*A	Fwd: TCTGCAATAGAGATAGCCGC Rev: GGAGTAGCTATCCCAGCATT	F(x)= -3.541x+33.078	376 bp	91.6 %	1.000	43	*E. faecium* B7641 vanA	(Klein et al. 1998)
*mec*A	Fwd: CGCAACGTTCAATTTAATTTTGTTAA Rev: TGGTCTTTCTGCATTCCTGGA	F(x)=-3,327x+34.887	91 bp	99.8 %	1.000	11	*S. Aureus* A1	(Volkmann et al. 2004)
mcr-1	Fwd: GGGCCTGCGTATTTTAAGCG Rev: CATAGGCATTGCTGTGCGTC	F(x)=-3.386x+35.349	183 bp	97.4 %	0.999	8	*E. coli* NRZ-14408	(Hembach et al. 2017)
*bla*NDM	Fwd: TTGGCCTTGCTGTCCTTG Rev: ACACCAGTGACAATATCACCG	F(x)= -3.293x+35.877	82 bp	101.2 %	0.999	66	*K. pneumoniae* ATCC BAA-2146	(Monteiro et al. 2012)

Target	Primer sequence	Equation of the calibration curve	Amplicon size	efficiency	R^2	LOD	Control strain	reference
House keeping gene								
16S rDNA	Fwd: TCCTACGGGAGGCAGCAGT Rev: ATTACCGCGGCTGCTGG	F(x)= -3.405x+35.350	195bp	95.5%	0.997		*E. coli* pNORM	Hembach et al. 2017)

Table SA 2: Water sample getting from poultry slaughterhouse. Abundance of facultative pathogenic bacteria (A), abundance of "commonly occurring resistance genes" (B), abundance of "intermediately occurring resistance genes" (C), and abundance of "rarely occurring resistance genes" (D). The data from each sampling campaign are listed together with the standard deviations SD. LOD: Limit of of detection.

A)

Targets (ESKAPE group) Cell equivalents per 100ml								
	Campaign date	**Waste water sources**	*Enterococcus spp.*	*E. faecalis*	*P. aeruginosa*	*K. pneumoniae*	*A. baumannii*	*E. coli*
Poultry slaughterhouse	**11.07.2022**	**Raw sewage**	2.2E+06	1.3E+04	1.5E+04	1.6E+03	2.7E+07	1.6E+08
		Biological treatment	1.1E+01	<LOD	2.6E+01	<LOD	4.3E+02	4.6E+03
		Ozonation effluent	<LOD	<LOD	<LOD	<LOD	<LOD	<LOD
	18.07.2022	**Raw sewage**	1.6E+07	2.5E+05	5.8E+03	3.6E+03	8.2E+05	2.0E+08
		Biological treatment	<LOD	<LOD	1.2E+02	<LOD	4.6E+02	1.4E+04
		Ozonation effluent	7.2E+00	<LOD	<LOD	<LOD	<LOD	1.4E+03
	Average value	**Raw sewage**	9.3E+06	1.3E+05	1.0E+04	2.6E+03	1.4E+07	1.8E+08
		Biological treatment	5.5E+00	<LOD	7.3E+01	<LOD	4.4E+02	9.1E+03
		Ozonation effluent	3.6E+00	<LOD	<LOD	<LOD	<LOD	6.8E+02

B)

Targets (Commonly occuring resistance genes) Cell equivalents per 100ml								
	Campaign date	**Waste water sources**	*ermB*	*IntI1*	*tetM*	*blaTEM*	*sul1*	*16S*
Poultry slaughterhouse	**11.07.2022**	**Raw sewage**	3.8E+07	1.0E+08	1.2E+08	2.9E+08	5.1E+08	2.1E+11
		Biological treatment	1.1E+01	5.1E+05	2.4E+03	8.4E+04	2.9E+06	1.4E+08
		Ozonation effluent	<LOD	1.4E+04	<LOD	6.5E+03	2.4E+04	9.7E+06
	18.07.2022	**Raw sewage**	4.1E+06	1.2E+08	6.6E+07	4.7E+08	2.1E+08	8.8E+09
		Biological treatment	2.3E+01	1.6E+06	2.1E+03	5.1E+04	1.3E+07	1.6E+08
		Ozonation effluent	<LOD	6.7E+04	3.4E+02	1.8E+04	1.1E+05	2.6E+07
	Average value	**Raw sewage**	2.1E+07	1.1E+08	9.1E+07	3.8E+08	3.6E+08	1.1E+11
		Biological treatment	1.7E+01	1.0E+06	2.3E+03	6.8E+04	8.0E+06	1.5E+08
		Ozonation effluent	<LOD	4.0E+04	1.7E+02	1.2E+04	6.5E+04	1.8E+07

C)

Targets (Intermediately occuring resistance genes)

Cell equivalents per 100ml

	Campaign date	Waste water sources	*blaCTX-M*	*blaCTX-M32*	*blaOXA-48*	*blaCMY-2*
Poultry slaughterhouse	**11.07.2022**	**Raw sewage**	3.1E+05	3.3E+06	8.5E+03	8.0E+05
		Biological treatment	7.8E+01	2.4E+04	3.0E+01	2.0E+01
		Ozonation effluent	9.4E+00	1.9E+03	<LOD	<LOD
	18.07.2022	**Raw sewage**	1.2E+06	1.2E+07	2.9E+05	1.5E+06
		Biological treatment	8.8E+00	8.2E+03	9.2E+01	<LOD
		Ozonation effluent	<LOD	2.3E+03	<LOD	1.4E+02
	Average value	**Raw sewage**	7.3E+05	7.8E+06	1.5E+05	1.2E+06
		Biological treatment	4.3E+01	1.6E+04	6.1E+01	7.7E+01
		Ozonation effluent	4.7E+00	2.1E+03	<LOD	6.9E+01

D)

Targets (Rarely occuring resistance genes)

Cell equivalents per 100ml

	Campaign date	Waste water sources	*blaVIM*	*vanA*	*mecA*	*mcr-1*	*blaNDM*
Poultry slaughterhouse	11.07.2022	Raw sewage	<LOD	2.2E+05	3.4E+05	1.8E+05	4.7E+02
		Biological treatment	<LOD	<LOD	2.7E+02	<LOD	1.2E+01
		Ozonation effluent	<LOD	<LOD	<LOD	<LOD	1.7E+01
	18.07.2022	Raw sewage	<LOD	2.2E+03	4.1E+04	3.3E+05	5.5E+01
		Biological treatment	<LOD	<LOD	<LOD	<LOD	1.8E+01
		Ozonation effluent	<LOD	<LOD	<LOD	<LOD	<LOD
	Average value	Raw sewage	<LOD	1.1E+05	1.9E+05	2.6E+05	2.6E+02
		Biological treatment	<LOD	<LOD	1.4E+02	<LOD	1.5E+01
		Ozonation effluent	<LOD	<LOD	<LOD	<LOD	8.6E+00

Table SA 3: Water sample getting from pig slaughterhouse. Abundance of facultative pathogenic bacteria (A), abundance of commonly occurring resistance genes (B), abundance of intermediately occurring resistance genes (C), and abundance of rarely occurring resistance genes (D). The data from each sampling campaign are listed together with the standard deviations SD. LOD: Limit of detection.

A)

			Targets (ESKAPE group)					
			Cell equivalents per 100ml					
	Campaign date	Waste water sources	*Enterococcus spp.*	*E. faecalis*	*P. aeruginosa*	*K. pneumoniae*	*A. baumannii*	*E. coli*
Pig slaughterhouse	19.10.2022	Raw water	4.6E+06	1.2E+04	1.6E+02	<LOD	1.9E+05	1.5E+07
		Biological treatment	9.8E+02	<LOD	<LOD	<LOD	<LOD	3.7E+04
	03.11.2022	Raw water	1.1E+07	1.1E+04	2.1E+04	1.9E+03	8.6E+06	7.5E+08
		Biological treatment	2.9E+01	<LOD	<LOD	<LOD	3.5E+02	3.7E+04
	Average value	Raw water	7.9E+06	1.1E+04	1.0E+04	9.3E+02	4.4E+06	3.8E+08
		Biological treatment	5.0E+02	<LOD	<LOD	<LOD	1.8E+02	3.7E+04

B)

			Targets (Commonly occuring resistance genes)					
			Cell equivalents per 100ml					
	Campaign date	Waste water sources	*ermB*	*IntI1*	*tetM*	*blaTEM*	*sul1*	*16S*
Pig slaughterhouse	19.10.2022	Raw water	1.6E+06	2.9E+07	2.5E+08	2.4E+07	1.4E+08	1.3E+11
		Biological treatment	7.0E+01	2.7E+06	2.7E+04	3.5E+04	6.7E+06	3.1E+08
	03.11.2022	Raw water	1.4E+07	3.6E+08	1.3E+09	4.0E+08	1.5E+09	1.7E+12
		Biological treatment	9.4E+00	2.1E+06	1.2E+04	4.9E+04	9.5E+06	3.2E+08
	Average value	Raw water	7.6E+06	1.9E+08	8.0E+08	2.1E+08	8.4E+08	9.4E+11
		Biological treatment	4.0E+01	2.4E+06	2.0E+04	4.2E+04	8.1E+06	3.2E+08

C)

Targets (Intermediately occuring resistance genes)

Cell equivalents per 100ml

	Campaign date	Waste water sources	*blaCTX-M*	*blaCTX-M32*	*blaOXA-48*	*blaCMY-2*
Pig slaughterhouse	**19.10.2022**	**Raw water**	3.4E+03	9.1E+04	8.4E+06	2.2E+05
		Biological treatment	1.6E+01	2.5E+03	1.9E+03	8.7E+01
	03.11.2022	**Raw water**	2.0E+05	2.5E+06	7.1E+07	6.1E+05
		Biological treatment	1.9E+01	2.8E+03	7.3E+03	4.8E+04
	Average value	**Raw water**	1.0E+05	1.3E+06	4.0E+07	4.2E+05
		Biological treatment	1.7E+01	2.6E+03	4.6E+03	2.4E+04

D)

Targets (Rarely occuring resistance genes)

Cell equivalents per 100ml

	Campaign date	Waste water sources	*blaVIM*	*vanA*	*mecA*	*mcr-1*	*blaNDM*
Pig slaughterhouse	**19.10.2022**	**Raw water**	<LOD	1.2E+03	9.4E+03	6.2E+03	1.3E+03
		Biological treatment	2.2E+01	<LOD	<LOD	<LOD	8.8E+01
	03.11.2022	**Raw water**	<LOD	5.9E+04	<LOD	2.4E+05	2.1E+03
		Biological treatment	<LOD	9.0E+00	<LOD	<LOD	1.4E+01
	Average value	**Raw water**	<LOD	3.0E+04	4.7E+03	1.2E+05	1.7E+03
		Biological treatment	1.1E+01	4.5E+00	<LOD	<LOD	5.1E+01

Table SA 4: Radiant intensity data were collected with a calibrated spectrophotometer (FLAME-S-XR1-ES, with optical fibre QP400-2-SR-BX; OceanInsight, Ostfildern, Germany) from the LED light source inside the incubator. Due to the fixed light emission of the LEDs, different light intensities, high and low, were performed by changing the light source – reaction vial distance.

Irradiation	High intensity	Low intensity
Radiant intensity [W/cm²] corresponds with J/s*cm^2	8.33E-02	5.43E-02
Irradiation time [h]	Time dependent energy input [J/cm²]	
1	300	196
2	600	392
3	900	588
4	1200	784

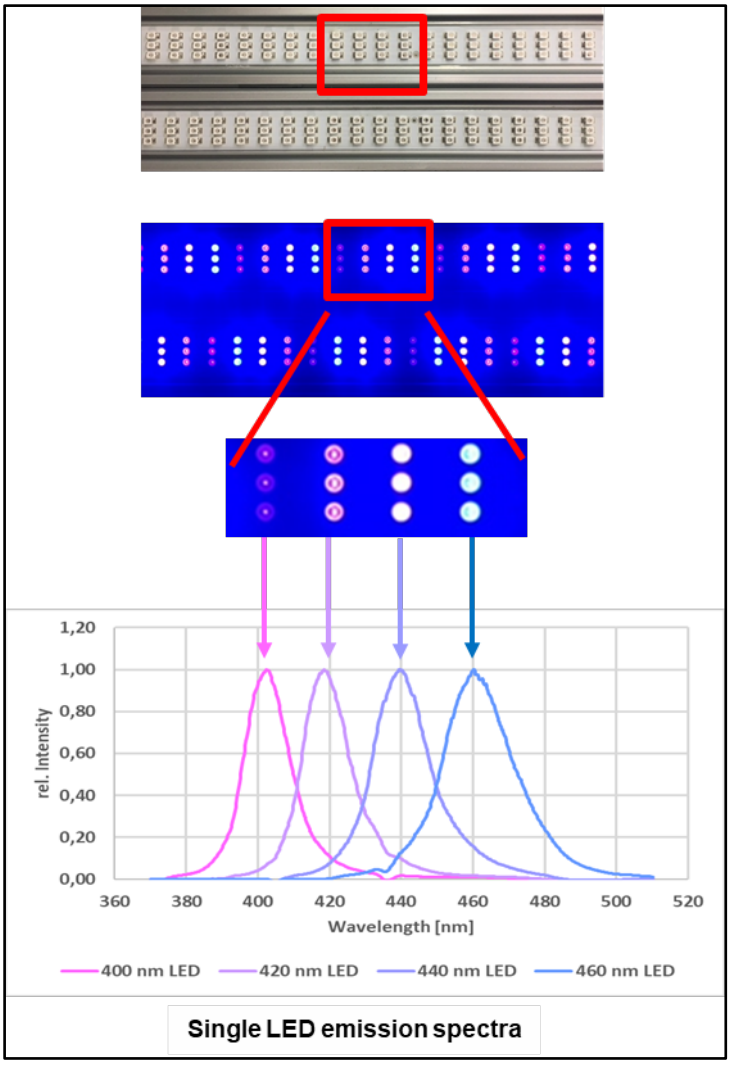

Figure SA 1: Exemplary: normalized entire emission spectrum of the LED bar (top); normalized emission spectra of each LED type on LED bar (bottom). A qualtitative characterization of the emitted spectrum was done with a spectrometer (FLAME-S-XR1-ES, OceanInsight, Ostfildern, Germany).

3 Inactivating facultative pathogen bacteria and antibiotic resistance genes in wastewater using blue light irradiation combined with a photosensitizer and hydrogen peroxide

Published as: *Cong, X., Schwermer, C. U., Krolla, P., & Schwartz, T. (2025). Inactivating facultative pathogen bacteria and antibiotic resistance genes in wastewater using blue light irradiation combined with a photosensitizer and hydrogen peroxide. Science of the Total Environment, 974, 179208.*

3.1 Introduction

The increasing prevalence of AMR in clinical, veterinary, and environmental contexts poses a serious public health threat (Ahmed et al., 2024). Currently, the spread of antibiotic resistance and antibiotic residues in the aquatic environment is unregulated, with no limit values and no indicator systems for their detection exist, and significant knowledge gaps about antibiotic resistance, its evolution, dissemination, and associated health risks. In this context, the German BMBF-funded project HyReKa 'Hygienic-medical relevance and control of antibiotic-resistant pathogens in clinical, agricultural, and municipal wastewater and their significance in raw water' was carried out (https://www.ifg.kit.edu/downloads/HyReKA%20Abschlussbericht%20Oktober%202020.pdf).

This project compared conventional disinfection techniques like membrane filtration, ozone treatment, and UV irradiation for wastewater effluent decontamination targeting clinically FPB and ARGs by cultivation and qPCR. The findings highlighted the need for innovative decentral measures for wastewater decontamination.

The propose EU urban wastewater treatment directive (https://eur-lex.europa.eu/legal-content/EN/TXT/?uri=CELEX%3A52022PC0541), emphasizes the importance of antibiotic resistance within the European 'One Health Action Plan'. The directive, referencing the World Health Organisation (WHO), identifies wastewater as an important source of antibiotic agents, their metabolites, ARB, and resistance genes. Consequently, mandatory monitoring of antibiotic resistance in municipal wastewater and initiation of appropriate regulations are deemed necessary. Hence, infection management should prioritize preventing the dissemination and spread of ARB carrying clinically relevant ARGs discharged from critical sources like hospitals, nursing homes, and industrial livestock

farming (Sib et al., 2019; WHO, 2019). The misuse of antibiotics continues to drive the selection of antibiotic resistance selection and evolution in pathogenic bacteria, potentially leading to untreatable infections in the near future (O' Neil, 2014).

Hospitals are known as potent hotspots for the emergence and dissemination of AMR and associated gene pools through clinic-associated pathways (Sib et al., 2019, 2020), while WWTPs serve as a final control point for discharging wastewater-born ARGs into receiving aquatic environments. Decentralized upstream monitoring of wastewater from selected urban areas has been conducted earlier (Alexander et al., 2020; Hembach et al., 2017). Local wastewater treatment at hospitals was initialized at a few hospitals in Germany, Switzerland, and Netherland. Pharmafilter is one commercially available system, while other more compact solutions, that often are based on advanced treatment principles, such as membrane filtration, ozonation, and UV-treatment are in research and pilot-stage. Besides hospitals, retirement homes and slaughterhouses have been identified as significant sources of ARG discharges, often exhibiting higher levels than residential sewer systems (Alexander et al., 2020; Cong et al., 2023). Conventional treatment methods have proven ineffectual in eradicating ARB and ARGs. Primary treatment achieves only modest reductions (ARB: 0–1 log units, ARGs: 0.09–0.55 log units) (Hazra & Durso, 2022), while suboptimal sedimentation exacerbates their downstream dissemination. Moreover, secondary processes such as activated sludge may trap ARGs and ARB, inadvertently reintroducing them into environmental settings (J. Wang & and Chen, 2022). Accordingly, the deployment of innovative advanced oxidative processes, particularly those light-based technologies are essential. Light-based wastewater disinfection employs various light sources to inactivate pathogens. Among these, UV disinfection remains predominant, inflicting irreparable damage to microbial nucleic acids without leaving chemical residues (Hazra et al., 2024). Emerging LED systems offer enhanced energy efficiency and durability (MacIsaac et al., 2024), while photocatalytic disinfection, which strengthen UV light with catalysts like titanium dioxide, being responsible for the decomposition of contaminants and the eradication of pathogens (Cong et al., 2024). Ozone can be generated by UV light and has strong disinfectant properties. It is often used in combination with other processes to increase the efficiency of disinfection. Besides these technologies, H_2O_2 is also a potent oxidant widely used in disinfection due to its ability to enhance antimicrobial effects while producing fewer by-products (Garcez et al., 2011; Herraiz-Carboné et al., 2021).

Our research focuses on the decentralized implementation of innovative, modular disinfection technologies. such as aBL irradiation combined with photosensitizers (e.g.,

porphyrins) or oxidative agents (H_2O_2), to effectively curb the spread of AMR (Cong et al., 2023).

Treating wastewater at AMR hotspots can prevent contamination of larger wastewaters volumes downstream, thus, unburden WWTPs in the load of these contaminants. This strategy would support a more cost-effective treatment compared to central actions at WWTPs alone.

The novel application of aBL irradiation in the 400-470 nm range offers a sophisticated, strategy to combat AMR (Cong et al., 2023; Woźniak & Grinholc, 2022). aBL disinfection is based on the activation of endogen photosensitizers within bacterial cells by specific wavelengths of blue light. This activation triggers the production of ROS, which are highly cytotoxic and lead to bacterial cell damage and death (Leanse et al., 2022; Ngo et al., 2023; Wainwright, 1998). The effectiveness of aBL treatment can vary significantly with changes in wavelength and dose (S. Huang et al., 2023). Endogenous porphyrins, critical chromophores in bacterial cells, act as inherent photosensitizers essential for photoinactivation (Maclean et al., 2009). We recently demonstrated that aBL in a static photoreactor holds significant potential for inactivating health-relevant FPB in polluted wastewater (Cong et al., 2023). In extension to the static photoreactor with small volumes of wastewater samples, this study is working with a continuous flow photoreactor using larger volumes of real WWTP effluent wastewater comparing the inactivation effectiveness for FPB and ARGs in a laboratory scaled reactor system. Here, three distinct LED wavelengths (i.e., 405, 420, and 460 nm) to assess their different inactivation effectiveness. The investigation used culturing and molecular biology techniques to evaluate the impact of aBL irradiation. The photodynamic porphyrin TMPyP (5,10,15,20-Tetrakis-(*N*-methyl-4-pyridyl)21,23-porphyrintetratosylate) (Figure SB1) and the oxidizing agents H_2O_2 were added to enhance the aBL irradation effectiveness. We also aimed to confirm that bacterial DNA damage induced by aBL irradiation plus TMPyP or H_2O_2. Understanding the extent of DNA lesion formation is important for elucidating aBL inactivation mechanisms. DNA damages in wastewater irradiated with aBL were quantified using the long-run real-time PCR-based method (LORD-Q). Semi-long amplicons of around 1.5-2 kb can also enhanced sensitivity for detecting DNA damage (Zhu & Coffman, 2017).

3.2 Material & Methods

3.2.1 Sampling and sample preparation

The wastewater effluent was collected biweekly from the local WWTP on the Karlsruhe Institute of Technology (KIT) campus in Karlsruhe Germany. It primarily consisted of

wastewater from scientific research institutes, serving approximately 3,300 individuals, including international scientists and students present during the week. The WWTP processes approximately 450 m^3 wastewater daily through a combination of conventional physical-chemical and biological treatment methods, including adsorption, precipitation, flocculation, and oxidation. Some chemical and physical average data collected are presented in Table SB1. The treated WWTP effluent is discharged into the River Rhine.

Due to its unique composition, WWTP effluent required comprehensive analysis, as wastewater from scientific institutes can pose potential risks to the environment. For each aBL treatment (i.e., (i) aBL alone, (ii) aBL combined with TMPyP, and (iii) aBL combined with H_2O_2) at each of the three wavelengths 405 nm, 420 nm, 460 nm, respectively, nine samples were collected from the WWTP, resulting in nine sampling campaigns per trial. The study was conducted over three independent trials (n=3). 4 liters of effluent was collected from the WWTP at each campaign. For each aBL treatment, a minimum of three independent trials were conducted to ensure the reliability and reproducibility of the results. The collected wastewater was pumped into the photoreactor (Figure 3.1; Figure SB2) using a peristaltic pump (1 L min^{-1}). The wastewater samples underwent a circulation of 4 h within the aBL reactor, resulting in an absolute aBL irradiation of 26 minutes by the LED lamp passing the photo-chamber. An aliquot of 0.7 L of aBL-treated samples were taken at regular intervals to assess the effectiveness of the aBL irradiation. Test were carried out at one of the three wavelengths 405 nm, 420 nm, or 460 nm, respectively. We further investigated the shading effects caused by the particulate matter contained in the WWTP treated effluent. In theory particles may block aBL irradiation, creating areas without exposed to the rays, and then reducing the effectiveness of ROS production as microorganisms in these shadowed areas may not exposed to the aBL and therefore may not be inactivated. However, a relatively low suspended solids content of <0.1 mg L^{-1} measured in the KIT WWTP treated effluent implies that this shading effect on our aBL irradiation tests was marginal or absent.

The aBL treated water samples were subsequently stored in darkness at room temperature to inhibit any additional photoreactive transformations. Aliquots of 150 mL from each sample were filtered through polycarbonate membranes (PC) with 47 mm diameter and 0.2 µm pore size (Whatman Nucleopore Track-Etched Membranes, Sigma-Aldrich, Munich, Germany). Following filtration, the membranes were treated with 20 µM of PMA for differentiating living from dead bacteria. PMA is able to enter the bacterial cell reaching the chromosomal and extrachromosomal nucleic acid due to the loss of cellular membrane integrity of injured/dead bacteria (Cong et al., 2023; Nocker et al., 2018). This modified DNA is blocked for subsequent qPCR analyses. The procedure was completed

by incubating the PMA-treated and filtered biomass in a dark environment for 10 minutes to prevent any photodegradation of the PMA. Then the filtered biomass on membranes were exposed to the PhAST Blue Photo-Activation System (GenIUL, Barcelona, Spain) at maximum intensity for a duration of 15 minutes for cross-linking of PMA with the DNA of the dead/injured bacterial cells.

3.2.2 Continuous flow aBL photoreactor

The continuous flow photoreactor, as described below, is initially designed as a laboratory system to test its inactivation efficiency. Decentralized use with up-scaling is planned for subsequent studies once the appropriate operating parameters have been determined.

The continuous flow aBL reactor experimental setup used for wastewater irradiation comprised of a sample tank, a peristaltic pump, a reactor cabinet (including one LED lamp with one wavelength), and a LED power supply. Additionally, a waste container was utilized for storing the treated wastewater, while 70% isopropanol was employed for disinfecting the setup (Figure 3.1). The aBL photoreaction chamber featured a dual glass cylinder setup, comprising an outer and an inner glass cylinder. Into the inner glass, a LED lamp was inserted centrally, whereby the flow of the test water was circulated upwards around the LED lamp. A peristaltic pump for transferring wastewater from the sample reservoir to the reactor cabinet, an LED cooling device to regulate system temperature, and a power supply for adjusting LED intensity.

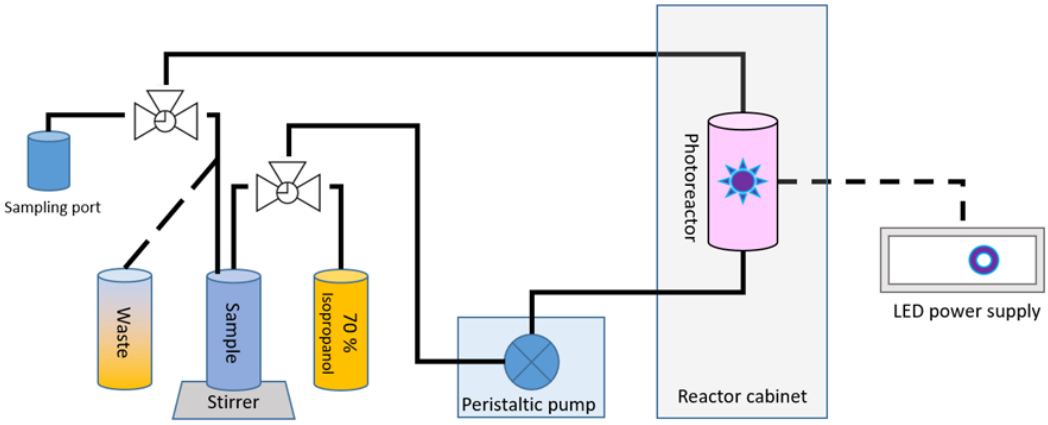

Figure 3.1: The experimental setup used in the water irradiation process using a continuous flow aBL photoreactor.

Figure 3.2 shows the calculated duration time of irradiation in the LED based reaction chamber's area (highlighted in blue), which spans 26 seconds by a given flow rate of 1 L min^{-1} dictated by the pump. The total volume of the chamber subjected to irradiation was 0.43 L. Within the inner cylinder, a LED mounting base equipped with four surfaces accommodates the LEDs. This base was hosted 12 LEDs arrayed in a row on each of its surfaces. The LED configuration delivered specific light intensities for aBL treatments at various wavelengths, where 420, 405, and 460 nm achieved 2,758, 3,282, and 3,486 W m^{-2}, respectively. The time dependent energy input corresponds with 430 J cm^{-2} at 420 nm, 512 J cm^{-2} at 405 nm, and 544 J cm^{-2} at 460 nm for 26 min. The energy input for 13 min irradiation was calculated with 215 J cm^{-2} at 420 nm, 256 J cm^{-2} at 405 nm, and 272 J cm^{-2} at 460 nm. Finally, the energy input for 6.5 min irradiation was 108 J cm^{-2} at 420 nm, 128 J cm^{-2} at 405 nm, and 136 J cm^{-2} at 460 nm. Based on a specified volume of 4 L of WWTP effluent being fed into the photoreactor without any pretreatment, the calculated entire irradiation time of the total volume of water sample in the photo reactor chamber for the residence time of (Δt = t1-t0) 26 minutes at a flow rate of 1 L min^{-1} for 4 h. The time points T0, T1, T2, and T4, corresponded to the untreated sample, one-hour treatment, two-hour treatment, and four-hour treatment, respectively, thus reflecting operation times. However, the total irradiation times differed with 6.5 minutes for T1, 13 minutes for T2, and 26 minutes for T4.

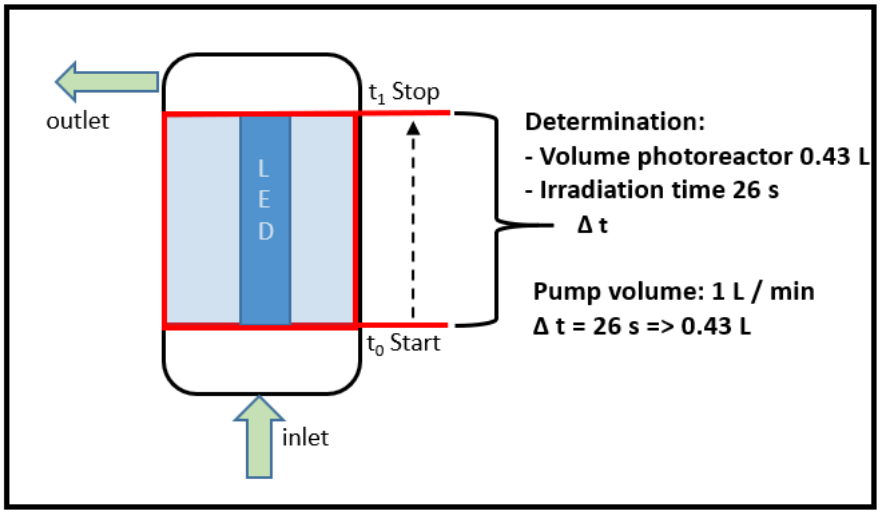

Figure 3.2: The schematic diagram of the reactor illustrates a total volume of 0.43 L and a retention of irradiation time of (Δt = t1-t0) 26 sec for the wastewater passing through the LED-irradiated volume at a flow rate of 1 L min^{-1}.

3.2.3 DNA extraction for molecular biological analyses

DNA was extracted using the FastDNA^{TM} Spin Kit for Soil (MP Biomedicals, Santa Ana, USA) and the FASTPREP® device (MP Biomedicals, Santa Ana, USA). For mechanical cell disruption, the filtered biomass on membranes were placed in the Lysing Matrix E tube and treated according to the manufacturer´s protocol. Proteins were separated by centrifugation and precipitation, and the DNA was finally purified by attachment to a silica matrix. The concentration of extracted DNA was measured using the NanoDrop (ND-1000, PEQLAB Biotechnologie GmbH, Germany) and the Quant-iTTM PicoGreen® dsDNA Assay Kit (Thermo Fisher Scientific, Nidderau, Germany).

3.2.4 Quantitative PCR (qPCR) analysis

SYBR Green qPCR assays were performed using a Bio-Rad Cycle CFX96 (CFX96 TouchTM Deep Well Real-Time PCR Detection System, Bio-Rad, Munich, Germany), and analysis was performed using the manufacturer's software (Bio-Rad CFX Manager Software). Reactions were performed in volumes of 20 µL containing 10 µL Maxima SYBR Green/ROX qPCR Master Mix (2×) (Thermo Scientific Nidderau, Germany), 7.4 µL nuclease-free water (Ambion, Life technologies, Karlsbad, Germany), 0.8 µL primer forward (10 µM), 0.8 µL primer reverse (10 µM) and 1 µL template DNA. In the denaturation phase, double-stranded DNA was converted into single strands by heating at a high temperature (about 95 °C) for 10 min. This was followed by 40 cycles of 15 s at 95 °C and 60 s at 60 °C. The melting curves were recorded by increasing the temperature from 60 °C to 95 °C (1 °C every 10 s) to assess the specificity of the application. The clinical relevance of the investigated ARGs and FPB are shown in Table 3.1. For each target (ARGs or FPB), the primer sequences used are listed in Table SB2. Information on the characteristics and quality of the qPCR systems used for the taxonomic genes and the ARGs is given in Table SB2. Cq (quantification of cycle) stands for Ct value and refers to the number of times a machine must copy a piece of genetic material before it can be detected in a PCR test. The value represents the amount of genetic material in a particular sample at a specific point in time. In general, the lower the Cq value, the higher the load that is found in the sample, while the higher the Cq value, the lower the load is. previous experience (Alexander et al., 2020; Cong et al., 2023; Hembach et al., 2022). The different ARG clusters categorize ARGs into common, moderate and rare gene targets and are based on previous experience (Alexander et al., 2020; Cong et al., 2023; Hembach et al., 2022).

3.2.5 The photosensitizer porphyrin TMPyP and the oxidative agent H_2O_2

The photosensitizer porphyrin TMPyP (5,10,15,20-Tetrakis-(*N*-methyl-4-pyridyl)21,23-porphyrintetratosylate) was obtained from Sigma-Aldrich in Darmstadt, Germany, and its structure is depicted in (Figure SB1). The 1×10^{-3} M TMPyP stock solution was preserved at a storage temperature of 4°C. For experimental purposes, a higher dilution, 1×10^{-6} M, was added to the water samples. The concentrations used for TMPyP are based on studies that have proven to be particularly effective in reducing antibiotic resistance (Cong et al., 2023). The molecular structure of TMPyP is characterized by a planar, tetracationic structure, centered around a porphyrin ring enabling porphyrin molecules to absorb light across a specific spectrum and making them effective in photodynamic applications. Additionally, 1 mM H_2O_2 was added to the water samples to explore the inactivation potential for ARG and FPB during aBL treatment.

1 mM H_2O_2 was used which is correlated with the optimal concentration used in the study (Truong et al., 2020). The higher concentration of H_2O_2 can cause scavenging of $OH^{\bullet}$ by H_2O_2. In principle, it has been shown that both TMPyP (1×10^{-6} M) and H_2O_2 (1 mM) has no antibacterial effects without blue light irradiation (data not shown). Only irradiation with blue light of the specified wavelengths showed an additional antibacterial capacity by the two components.

3.2.6 Cultivation of facultative pathogenic bacteria

Before (untreated wastewater) and after (treated wastewater) aBL irradiation, 50 mL of each sample were filtered through a nitrocellulose membrane (0.45 µm, GE Healthcare Life Sciences, Solingen, Germany) in preparation for cultivation. Selective agar plates were assessed by cultivation for the efficiency of aBL treatment. Four different agar plates were used in this investigation: CHROMagar™ ESBL, Enterococci agar plates, Pseudomonas agar plates, and CHROMagar™ Acinetobacter. CHROMagar™ ESBL allows enrichment of ESBL producing bacteria, enzymes confer resistance to a wide range of beta-lactam antibiotics, including penicillins and cephalosporins. Enterococci agar plates are used for the selective isolation and identification of *Enterococcus* species from clinical and environmental samples. Pseudomonas agar plates are used for the selective isolation and identification of *Pseudomonas* species, particularly *Pseudomonas aeruginosa*, from clinical and environmental samples. CHROMagar™ Acinetobacter are used to selectively isolate and identify *Acinetobacter* species. The CFU were quantified for 50 mL water sample volumes after overnight incubation. The fold change in bacterial count was calculated by taking the ratio of the bacterial count after treatment (C_t) to the

initial bacterial count (C_0), expressed as C_t/C_0. A fold change of 1 means no change, greater than 1 indicates an increase, and less than 1 indicates a decrease.

3.2.7 DNA damage analysis by qPCR

The methodology involves amplifying genomic DNA extracted from aBL-irradiated samples (aBL treatment alone, aBL treatment with TMPyP, and aBL treatment with H_2O_2) using “short” and “long” qPCR reactions. We used with approximately 1,500 bp long amplicons to balance sensitivity and efficiency in quantifying DNA damage. The resulting Cq values and the amplification efficiencies of the two reactions are calculated using the equation $E = [10^{-(1/slope)}-1]$. Correlation coefficients (R^2) are derived from standard curves generated by running qPCR reactions on serial dilutions of the samples. In the investigation of DNA damage, a diverse array of primer types, as specified in Table SB2, was utilized. The primer 27F, referred to as primer F_L, and BacUni-1387F, referred to as primer F_S, were each paired with the identical reverse primer BacUni-1492R, identified as primer R. This configuration facilitated the generation of both long and short amplicons. All qPCR reactions were executed in volumes of 20 µL, consistent with the established protocol for detecting target sequences through qPCR. For the elongation of sequences with approximately 1,500 base pairs in length, the cycling protocol commenced with a three-minute polymerase activation phase at 95°C, followed by 39 cycles of 15 seconds at 95°C, 20 seconds at 55°C, and 80 seconds at 72°C. Conversely, the amplification of shorter (approximately 100 base pairs) sequences, adhered to a similar initial step of three minutes at 95°C for polymerase activation, but was followed by 39 cycles of 15 seconds at 95°C, 20 seconds at 55°C, and 15 seconds at 72°C. The Cq values was automated via the Bio-Rad CFX Manager software, and the subsequent data analysis was conducted using Microsoft Excel. This method ensured precise and repeatable measurement of DNA amplification across varying experimental conditions. To quantify DNA lesions per 10 kb, the Cq values correlate to the number of target copies obtained from the experiments. Together with the amplification efficiencies of the two reactions and the amplicon lengths, were processed using the LORD-Q equation (Dannenmann et al., 2017).

3.2.8 Statistics

For statistical evaluation, the median cell equivalent from all sample collection campaigns was used to calculate p-values for the significance displayed in our figures. The statistical significance of the experimental data was rigorously evaluated using Analysis of Variance (ANOVA) tests, followed by Tukey's multiple comparisons analysis. The comparisons were

made between the control group, aBL treatment alone, and aBL treatment in conjunction with either TMPyP or H_2O_2. The outcomes of these analyses are reported as follows: non-significant (ns), *P≤0.5, **P≤0.05, ***P≤0.01. The median abundance of WWTP effluent was calculated by averaging the cell equivalents obtained from three sample trials. The Median Absolute Deviation (MAD) represents the statistical dispersion, and was calculated as

$$XY = (|x_i - \text{median}(x_i)|),$$

where x_i represents the cell equivalents of each individual data point in the dataset, and i denotes the index corresponding to each specific data point.

3.3 Results and Discussion

3.3.1 Reduction effectiveness of FPB in the aBL photoreactor determined by cultivation

The presence of FPB and ESBL producing bacteria was elucidated by culturing. Specifically, the Gram-positive bacteria *Enterococcus spp*. and Gram-negative *Acinetobacter spp*. and *Pseudomonas spp.* were selected for cultivation on selective media from untreated and treated wastewater samples with blue light and in combination with TMPyP or H_2O_2. Additionally, bacteria producing extended spectrum of beta-lactamases (ESBL) from the ESKAPE group were studied by cultivating experiments. The initial CFUs for *Enterococcus spp.*, *Acinetobacter spp.*, and ESBL agar plates were determined to be 1,326 ± 75, 837 ± 43, and 390 ± 82 CFUs per 100 mL, respectively. These values represent the mean results and standard deviations obtained from three independent trials.

As shown in Figure 3.3, a progressive reduction in CFU counts was observed from 0h (no treatment) to 4h (i.e. 26 min real aBL irradiation). This was observed for 405, 420, and 460 nm of aBL treatment, as well as in presence of TMPyP or H_2O_2 together with aBL irradiation. This trend was observed across all tested FPB, irrespective of the wavelengths applied. When evaluating the susceptibilities of these bacterial species, *Enterococcus spp.* (Figure 3.3a) exhibited higher sensitivity to aBL treatment than *Acinetobacter spp.*, *Pseudomonas spp*., and ESBL-producing bacteria. One-hour aBL irradiation, regardless of the wavelength, completely inhibited the growth of this Gram-positive bacterium *Enterococcus spp.*, indicating complete inactivation by aBL alone and when combined with TMPyP or H_2O_2 (Figure 3.3a). This increased sensitivity may be due to the absence of the

specific outer membrane in Gram-negative bacteria, making them more resistant to oxidative stress than Gram-positive bacteria (Maldonado-Carmona et al., 2022).

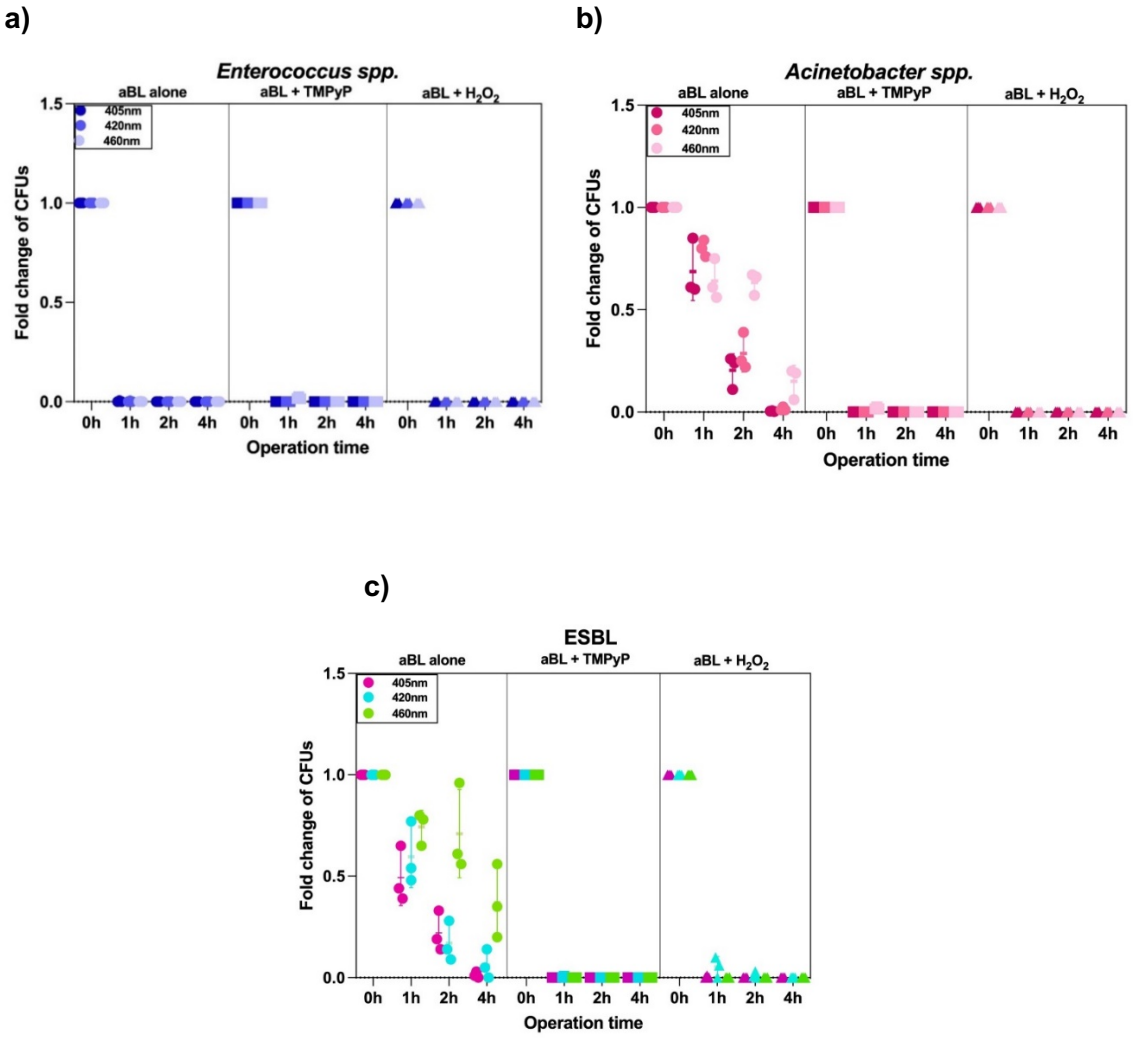

Figure 3.3: The fold change of CFU from subsequent (Ct) to initial (C0) concentration values at four time points (0h, 1h, 2h, 4h) following nine different aBL treatments, including aBL alone, aBL combined with H_2O_2, and aBL combined with TMPyP at three distinct wavelengths. In total, nine sampling campains were done. Each dot represents the results of an individual trial for each wastewater treatment condition (n=3).

For *Acinetobacter spp.* (Figure 3.3b) as well as for ESBL producing bacteria (Figure 3.3c), the combination of aBL with TMPyP or H_2O_2 demonstrated superior effectiveness in CFU reduction compared to aBL treatment alone, as evidenced by the complete absence of colonies on the specific agar plates after 4 h irradiation. Nevertheless, it became evident that the effectiveness of aBL treatment is dynamic and influenced by multiple factors beyond just wavelength (e.g. Gram-positive vs Gram-negative). However, its impact on

inactivating FPB becomes increasingly evident over time. *Pseudomonas spp*. count numbers were too high to quantify in all untreated wastewater samples, making fold change calculation impossible. However, aBL irradiation reduced CFUs. Compared to other pathogens, *Pseudomonas spp.* was less sensitivity to the treatment highlighting their high resilience compared to the other FPBs. In conclusion, aBL treatment combined with TMPyP or H_2O_2 enhanced the reduction of FPB and ESBL bacteria. Comparing the CFU reduction data 405 and 420 nm were slightly more effective compared to 460 nm after 1 hour of treatment. These differences disappeared in case of longer treatment times. This may be due to the higher photon energy of 405 nm and 420 nm aBL compared to 460 nm at the beginning of the treatment, when all intracellular involved structures are more or less intact (Enwemeka et al., 2021; S. Huang et al., 2023), which induces more ROS and increases oxidative stress potentially leading to more VBNC states in bacteria. It was shown, that more than 100 bacterial species have been found to enter a VBNC state under oxidative stress conditions (Ayrapetyan et al., 2018). Additionally, bacteria that are unable to withstand multiple stressors have also been shown to transition into the VBNC state (Idil et al., 2011; Barber, 2015). Hence, the VBNC state need to be analysed by living/dead staining in planed subsequent studies. It should be noted that cultivation experiments may be biased due to the limitations of cultivation methods in general. Therefore, incorporating molecular biology techniques was crucial to accurately assess bacterial viability and response to aBL treatments.

3.3.2 Reduction effectiveness of FPB and ARB during aBL irradiation as determined by qPCR.

3.3.2.1 FPB and ARGs abundances in WWTP effluent

The total bacterial load in the WWTP effluent, quantified via the eubacterial ribosomal 16S rDNA using qPCR, averaged 6.39×10^8 cell equivalents per 100 mL (Table 3.1). The *intI1* gene, coding for a transposon-based Class I integrase, serves as a specific marker for class 1 integrons and indicates the potential for HGT, was present at 1.79×10^6 gene copies per 100 mL. An increased gene transfer rate facilitated by the dissemination of *intI1*, may facilitate to its spread through the corresponding gene cassettes in mobile genetic elements.

Lower abundances for specific taxonomic gene markers were detected for the FPB of the ESKAPE group (Table 3.1): Detected species included enterococci (23S rDNA gene), *Pseudomonas aeruginosa* (*ecf*X gene), *Acinetobacter baumannii* (*sec*E gene), and *Escherichia coli* (*ycc*T gene) (Table 3.1). *E. coli,* detected using the *ycc*T was the dominant species with an average of 4.18×10^5 cell equivalents per 100 mL. *E. coli,* serving as a well-

known indicator for fecal contaminations. *Enterococci* were also abundant, with $4.18x10^3$ cell equivalents per 100 mL. *P. aeruginosa* and *A. baumannii* were detected in lower concentrations, with 1-2 logs per 100 mL. The abundance of ARGs was categorized into 'commonly detected genes' and 'intermediately detected genes' based on previous studies (Hembach et al., 2019) (Table 3.1). 'Commonly detected genes' include *erm*B (resistance to erytrhomicin in Gram positive bacteria like *Enterococcus*, *Staphylococcus*, and *Streptococcus*), *sul*1 (resistance to sulfonamides, often found in mobile genetic elements, such as plasmids, transposons, and integrons), *tet*M (tetracycline resistance, frequently detected in wastewater from hospitals, agricultural runoff, and residential areas), and bla_{TEM} (a beta-lactam resistance gene, commonly detected ESBL gene) (P. Gao et al., 2012; Sah and Hemalatha, 2015; Y. Wang et al., 2022; Wen et al., 2016). These genes exhibited cell equivalent concentrations ranging from 10^4 to 10^7 log units per 100 mL in the WWTP effluent making them suitable for assessing ARG inactivation effectiveness in wastewater treatment. 'Intermediately detected genes' include bla_{CTX-M}, $bla_{CTX-M32}$, bla_{OXA-48}, bla_{CMY-2}, and bla_{VIM}, which are beta-lactam resistance genes associated with FPB with two and three log level abundances. The colistin resistance gene *mcr-1,* carried by *Enterobacteriaceae* on transmissible plasmids, has previously been reported in municipal and husbandry WWTPs (Savin et al., 2021). We found *mcr-1* at low abundance, indicating its presence but at lower concentrations compared to other ARGs. Other critical ARGs, including *van*A, bla_{NDM}, and *mec*A were not detected in the WWTP effluent.

Our results imply high contamination of FPB from the ESKAPE group in WWTP effluent. ESKAPE group pathogens, amongst other health-concerning microorganisms of, are clinically important bacteria responsible for many community and hospital-acquired infections (Mathur et al., 2023). Even without direct inputs from clinical facilities, industry, or agriculture, critical FPB (Table 3.1, Figure 3.3) enter local wastewater, persist through and remain unaffected by most conventional treatment processes, and ultimately reach receiving water bodies. Our study suggests that the international community at the KIT campus contributes to the dissemination of a broad spectrum of ARGs and FPB to the KIT WWTP due to the incomplete effectiveness of the current wastewater treatment processes. Therefore, it is essential to consider implementing a supplementary quaternary treatment step for hygienization with advanced wastewater treatment methods, such as aBL-photo disinfection, and to evaluates its effectiveness.

Table 3.1: Categorization of various FPB and ARGs is based on their abundance, stated as median of cell equivalents per 100 mL (n=3), within the KIT WWTP.

	Targets	Median of cell equivalents per 100 mL	Median absolute deviation (MAD)
Eubacteria	**16S rDNA**	6.39E+08	1.72E+08
Facultative pathogenic bacteria (ESKAPE group)	***yccT (E. coli)***	4.18E+05	1.62E+05
	23S *(enterococci)*	4.18E+03	1.82E+03
	secE (A. baumannii)	2.02E+02	5.38E+00
	ecfX (P. aeruginosa)	9.34E+01	2.24E+01
Commonly detected	***sul*1**	3.54E+07	4.56E+06
	***Intl*1**	1.79E+06	4.02E+05
	***tet*M**	1.45E+05	6.49E+04
	***erm*B**	1.26E+05	1.88E+04
	bla_{TEM}	8.40E+04	2.06E+04
Intermediately detected	bla_{VIM}	3.67E+03	1.41E+03
	$bla_{CTX-M32}$	2.58E+03	1.51E+03
	bla_{OXA-48}	6.87E+02	5.44E+02
	bla_{CTX-M}	3.32E+02	2.12E+02
	bla_{CMY-2}	2.35E+02	8.33E+01
	***mcr*-1**	8.56E+01	5.85E+01

3.3.2.2 Effectiveness of aBL irradiation at different wavelength to inactivate FPB and ARG

The effectiveness of three aBL wavelengths in inactivating FPB and ARG in KIT WWTP effluent was evaluated (Table SB3). Among the detected FPB, enterococci demonstrated sensitivity to all three aBL wavelengths. Notably, treatment with 420 nm aBL achieved a maximum reduction of 2.6 log_{10} units (Figure 3.4a). Although the 405 nm aBL wavelength resulted in a comparatively lower reduction of enterococci, the bacteria remained susceptible to aBL treatment alone. This finding is further corroborated by results obtained through cultivation-based methods. For other Gram-negative bacteria, aBL treatment alone appears insufficient for effective inactivation (Figure 3.4a). *P. aeruginosa* exhibited a higher tolerance to aBL, showing no significant reduction in gene copy numbers after 4 hours of exposure, regardless of the wavelength. This observation aligns with the

cultivation-based results, further confirming the bacteria resistance to aBL treatment alone. When using aBL treatment alone for bacterial inactivation, the specific wavelength of aBL does not appear to be a critical factor in the removal of FPB. Instead, the intrinsic characteristics of the bacteria themselves may play a more significant role in determining their susceptibility to aBL treatment (i.e., Gram-positive vs Gram-negative bacteria). The incomplete disinfection may be due to insufficient irradiation during the 4-hour flow reactor experiment, which did not achieve high enough intracellular ROS concentrations to inactivate targeted FPB/ARGs.

Among the examined ARGs, the susceptibility to aBL treatment varied which might depend on the bacterial host carrying the gene under investigation. Frequently detected ARGs, such as *erm*B, which encodes resistance to erythromycin, exhibited the strongest reduction, reaching up to 1.9 $\log_{10}$ units following irradiation with 420 nm aBL (Figure 3.4b). Similarly, the *tet*M gene, responsible for tetracycline resistance, displayed moderate susceptibility to aBL treatment, with a reduction of up to 1.8 $\log_{10}$ units at 420 nm (Figure 3.4b). Other intermediately detected ARG targets, including $bla_{\text{CTX-M}}$, $bla_{\text{CTX-M32}}$, $bla_{\text{CMY-2}}$ were less efficiently inactivated by aBL irradiation. The bla_{VIM} and *mcr*-1 genes exhibited relatively high sensitivity to aBL treatment alone, with reductions in gene copy numbers of 1.9 $\log_{10}$ and 0.9 $\log_{10}$, units respectively, following irradiation with 420 nm aBL (Figure 3.4c). When aBL was applied alone, the extent of ARG reduction appeared to be highly dependent on the specific bacterial hosts carrying the genes as part of the real wastewater effluent. Furthermore, the additional wavelengths of aBL (405 nm and 460 nm) did not appear to have a significant or decisive impact on ARG reduction.

There are clear differences in the results (1) when comparing culture methods with qPCR, and (2) when comparing the flow-through reactor with the static aBL photosystem reported by Cong et al. (2023). In the culture method, FPB contamination in the wastewater was reduced to 0 CFU after 4 h aBL irradiation (26 min, without addition of photosensitizers or oxidative agents) (Figure 3.3). However, qPCR analysis showed a less acceptable reduction. This discrepancy could be due to sufficient cellular DNA still being available for qPCR, despite the bacterial cells losing cultivability due to aBL treatment. Possible reasons include shading effects, bacterial aggregating, insufficient DNA degradation by ROS, and matrix effects impacting PMA treatment for living/dead discrimination. Irradiation exceeding 4 hours and a simultaneous application of 405 nm, 420 nm, and 460 nm wavelengths are recommended for future applications of the aBL method to achieve higher inactivation. Cong et al. (2023) showed that simultaneous irradiation of wastewater from slaughterhouses with the three wavelengths of blue light in the static photoreactor resulted in strong reductions up to elimination within 4 hours; with the photosensitizers significantly

increasing reduction performance. The energy input in J cm^{-2} was generally 10 times higher in the static aBL photosystem compared with the recently used flow through photoreactor (Cong et al, 2023).

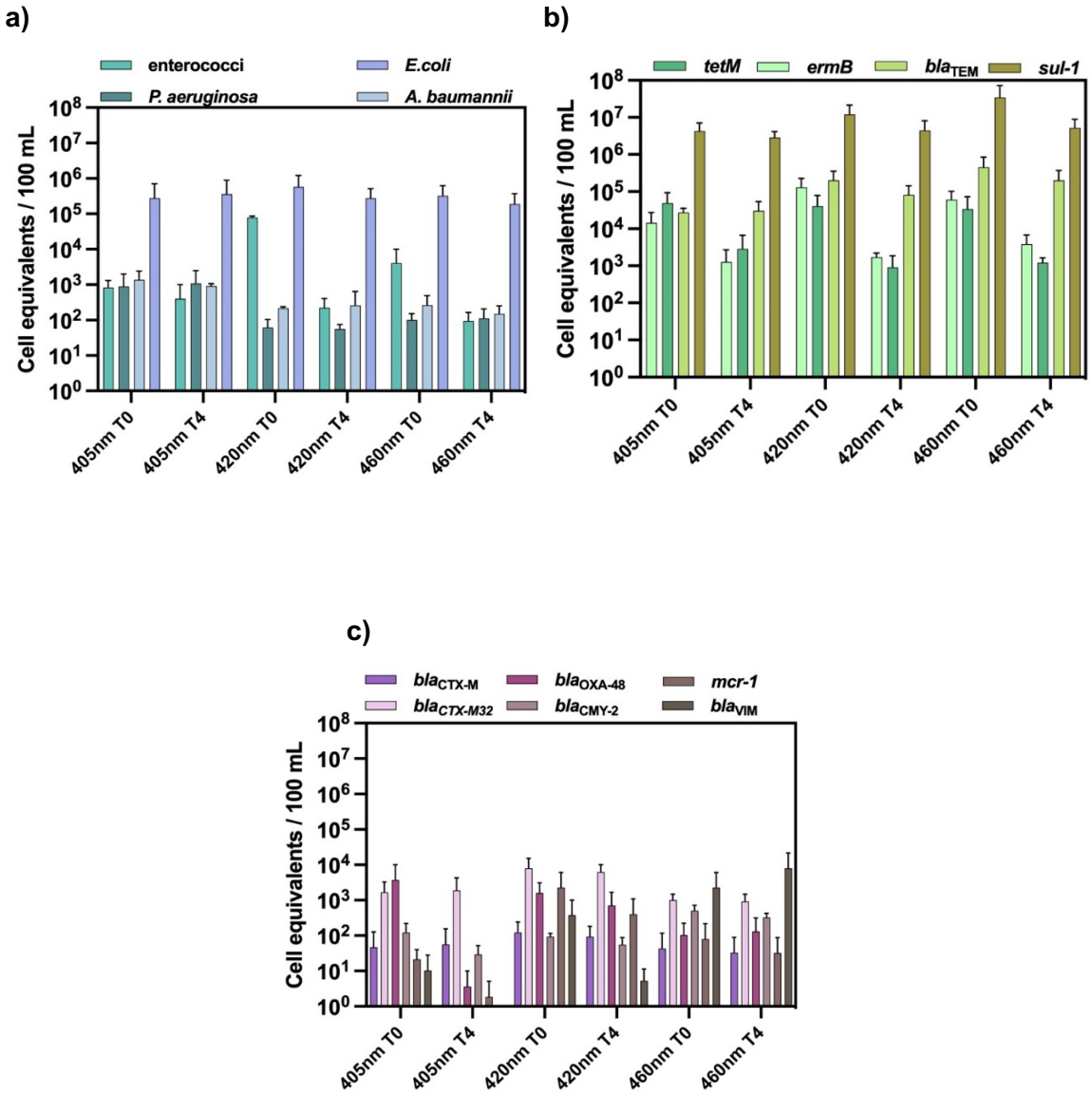

Figure 3.4: FPB and ARG cell equivalents per 100 mL of s following irradiation with aBL alone at 405, 420 and 460 nm after 4 h illumination (equal to 26 min net irradiation. The results are categorized into three groups: (a) FPB, including enterococci, *Pseudomonas aeruginosa*, *Acinetobacter baumannii*, and *Escherichia coli*, (b) commonly detected ARGs, including genes such as *ermB*, *tetM*, bla_{TEM}, and *sul1*, (c) intermediately detected ARGs, including bla_{CTX-M}, $bla_{CTX-M32}$, bla_{OXA-48}, bla_{CMY-2}, *mcr-1*, and bla_{VIM}. Values are averages from n = 3 tests at each condition.

Consistent with the results for taxonomic gene markers, the calculated ARGs reduction rates (Figures 3.4b and 3.4c) imply that no full inactivation was achieved by aBL at the maximum irradiation of 26 minutes (equal to 4 h of operation). This demonstrates that aBL irradiation could inactivate FPB and ARGs to a certain extent within the applied treatment period, independent of the wavelength, although effectiveness was likely limited by insufficient internal ROS production. Matrix effects of the wastewater, aggregate formation (hindering light penetration), and shading effects are plausible explanations for the limitation of aBL irradiation. Therefore, the application of effective additional photosensitizers is crucial for enhancing the efficiency of aBL treatment, particularly in overcoming the limitations of aBL alone in inactivating certain FPB and ARGs.

3.3.3 Comparative effectiveness of added TMPyP or H_2O_2

TMPyP, a photoactive dye, has been shown to inactivate microorganisms in combination with aBL irradiation very efficiently (Cong et al. 2023). Porphyrins are organic chemical structures with four pyrrole rings, connected by four methine groups, forming cyclic structures and are present in different bacterial cytochromes (Figure SB1). The integration of blue light therapy with exogenously applied oxidizing agents like H_2O_2, has been adopted in medical photodynamic therapies (Ngo et al., 2023). H_2O_2 enhances the efficiency of light-induced processes, such as UV-C, in eliminating pollutants by generating free radicals ($HO^{\bullet}$ or/and $SO_4^{\bullet-}$) (Meng et al., 2022). While aBL is effective in removing FPB, its successful application in eliminating ARB/ARGs from wastewaters has not been thoroughly investigated. The usefulness of aBL irradiance alone and in combination with TMPyP and H_2O_2 in inactivating selected FPB and ARG targets in WWTP effluents was investigated (Table SB4). Figure 3.5 shows the effectiveness of three different aBL treatments, expressed as cell equivalence per 100 mL for selected gene targets categorized into four groups, with (a) 16S rRNA gene and *intI1*; (b) FPB, including enterococci, *P. aeruginosa*, *A. baumannii*, and *E. coli*; (c) Commonly detected ARGs, including *erm*B, *tet*M, bla_{TEM}, and *sul*1; (d) Intermediately detected ARGs, including $bla_{CTX\text{-}M}$, $bla_{CTX\text{-}M32}$, $bla_{OXA\text{-}48}$, $bla_{CMY\text{-}2}$, *mcr-1*, and bla_{VIM}. As 420 nm proved to be quite similar effective among the three tested wavelengths, we focused on it.

In our study, an antibacterial effect of added H_2O_2 (1 mM) is only seen in combination with aBL irradiation (data not shown). H_2O_2 itself does not absorb light strongly in the visible spectrum or in the spectral range of the emitted blue light. But when combined with certain catalysts or photosensitizers (like titanium dioxide, silver nanoparticles, or certain organic

compounds like photoenhancers or intracellular light sensitive compounds), the system can absorb light in the blue range (400-460 nm).

Photosensitizers which absorb blue light enter an excited state, either a singlet or a triplet excited state, depending on the nature of the sensitizer. In its excited state, the photosensitizer can interact with H_2O_2 molecules. This interaction can lead to the enhanced production of reactive ROS, such as $OH^{\bullet}$ and $^1O_2$. In summary, the activation of H_2O_2 under blue light involves the absorption of light by a photosensitizer, which then produces ROS that decompose H_2O_2. The presence of blue light and a suitable catalyst is critical to this process. Further, although H_2O_2 is described as a toxic molecule and also occurs naturally as part of the bacterial energy metabolism, it is naturally degraded or intercepted by scavenger molecule activities like porphyrins and can then no longer show its bactericidal potential. However, if these intracellular scavenger molecules are altered by aBL irradiation, their scavenger potential is lost and the antibacterial potential of H_2O_2 comes into play. The different behavior of bacteria in natural communities or reference bacteria can therefore be attributed to different intracellular concentrations of natural scavenger molecules or their enzymatic activities (Mishra & Imlay, 2012; H. Yoon et al., 2022).

It must be noted that the added photosensitizer TMPyP (10^{-6} M) and the oxidative agent H_2O_2 (1 mM) showed no reducing effect on bacterial communities without aBL irradiation. Only with simultaneous aBL irradiation did the additional reduction performance of aBL develop in wastewater effluent (data not shown, but available upon request). The combination of aBL with TMPyP significantly decreased 16S rRNA gene abundance, indicating a strong bactericidal effect and reduced overall bacterial load (Figure 3.5a). In contrast, aBL alone and its combination with H_2O_2 did not significantly reduce 16S rRNA genes, suggesting these treatments were less effective at lowering bacterial load. Regarding the *intI1* gene, Figure 3.5a shows varying levels of effectiveness among the three treatments: aBL alone led to a reduction of less than 1 $\log_{10}$ in *intI*1 gene copies, indicating a modest impact on the HGT marker. The combination of aBL with H_2O_2 resulted in greater reduction, achieving a 1.4 $\log_{10}$ decrease. aBL combined with TMPyP achieved the strongest reduction, reaching up to approximately 4 $\log_{10}$ units, highlighting TMPyP's significant role in enhancing aBL's ability to target and reduce ARGs, particularly those associated with integrons like *intI1*. This implies that the combination of aBL with TMPyP exhibits enhanced ability to inactivate ARGs compared to H_2O_2. aBL irradiation alone led to a significant reduction in gene copy numbers, specifically a 2.5 $\log_{10}$ decrease observed in enterococci (Figure 3.5b). In contrast, gene copy numbers of *P. aeruginosa*, *A.*

baumannii, and *E. coli* remained unchanged, even after 4 h of aBL irradiation (equal to 26 minutes of aBL net irradiation). This discrepancy highlights the varying susceptibility of different FPB to aBL irradiation, confirmed by our cultivation methods. The combination of aBL with TMPyP resulted ina 3.3 $\log_{10}$ reduction for enterococci, 1.2 $\log_{10}$ for *P. aeruginosa*, 1.8 $\log_{10}$ for *A. baumannii*, and 2.4 $\log_{10}$ for *E coli (*Figure 3.5b). This demonstrated that combining TMPyP with violet-blue light significantly enhanced the reduction of multidrug-resistant strains of *P. aeruginosa* and *Klebsiella pneumoniae***,** supporting previous studies such as by Mušković et al. (2023). However, adding H_2O_2 appears more selective strongly inactivating *A. baumannii*, a bacterium known for its resistance mechanisms, but not enhancing the inactivation of enterococci, *P. aeruginosa*, and *E. coli* beyond what was achieved with aBL with TMPyP.

Based on the results of each specific target gene (Table 3.1, Figure 3.5), ARGs in the KIT WWTP effluent can be categorized into two groups. The first group includes commonly detected ARGs, such as *erm*B and *tet*M genes, which are more susceptible to aBL irradiation (Figure 3.5c). These genes were reduced of approximately 1.5 orders of magnitude with aBL alone. Adding H_2O_2 at 1 mM enhanced effectiveness by 2 orders of magnitude. Notably, combining TMPyP with aBL irradiation increased reduction effectiveness, resulting in a 3 $\log_{10}$ unit decrease. In contrast, the *sul*1 gene, less susceptible to aBL alone, was better inactivated with aBL and TMPyP, showing a 4.2 $\log_{10}$ unit decrease.

The combination of aBL with H_2O_2 also leads to a notable reduction, though less pronounced, with a decrease of 2.1 $\log_{10}$ units. The bla_{TEM} gene was more robust to all three aBL-treatments suggesting that bacteria with bla_{TEM} gene are less susceptible to the oxidative and photodynamic effects of aBL, whether used alone or in with TMPyP or H_2O_2. Regarding the second group (Table 3.1), the intermediately detected ARGs, including $bla_{\text{CTX-M}}$, $bla_{\text{CTX-M32}}$, $bla_{\text{OXA-48}}$, and $bla_{\text{CMY-2}}$, aBL irradiation alone did not substantially change gene copy concentrations, indicating minimal impact. However, the addition of TMPyP reduced $bla_{\text{CTX-M}}$ and $bla_{\text{CMY-2}}$ gene copy numbers by approximately 2 $\log_{10}$ units, suggesting that TMPyP significantly enhanced aBL irradiation effectiveness for these ARGs. In contrast, $bla_{\text{CTX-M32}}$ was more robust against aBL under similar conditions. Conversely, $bla_{\text{OXA-48}}$ was highly susceptible to aBL combined with H_2O_2, indicating that it can be effectively affected. The *mcr-1* gene was notably susceptible to both aBL with TMPyP and aBL with H_2O_2, demonstrating significant inactivation. This suggests that the combined oxidative and photodynamic effects are sufficient to significantly eliminate these gene or bacteria carrying them, which is crucial given the clinical importance of colistin

resistance. On the other hand, *bla*$_{VIM}$, associated with carbapenem resistance, was unaffected by aBL treatment.

The maximum aBL irradiation time in this study was limited to 26 minutes, resulting from a total circulation time of 4 hours for 4 liters of WWTP effluent in the photoreactor. A longer circulation period or aBL irradiation time in combination with photosensitizers or H_2O_2 in an up-scaled variant is expected to result into a greater inactivation or elimination of FPB and ARGs. This was confirmed by experiments using a static aBL reactor with TMPyP as a photosensitizer, exhibiting much longer continuous irradiation durations in the range of several hours (Cong et al., 2023).

Conventional treatment processes at WWTPs often fail to completely eliminate ARB or ARGs, allowing them to enter downstream aquatic environments through effluent discharge (Maldonado-Carmona et al., 2022). Implementing strategies to disrupt these transmission pathways and prevent selection processes can effectively mitigate the evolution and spread of antibiotic resistance. Identifying critical control points in sewer systems is crucial, with special attention to ARGs against reserve antibiotics, which are detected in intermediate or low abundances in wastewater systems via genetic detection methods (Hembach et al., 2019).

As an outlook, after further optimization to real-live applications, modular designs of this aBL photodisinfection could be installed at critical AMR hotspots for decentralized advanced wastewater treatment. This can significantly unburden the load of contaminants in wastewater received by the WWTPs, and safeguarding aging and leaking pipeline systems. As urban WWTPs are currently ineffective at to fully remove pathogens, quaternary treatment of WWTP effluents for hygienization, are urgently required. Through this, the dissemination of AMR determinants through the wastewater system can be reduced and ultimately lowing the risks for human and animal health. Targeted and innovative light-based on-site measures relieve downstream wastewater areas of AMR contamination, reducing their release into the environment (Mulani et al., 2019).

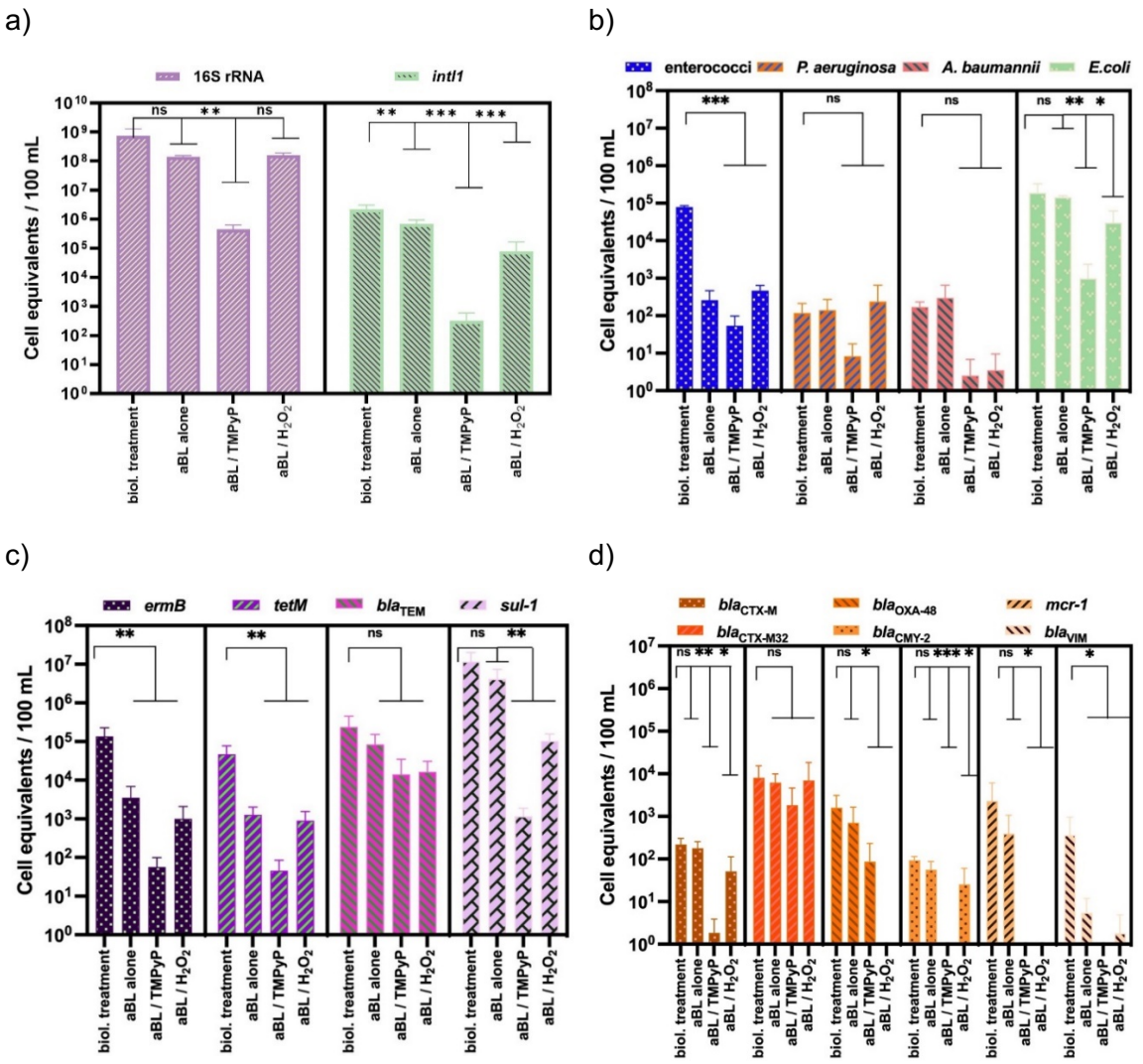

Figure 3.5: Cell equivalents per 100 mL of FPB and ARGs at aBL irradiation for 4 h (equal to 26 min irradiation) using aBL alone at 420 nm, aBL + TMPyP (10^{-6} M), and aBL + H_2O_2 (1 mM). Results are categorized into four groups: (a) 16S rRNA and *intI*1, (b) FPB, including *enterococci*, *Pseudomonas aeruginosa*, *Acinetobacter baumannii*, and *Escherichia coli*, (c) commonly detected ARGs, including *ermB*, *tetM*, bla_{TEM}, and *sul1*, (d) intermediately detected ARGs, including bla_{CTX-M}, $bla_{CTX-M32}$, bla_{OXA-48}, bla_{CMY-2}, *mcr-1*, and bla_{VIM}. Values are average from n = 3 tests at each condition. The statistical significance of the differences in treatment effects is indicated by asterisks.

Since, it was initially a flow reactor for laboratory operation, in which the operating parameters were set to a maximum operating time of 4 h (equal to 26 min net irradiation), it can be assumed that an extension of the actual irradiation time would be even more effective. As the previously described energy input of our flow aBL-reactor was already set to maximum. For optimization, this would be obtained by either increasing the irradiation time (> 4 hours) and/or reduce the total volume of liquid to be irradiated during circulation

(< 4 L total volume). Previous studies with static conditions where significantly longer irradiation times (>26 min) where achieved, support this hypothesis (Cong et al.2023). To demonstrate this with a flow reactor, up-scaling of the apparatus would be required. Decentralized modular inactivation technologies, such as aBL, would be the preferred intervention at AMR hotspots for combating AMR dissemination through sewage systems.

3.3.4 aBL irradiation induced DNA damages

Our goal was to determine whether aBL-mediated irradiation directly induces DNA lesions. The number of DNA damages per 10 kb length in bacteria before and after aBL irradiation, alone and combined with TMPyP or H_2O_2, was quantified via qPCR analyses. The qPCR amplification efficiency (E) and the correlation coefficients for each sample are presented in Table SB5. The results (Figure 3.6) show that aBL irradiation alone caused approximately 10 lesions per 10 kb DNA, while the combination with TMPyP and H_2O_2 resulted in about 13 and 12 lesions per 10 kb DNA, respectively. This indicates slightly higher DNA damage with TMPyP and H_2O_2 additions, though the overlapping error bars indicate no statistically significant difference between treatments.

More generally, aBL treatment itself is considered low risk for the development of bacterial resistance and tolerance due to its multitarget mode of action. This was studied by the tolerance (resistance development in *E. coli*, *K. pneumoniae*, and *P. aeruginosa* to aBL. The observed adaption was a stable feature (Rapacka-Zdonczyk et al., 2021). The impact of aBL in combination with TMPyP or H_2O_2 on the tolerance/resistance development is so far not clarified. Nevertheless, we observed a direct or in direct impact on the DNA in bacteria. The resulting consequence will be studies in a following up project.

UV-C (100 – 289 nm) is widely used for (waste)water disinfection, with germicidal effects based on DNA, RNA, and protein absorption at specific wavelengths, causing molecular damage. The germicidal effect for many bacteria is achieved at near 254 nm, where DNA has its maximum absorption (Jungfer et al., 2007; Süß et al., 2009). Lethal damages, mainly thymine dimers, blocks DNA replication leading to reproductive cell death. UV-C-induced DNA lesions were quantified in a UV-C reactor used for drinking water treatment (113.9 - 114.5 mJ cm^{-2}), with up to 2-3 lesions per kilobase reported (Nocker et al., 2018). Bacteria have evolved molecular mechanisms, such as photo-reactivation and dark repair systems, to restore such DNA lesions regulated by the *rec*A gene (Jungfer et al, 2007).

Opposed to UV inactivation, aBL irradiation activates ROS in the bacterial cells, targeting various cellular structures and causing lethal effects. Blue light can cause DNA damage

either directly or indirectly. Lawrence et al. (2018) found that light at 385 nm induced cyclobutane pyrimidine dimers (CPDs), while 405 nm did not. ROS can target guanine bases in DNA, forming oxidized derivatives like 8-hydroxy-deoxyguanosine (8-OHdG). Yoshida et al. (2017) confirmed that $^1O_2$, a specific ROS, significantly increases 8-OHdG levels in bacterial cells exposed to aBL irradiation. However, there is limited information on whether aBL (405-460 nm) induces DNA lesions, requiring further investigation. Unlike UV-C which primarily causes nucleic acid alterations and bacteria during evolution developed DNA directed repair mechanisms against, until now no repair mechanisms are known to repair the manifold target structures impaired by aBL irradiation (Hadi et al., 2020). Thus, aBL combined with porphyrin photosensitizer is expected to be more sustainable.

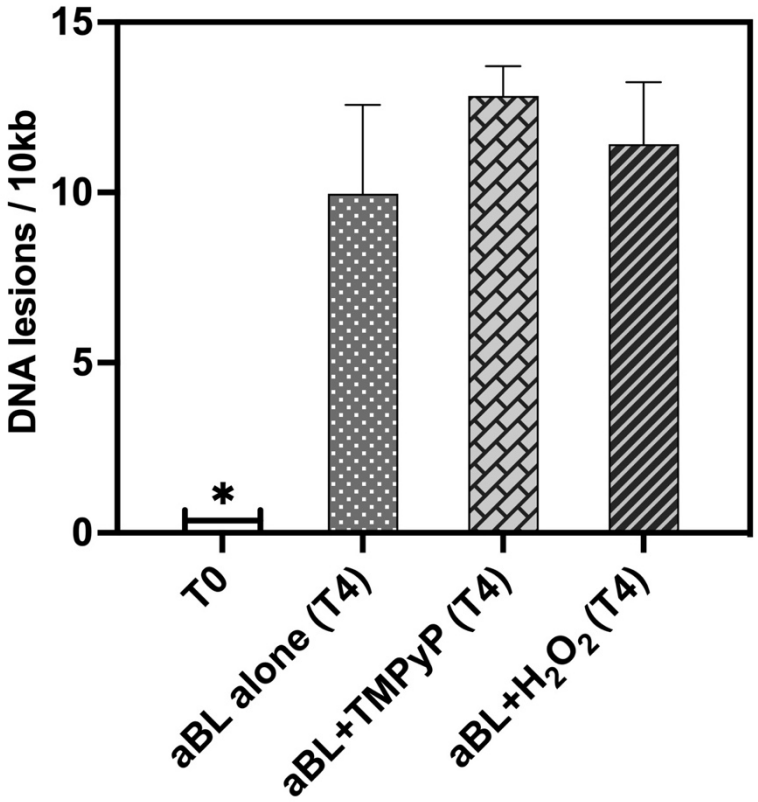

Figure 3.6: DNA lesions per 10kb DNA in the genomic DNA bacterial populations after aBL irradiation alone, or when combined either TMPyP or H_2O_2. Columns present averages of n=2 lesion measurements after 4h aBL irradiation (equal to 26 min effective irradiation). aBL treatments was performed using 420 nm LED lamps. The statistical significance is indicated by asterisks.

Although our data does not imply direct DNA damage induced by aBL, it suggests that it induces indirect DNA damage through ROS generation. It yet remains uncertain whether *Eubacteria's* DNA repair mechanisms could regenerate damaged DNA. Given that aBL, especially with TMPyP, has multiple attack points, long-term DNA repair may not be effective. This suggests that aBL, particularly with TMPyP, poses a potent challenge for bacterial survival due to the compounded effects on cellular integrity. The extent to which DNA lesions affect regrowth after regeneration is a subject of future investigations. Increasing the energy input is relevant for enhancing the inactivation performance of aBL-induced processes for contaminated wastewater.

3.4 Conclusion

This study evaluated the potential and effectiveness of aBL irradiation at 405, 420, and 460 nm in deactivating ARB, FPB, and ARGs in wastewater effluents from AMR-contaminated WWTP. The reduction of ARB, FPB, and ARGs was examined under continuous-flow conditions using an aBL photoreactor, with and without the addition of TMPyP porphyrin photosensitizers or oxidative agent H_2O_2 to enhance the effect of aBL irradiation by up to five $\log_{10}$ units.

Among the investigated FPB targets, enterococci were more sensitive to aBL irradiation than *A. baumannii*, *P. aeruginosa*, and *E. coli*. Among the ARG targets, *ermB*, *tetM*, *sul1*, and bla_{VIM} were more sensitive to aBL irradiation, resulting in significant gene copy number reduction. Additionally, aBL irradiation induced DNA damage, leading to lesions in the genomic DNA of treated wastewater. These findings indicate that aBL irradiation enhanced with photosensitizer and the oxidative agent H_2O_2 is highly effective for inactivating FPB, ARB, and ARGs in wastewater. This approach shows promising for decentralized wastewater treatment at AMR hotspots, providing a viable solution for the mitigation AMR spread through sewage. Compared to static reactors, the energy input via parallel-connected aBL LED lamps in continuous-flow reactors is assumed to be significantly higher, resulting in more effective inactivation. Based on these promising aBL flow reactor results, approaches for optimizing up-scaling were indicated. Therefore, to enhance intracellular ROS generation and promote increased cell death, the aBL irradiation should have been combined with additional photosensitizers or oxidizing agents. Another possible optimization is the up scaling of the aBL reactor, where stronger aBL intensities could be used for the treatment of contaminated wastewaters (i.e. more photoenergy, different LED lamps in parallel, etc). Such alterations would increase the effectiveness of aBL when used alone, without phosensitizer or oxidant addition. Future investigations should also explore the feasibility of adding photosensitizers or oxidizing agents to aBL treatments, and how

this can be practically implemented in larger scale applications (with regard to recovery, regeneration, or immobilization).

3.5 Supporting Information B

Table SB 1: Characteristics of secondary effluent from KIT WWTP

Parameter	Secondary effluent from WWTP	Unit
TOC	7.88	mgL^{-1}
BOD_5	1.9	mgL^{-1}
Temperature	16	°C
Turbidity	≤0.1	mgL^{-1}
pH	7.29	
Ammonium-N	≤0.44	mgL^{-1}
Nitrat-N	5.27	mgL^{-1}
Nitrit-N	≤0.2	mgL^{-1}
Phosphor total	1.25	mgL^{-1}

Table SB 2: The table summarizes primer sequences, calibration curve equations, amplicon sizes, qPCR efficiency values, correlation coefficients, and control strains with associated references. It groups the qPCR systems used for quantifying facultative pathogenic bacteria and antibiotic resistance genes, following Hembach et al. (2017, 2022) and Alexander et al. (2020, 2022). The primer sets employed for DNA lesion quantification are based on methods described by Nocker et al. (2018).

Target	Primer sequence	Equation of the calibration curve	Amplicon size	Efficiency	R^2	Control strain	Reference
Facultative pathogenic bacteria							
Enterococcus spp.	Fwd: AGAAATTCCAAACGAACTTG Rev: CAGTGCTCTACCTCCATCATT	F(x)= -3.585x+35.283	93 bp	90.1 %	1.000	*E. faecium* DSM20477	(Frahm und Obst 2003)
P. aeruginosa	Fwd: AGCGTTCGTCCTGCACAAGT Rev: TCCACCATGCTCAGGGAGAT	F(x)= -3.282x+35.276	81 bp	101.7 %	0.999	*P. aeruginosa* DSM1117	(Clifford et al. 2012)
A. baumannii	Fwd: GTTGTGGCTTTAGGTTTATTATACG Rev: AAGTTACTCGACGCAATTCG	F(x)= -3.380x+35.679	94 bp	97.6 %	1.000	*A. baumannii* DSM30007	(Clifford et al. 2012)
E. coli	Fwd: GCATCGTGACCACCTTGA Rev: CAGCGTGGTGGCAAAA	F(x)= -3.361x+35.797	59 bp	98.4 %	0.994	*E. coli* DSM1103	(Clifford et al. 2012)
Antibiotic resistance genes							
*erm*B	Fwd: TGAATCGAGACTTGAGTGTGCAA Rev: GGATTCTACAAGCGTACCTT	F(x)=-3.328x+35.901	71 bp	100 %	1.000	*S. hyointestinalis* DSM20770	(Alexander et al. 2015)
*Int*I1	Fwd: GCCTTGATGTTACCCGAGAG Rev: GATCGGTCGAATGCGTGT	F(x)= -3.472x+34.720	196 bp	94.1 %	1.000	*E. coli* pNORM	(Rocha et al. 2018)
*tet*M	Fwd: GGTTTCTCTTGGATACTTAAATCAATC Rev: CCAACCATAAATCCTTGTTCRC	F(x)=-3.424x+38.747	88 bp	95.9 %	0.998	*E. coli* DH5α	(Peak et al. 2007)
*bla*TEM	Fwd: TTCCTGTTTTTGCTCACCCAG Rev: CTCAAGGATCTTACCGCTGTTG	F(x)=-3.303x+38.559	112 bp	10.8 %	0.999	*E. coli* pNORM	(Rocha et al. 2018)
*sul*1	Fwd: CGCACCGGAAACATCGCTGCAC Rev: TGAAGTTCCGCCGCAAGGCTCG	F(x) -3.387x+39.802	161 bp	97.6 %	0.999	*E. coli* pNORM	(Rocha et al. 2018)
*bla*CTX-M	Fwd: CGCTTTGCGATGTGCAG Rev: ACCGCGATATCGTTGGT	F(x)= -3.504x+34.255	551 bp	92.9 %	1.000	*E. coli* pNORM	(Rocha et al. 2018)
*bla*CTX-M-32	Fwd: CGTCACGCTGTTGTTAGGAA Rev: CGCTCATCAGCACGATAAAG	F(x)= -3.517x+37.800	155 bp	92.5 %	1.000	*E. coli* pNORM	(Rocha et al. 2018)

Target	Primer sequence	Equation of the calibration curve	Amplicon size	Efficiency	R^2	Control strain	Reference
*bla*OXA-48	Fwd: TGTTTTTGGTGGCATCGAT Rev: GTAAMRATGCTTGGTTCGC	F(x)= -3.540x+36.913	177 bp	91.6 %	0.998	*K. pneumoniae* TGH Isolate 2	(Monteiro et al. 2012)
*bla*CMY-2	Fwd: CGTTAATCGCACCATCACC Rev: CGTCTTACTAACCGATCCTAGC	F(x)=-3.591x+34.025	172 bp	89.9 %	0.998	*K. pneumoniae* NRZ-01013	(Kurpiel&Hanson, 2012)
*bla*VIM	Fwd: GAGATTCCCACGCACTCTCTAGA Rev: AATGCGCAGCACCAGGATAG	F(x)=-3.829x+40.858	61 bp	82.5 %	0.999	*P. aeruginosa* PA49	(Van der Zee et al. 2014)
mcr-1	Fwd: GGGCCTGCGTATTTTAAGCG Rev: CATAGGCATTGCTGTGCGTC	F(x)=-3.386x+35.349	183 bp	97.4 %	0.999	*E. coli* NRZ-14408	(Hembach et al. 2017)

Target	Primer sequence	Equation of the calibration curve	Amplicon size	Efficiency	R^2	Control strain	Reference
Ribosomal DNA							
16S rDNA	Fwd: TCCTACGGGAGGCAGCAGT Rev: ATTACCGCGGCTGCTGG	F(x)= -3.405x+35.350	195bp	95.5%	0.997	*E. coli* pNORM	Hembach et al. 2017)
DNA damage	**Primer sequence**	**Primer type**	**Amplicon size**	**Efficiency**	**R^2**	**Control strain**	**Reference**
16S rDNA-27F	AGAGTTTGATCCTGGCTCAG	Forward (F_L)	1465 bp	75%	0.999	*E. coli DSM 787*	(Muyzer et al. 1993)
BacUni-1387F	GCCTTGTACACWCCGCCC	Forward (F_S)	105 bp	97%	0.999	*E. coli DSM 787*	(Marchesi et al. 1998)
BacUni-1492R	GGYTACCTTGTTACGACTT	Reverse				*E. coli DSM 787*	(Lane, 1991)

Table SB 3: Cell equivalents of FPB and ARGs per 100 mL were quantified and normalized following aBL irradiation at 405, 420, and 460 nm after 4 h of reactor operation (corresponding to 26 min net irradiation). T0 refers to untreated samples, while T4 denotes samples collected after 26 min of irradiation. The results are categorized into three groups: (A) FPB, including enterococci, *Pseudomonas aeruginosa*, *Acinetobacter baumannii*, and *Escherichia coli,* (B) commonly detected ARGs, including *erm*B, *tet*M, bla_{TEM}, and *sul*1, (d) intermediately detected ARGs, including bla_{CTX-M}, $bla_{CTX-M32}$, bla_{OXA-48}, bla_{CMY-2}, *mcr*-1, and bla_{VIM}. Values are average from n = 3 tests at each condition. LOD: Limit of detection.

A)

Targets (ESKAPE group) Cell equivalents per 100 mL												
	enterococci			*P. aeruginosa*			*A. baumannii*			*E. coli*		
405nm T0	3.60E+02	1.30E+03	8.30E+02	2.80E+02	1.90E+02	2.20E+03	2.50E+03	1.20E+03	4.00E+02	2.00E+04	7.70E+05	3.70E+04
405nm T4	6.50E+01	1.10E+03	4.50E+01	3.80E+02	1.90E+02	2.70E+03	1.10E+03	8.50E+02	8.10E+02	2.20E+04	9.80E+05	8.40E+04
420nm T0	8.30E+04	7.10E+04	8.36E+04	2.90E+01	1.10E+02	4.60E+01	2.00E+02	2.10E+02	2.40E+02	3.50E+05	8.30E+04	1.30E+06
420nm T4	3.80E+02	2.20E+01	2.66E+02	6.20E+01	7.20E+01	3.40E+01	4.90E+01	7.00E+02	3.30E+01	1.30E+05	1.50E+05	5.50E+05
460nm T0	6.30E+02	1.10E+04	5.30E+02	7.90E+01	6.20E+01	1.60E+02	3.60E+02	9.70E+00	4.30E+02	1.80E+04	3.40E+05	6.20E+05
460nm T4	1.30E+02	1.60E+01	1.40E+02	2.20E+02	3.70E+01	7.90E+01	2.10E+02	3.20E+01	2.10E+02	1.30E+04	1.70E+05	3.80E+05

B)

	Targets (commonly detected genes) Cell equivalents per 100 mL											
	ermB			*tetM*			bla_{TEM}			*sul*1		
405nm T0	2.70E+02	1.80E+04	2.50E+04	1.00E+05	2.00E+04	2.60E+04	2.20E+04	2.30E+04	3.70E+04	4.20E+06	1.40E+06	7.00E+06
405nm T4	3.80E+01	9.80E+02	2.80E+03	7.30E+03	5.00E+02	7.30E+02	2.10E+04	5.70E+04	1.30E+04	4.10E+06	2.80E+06	1.60E+06
420nm T0	2.10E+05	1.60E+05	2.30E+04	4.00E+03	8.10E+04	3.70E+04	1.90E+05	5.10E+04	3.60E+05	2.20E+07	9.00E+06	4.70E+06
420nm T4	1.20E+03	2.10E+03	1.90E+03	2.10E+02	5.20E+02	2.00E+03	6.60E+04	2.70E+04	1.50E+05	8.50E+06	1.50E+06	3.20E+06
460nm T0	6.50E+04	1.00E+05	1.60E+04	1.90E+04	7.80E+04	5.20E+03	4.50E+05	8.50E+05	5.60E+04	7.40E+07	3.30E+06	2.50E+07
460nm T4	7.20E+03	1.60E+03	2.70E+03	1.30E+03	1.60E+03	7.40E+02	3.70E+05	2.00E+05	3.10E+04	8.10E+06	9.90E+05	6.30E+06

C)

	Targets (Intermediately detected genes) Cell equivalents per 100 mL											
	bla$_{CTX-M}$			*bla*$_{CTXM-32}$			*bla*$_{OXA-48}$			*bla*$_{CMY-2}$		
405nm T0	1.40E+02	<LOD	<LOD	3.30E+03	1.50E+03	1.60E+02	1.10E+04	2.00E+02	1.40E+01	2.10E+02	1.40E+02	2.10E+01
405nm T4	1.70E+02	<LOD	<LOD	1.10E+03	4.50E+03	2.90E+01	<LOD	1.10E+01	<LOD	3.20E+01	5.10E+01	5.00E+00
420nm T0	1.30E+02	2.40E+02	<LOD	3.90E+03	3.80E+03	1.60E+04	3.00E+03	1.80E+03	<LOD	1.20E+02	7.90E+01	8.20E+01
420nm T4	1.00E+02	1.80E+02	<LOD	7.50E+03	2.00E+03	9.00E+03	3.10E+02	1.80E+03	1.10E+01	8.60E+01	5.90E+01	2.20E+01
460nm T0	1.30E+02	<LOD	<LOD	6.10E+02	1.50E+03	8.70E+02	2.40E+02	5.30E+01	1.70E+01	6.70E+02	2.60E+02	5.90E+02
460nm T4	9.80E+01	<LOD	<LOD	3.00E+02	1.00E+03	1.40E+03	3.40E+02	4.60E+01	5.80E+00	3.10E+02	2.30E+02	4.30E+02

	mcr-1			*bla*$_{VIM}$		
405nm T0	3.50E+01	2.90E+01	<LOD	3.10E+01	<LOD	<LOD
405nm T4	5.60E+00	<LOD	<LOD	<LOD	<LOD	<LOD
420nm T0	2.90E+01	6.70E+03	1.30E+02	1.10E+03	1.30E+01	2.00E+01
420nm T4	<LOD	1.20E+03	3.50E+00	<LOD	1.20E+01	3.90E+00
460nm T0	2.40E+02	<LOD	<LOD	6.70E+03	4.10E+01	3.50E+01
460nm T4	9.70E+01	<LOD	<LOD	2.40E+04	2.80E+01	<LOD

Table SB 4: Cell equivalents per 100 mL of FPB and ARGs at aBL irradiation for 4 h (equal to 26 min irradiation) using aBL alone at 420 nm, aBL + TMPyP (10^{-6} M), and aBL + H_2O_2 (1 mM). Results are categorized and normalized into four groups: (a) 16S rRNA and intI1, (b) FPB, including enterococci, *Pseudomonas aeruginosa*, *Acinetobacter baumannii*, and *Escherichia coli*, (c) commonly detected ARGs, including *erm*B, *tet*M, *bla*$_{TEM}$, and *sul*1, (d) intermediately detected ARGs, including *bla*$_{CTX-M}$, *bla*$_{CTX-M32}$, *bla*$_{OXA-48}$, *bla*$_{CMY-2}$, *mcr*-1, and *bla*$_{VIM}$. Values are average from n = 3 tests at each condition. LOD: Limit of detection.

A)

Targets Cell equivalents per 100 mL						
	16s rRNA			*Intl*1		
biol. treatment	1.12E+09	3.43E+08	5.98E+07	3.13E+06	1.38E+06	2.08E+06
aBL alone	1.53E+08	1.33E+08	2.43E+07	5.05E+05	5.42E+05	9.78E+05
aBL / TMPyP	5.75E+05	3.17E+05	4.14E+05	6.19E+02	2.38E+02	1.12E+02
aBL / H_2O_2	1.41E+08	1.81E+08	1.73E+06	1.77E+05	4.01E+04	1.92E+04

B)

Targets (ESKAPE group) Cell equivalents per 100 mL												
	enterococci			*P. aeruginosa*			*A. baumannii*			*E. coli*		
biol. treatment	8.30E+04	7.10E+04	8.34E+04	2.87E+01	1.11E+02	2.16E+02	2.05E+02	2.10E+02	9.75E+01	3.51E+05	8.27E+04	1.33E+05
aBL alone	3.80E+02	2.20E+01	3.80E+02	6.16E+01	7.16E+01	2.92E+02	4.91E+01	7.02E+02	1.52E+02	1.28E+05	1.54E+05	1.51E+05
aBL / TMPyP	8.96E+01	5.36E+00	6.74E+01	<LOD	6.38E+00	1.85E+01	<LOD	<LOD	7.54E+00	2.56E+03	3.13E+01	3.57E+02
aBL / H_2O_2	4.25E+02	6.57E+02	3.08E+02	8.93E+00	7.10E+02	<LOD	<LOD	1.06E+01	<LOD	6.72E+04	1.12E+04	1.18E+04

C)

Targets (commonly detected genes) Cell equivalents per 100 mL												
	*erm*B			*tet*M			*bla*$_{TEM}$			*sul*1		
biol. treatment	2.13E+05	1.58E+05	3.41E+04	8.09E+04	3.69E+04	2.29E+04	1.94E+05	5.15E+04	4.69E+05	9.02E+06	4.66E+06	2.09E+07
aBL alone	1.15E+03	2.08E+03	7.37E+03	5.24E+02	1.98E+03	1.32E+03	6.55E+04	2.75E+04	1.60E+05	1.49E+06	3.17E+06	7.64E+06
aBL / TMPyP	9.11E+01	6.96E+01	9.54E+00	6.77E+01	6.99E+01	<LOD	3.84E+03	2.44E+02	3.80E+04	1.81E+03	3.95E+02	1.23E+03
aBL / H_2O_2	8.33E+02	2.15E+03	2.62E+01	1.42E+03	1.12E+03	1.82E+02	1.34E+04	3.67E+03	3.23E+04	4.24E+04	1.25E+05	1.39E+05

D)

Targets (Intermediately detected ARGs) Cell equivalents per 100 mL												
	bla$_{CTX-M}$			*bla*$_{CTXM-32}$			*bla*$_{OXA-48}$			*bla*$_{CMY-2}$		
biol. treatment	2.43E+02	1.27E+02	2.89E+02	3.95E+03	3.84E+03	1.65E+04	3.02E+03	1.78E+03	1.13E+01	1.17E+02	7.94E+01	8.19E+01
aBL alone	1.79E+02	1.02E+02	2.55E+02	7.50E+03	1.98E+03	9.04E+03	3.09E+02	1.78E+03	4.26E+01	8.60E+01	5.89E+01	2.20E+01
aBL / TMPyP	<LOD	1.57E+00	3.99E+00	3.22E+02	8.44E+01	5.08E+03	2.55E+02	4.35E+00	0.00E+00	0.00E+00	0.00E+00	0.00E+00
aBL / H_2O_2	1.22E+02	1.60E+01	1.57E+01	2.02E+04	6.30E+02	0.00E+00	0.00E+00	0.00E+00	0.00E+00	0.00E+00	6.52E+01	1.09E+01
	mcr-1			*bla*$_{VIM}$								
biol. treatment	6.68E+03	1.26E+02	2.93E+01	1.05E+03	2.04E+01	1.32E+01						
aBL alone	1.16E+03	3.51E+00	<LOD	<LOD	3.91E+00	1.25E+01						
aBL / TMPyP	<LOD	<LOD	<LOD	<LOD	<LOD	<LOD						
aBL / H_2O_2	<LOD	<LOD	<LOD	<LOD	<LOD	5.33E+00						

Table SB 5: The reaction equations derived from the amplification of standard curves by serial dilutions of genomic DNA from both non-irradiated and irradiated samples. It also includes the qPCR amplification efficiency (E) and correlation coefficient (R^2) for each of the standards.

Target	Equation	E	R^2
Short qPCR			
T0/alone	y = -3.54x + 41.91	0.92	0.99
T4/alone	y = -3.64x + 39.32	0.88	0.99
T0/TMPyP	y = -3.52x + 37.55	0.92	0.99
T4/TMPyP	y = -4,38x + 46.53	0.69	0.99
T0/H_2O_2	y = -3.52x + 37.51	0.93	0.99
T_4/H_2O_2	y = -3.57x + 46.43	0.91	0.99
Long qPCR			
T0/alone	y = -4.61x + 50.31	0.66	0.99
T4/alone	y = -4.33x + 46.56	0.71	0.99
T0/TMPyP	y = -4.68x + 43.91	0.64	0.99
T4/TMPyP	y = -4.63x + 49.59	0.65	0.99
T0/H_2O_2	y = -4.67x + 42.18	0.64	0.99
T4/H_2O_2	y = -4.04x + 47.79	0.77	0.99

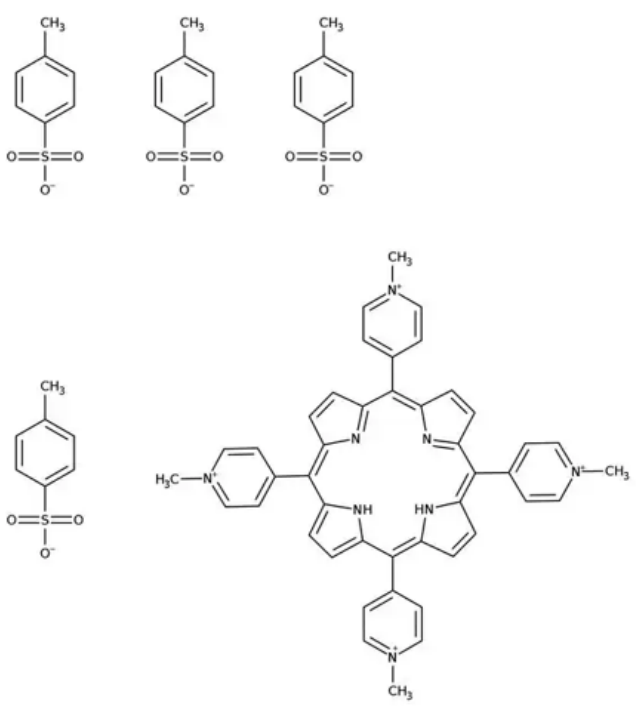

Figure SB 1: The structure of photosensitizer porphyrin TMPyP (5, 10, 15, 20-Tetrakis-(N-Methyl-4-pyridyl) 21, 23-porphyrin tetratosylate). The molecular formular is $C_{72}H_{66}N_8O_{12}S_4$. The central structure features a porphyrin core, a large, planar, and cyclic compound. The nitrogen-containing heterocycles form an integral part of the porphyrin ring. The sulfonic acid groups contribute to balancing the overall charge of the molecule while enhancing its stability.

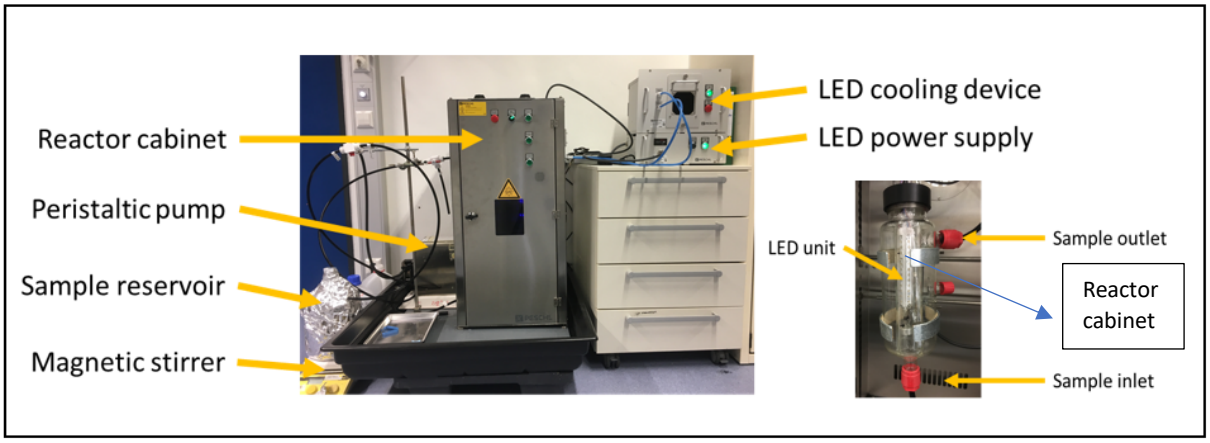

Figure SB 2: The laboratory setup for the continuous-flow photoreactor includes a reactor cabinet housing the LED unit and a peristaltic pump, which facilitates the movement of the water sample. A magnetic stirrer is employed to ensure continuous mixing of the sample in the reserveoir, maintaining homogeneity and preventing sedimentation throughout the experiment.

4 Cellular insights into reactive oxidative species (ROS) and bacterial stress responses induced by antimicrobial blue light (aBL) for inactivating antibiotic resistant bacteria (ARB) in wastewater

Published as: *Cong, X., Hillert, J., Krolla, P., & Schwartz, T. (2025). Cellular insights into reactive oxidative species (ROS) and bacterial stress responses induced by antimicrobial blue light (aBL) for inactivating antibiotic resistant bacteria (ARB) in wastewater. Science of the Total Environment, 1005, 180878.*

4.1 Introduction

Antibiotics are recognized as a new type of environmental pollutants because of their persistence and potential ecotoxicological effects (Shao et al., 2018). The selective pressure from long-term antibiotic use drives the evolution of resistant bacterial variants (Amarasiri et al., 2020; Li and Zhang, 2022), leading to AMR, which is estimated to lead to 10 million deaths annually globally by 2050 (Tang et al., 2023; O'Neill, 2016). ARB and ARGs are gaining gradual acceptance as environmental pollutants, raising considerable public health concerns (Ding et al., 2023; Ondon et al., 2021) and are found to contribute to hospital-acquired infections (Li et al., 2023).

Conventional wastewater treatment strategies generally cannot effectively remove ARB/ARGs and this urges the development of novel and efficient remediation measures (Mandal, 2024; Wang and Chen, 2022). Of the possibilities currently under examination, the AOPs have been extensively studied for the elimination of ARB and ARGs (Alexander et al., 2016; Ferro et al., 2017), but their broader application is hindered by high cost, high energy demand, and the formation of potential harmful by-products (Han et al., 2024). aBL has emerged as a promising, environmentally sustainable alternative to conventional UV-based approaches. Compared with medium-pressure UV lamps, LED-based aBL systems are substantially more efficient in the 405 nm range (Martín-Sómer et al., 2023), roughly 20 times higher radiation output for the same energy input, while avoiding undesired side reactions. Their mercury-free, modular design further enables safe, scalable deployment at critical hotspots in wastewater treatment and facilitates retrofitting of legacy infrastructure. Given that effluents can still contain trace pollutants and multi-resistant

bacteria, extending hygienisation with LED-based aBL offers an environmentally sustainable option to safeguard public health and the environment (Mandal, 2024).

Mechanistically, aBL acts by stimulating native bacterial chromophores irradiating bluelight with the help of LED lamp technology. In subsequence, the formed ROS include $OH^{\bullet}$, $O_2^{\bullet-}$, $^1O_2$, and H_2O_2 contribute to the bactericidal effect (Feuerstein et al., 2005; Wang et al., 2019). These ROS cause oxidative damages to DNAs, proteins, and membranes, which ultimately result in microorganism death. Our previous study demonstrated the feasibility of aBL in a continuous flow reactor, achieving substantial reductions of 4 FPB, 10 ARGs, as well as 16S rRNA and *Intl*1 genes (Cong et al., 2025). While these findings verified the feasibility of aBL in practice, the specific cellular mechanisms of action under wastewater conditions remain unclear.

ROS are generated under aBL through two distinct photochemical pathways: One, the type I mechanism, involves electron transfer to produce H_2O_2, $OH^{\bullet}$, and $O_2^{\bullet-}$. In the mechanism type II energy transfer to molecular oxygen results mainly in $^1O_2$ (Dąbrowski, 2017; Baptista et al., 2021). Exogenous photosensitizers (PS) such as porphyrins can be added to increase ROS production and consequently aBL efficiency (Cong et al., 2023; Bulit et al., 2014). Our own studies (Cong et al., 2023; 2025) have demonstrated that the application of photosensitizers and oxidative agent (TMPyP or H_2O_2) in aBL irradiation could greatly improve ARGs and FPB elimination by raising hypothesized oxidative stress.

Although the bactericidal activity of aBL is widely attributed to ROS, the specific contributions of individual ROS species during disinfection in wastewater matrices remain unclear. To address this gap, we applied selective scavengers to determine the relative contributions of individual ROS. The effect of each ROS was further assessed by qPCR with respect to a gene copy number determination of *erm*B, *sec*E (specific for *A. baumannii*), bla_{TEM}, 16S rRNA genes. Since VBNC cells escape detection by conventional cultivation methods (Colwell, 2000), culture-independent molecular tools are essential. In this study, living/dead differentiation combined with qPCR provided a more comprehensive and reliable assessment of ARB and ARG persistence under aBL treatment.

Under aerobic conditions, molecular oxygen freely diffuses across biological membranes, participating in intracellular ROS formation. To survive in such oxidative environments, bacteria have evolved sophisticated stress response systems. While ROS are central to microbial inactivation, they can also contribute to the development of antibiotic resistance by inducing DNA damage and mutagenesis during DNA repair mediated by *rec*A gene activation (Taylor et al., 2024; Qi et al., 2023). In response to such oxidative stress,

bacteria have constitutive expression of an array of antioxidant enzymes that scavenge ROS and repair oxidative damage. Moreover, the synthesis of most of these enzymes is induced as intracellular ROS resulting in a dynamic and inducible protection system. OxyR and SoxRS are major regulatory proteins that are activated by oxidants to promote the up-regulation of genes associated with detoxification and repair in response to H_2O_2 exposure (Chiang and Schellhorn, 2012; Choudharz et al., 2024). On reversible oxidation, the oxidized OxyR positively interacts with the RNA polymerase and thereby increases transcription of its target genes (Bang et al., 2016). The sodA gene, encoding superoxide dismutase (SOD), catalyzes the disproportionation of $O_2^{\bullet-}$ to H_2O_2 and oxygen, and represents the main protection system against oxidative stress (Wang et al., 2024). *rec*A is a key regulator gene central to the SOS response, promoting DNA repair during oxidative damage (Sanchez-Alberola et al., 2012). Notably, activation of *rec*A not only promotes DNA repair but also facilitates horizontal gene transfer, thereby accelerating the evolution of resistance. Membrane-associated stress-response genes such as *tol*C (efflux pump) and *omp*F (porin) help bacteria adapt to redox stress and maintain membrane integrity (Sorn et al., 2023; Wang et al., 2024).

In our previous study, we demonstrated the feasibility of aBL for the removal of 4 FPB, 10 ARGs, as well as 16S rRNA and *Intl*1 genes, confirming its practical applicability in wastewater matrices. Here, we report on the inactivation of two relevant facultative pathogenic bacterial strains both carrying ARGs with clinical relevance, namely *P. aeruginosa* PA49 and *E. faecium* B7641, after different aBL treatment. The study uses both culture-based (CFU) and qPCR methods to compare how various analytical methods can affect the interpretation of treatment efficacy. Furthermore, the expression levels of genes involving the bacterial responses to stress under oxidative environments induced by aBL have been determined by reverse transcription quantitative PCR (RT-qPCR). The levels of expression of oxidative stress responsive genes (*oxy*R, *sod*A, *rec*A, *omp*F, and *tol*C) monitored provided an insight into the mechanism of bacterial adaptation and survival. Several studies have documented the evolution of aBL resistance. We therefore see an urgent need to understand the cellular mechanisms of aBL in the wastewater matrix (Kruszewska-Naczk et al., 2024; Rapacka-Zdończyk et al., 2021). By integrating ROS scavenger assays with RT-qPCR analysis of oxidative stress responsive genes, this study for the first time elucidates the cellular mechanisms of aBL disinfection within a complex wastewater matrix, providing novel insights into bacterial adaptation and highlighting the potential of aBL as a sustainable light-based technology for decentralized wastewater treatment. The final goal is the development of an optimized strategy to inactivate hygienically relevant microorganisms in wastewater hotspots.

4.2 Methods

4.2.1 Strains and culture conditions

The bacterial strains used in the aBL assays were *P. aeruginosa* PA49 which is a multi-resistant wastewater isolate (Berditsch et al., 2015) and *E. faecium* B7641 which is a strain of the German collection of microorganisms and contains the *van*A Vancomycin resistance gene (Patel et al., 1997). Primer sequences, amplicon sizes, qPCR conditions, and control strains are provided in Table SC1. *P. aeruginosa* and *E. faecium* cultures were performed by transferring 1.5 mL of an overnight culture to 13.5 mL of LB medium (Luria-Bertani, Sigma-Aldrich, Darmstadt, Germany) and incubated at 37°C with shaking (56 rpm) (CERTOMAT H, Labexchange, Burladingen, Germany). The growth of bacteria was assessed by measuring the optical density at 600 nm (OD_{600}) to be 0.8 with a Hitachi photometer (Hitachi High-Tech Corporation, Tokyo, Japan), which indicates bacterial exponential growth. Following a seven-step serial dilution of the bacterial suspension at a ratio of 1:10 using PBS, five drops of each dilution, each with a volume of 10 µL, were plated onto agar media. Colony counts were determined after incubating using the drop plate method (Herigstad et al., 2001). The CFU were then calculated by averaging the number of colonies across the five drops and converting the result to CFU/mL according to the respective dilution factor.

4.2.2 Chemical reagents and ROS quantification in scavenger studies

Chemical scavengers were applied to explore the roles of individual ROS in aBL. Based on their established specificity in biological ROS studies, 10 mM L-histidine (ITW Reagents) for $^1O_2$ (Méndez-Hurtado et al., 2012), 10 mM Tiron (Thermo Scientific) for $O_2^{\bullet-}$ (Taiwo, 2008), 10 mM tert-butanol (VWR International GmbH) for $OH^{\bullet}$ (Piechowski et al., 1992), and 10 mM Na_2SO_3 (Sigma-Aldrich) for H_2O_2 (Wang et al., 2013) were added to water samples separately for quenching the respective ROS. Preliminary dose–response pre-experiments (1, 5, and 10 mM) confirmed that 10 mM provided consistent scavenging activity without affecting bacterial viability in dark controls. Parallel control samples without scavenger treatment were prepared for comparison. The degradation rate for each aBL-related treatment, both with and without additional scavengers, was determined by calculating the rate constant based on a pseudo-first-order kinetic model, as described by the following equation (Eq. 1):

$$\mathrm{In}(\frac{C_0}{C_t}) = kt \quad (1)$$

In this equation, C (mg/L) represents the gene copy number of the 16S rRNA gene, t (min) is the reaction time, and k (min^{-1}) is the pseudo-first-order rate constant. Additionally, the contribution rate of each ROS, denoted as RC, was estimated using the following equation:

$$RC \cdot OH^{\bullet} = \frac{k_{OH^{\bullet}}}{k_{app}} \approx \frac{k_{app} - k_{tert-butanol}}{k_{app}} \quad (2)$$

$$RC \cdot O_2^{\bullet -} = \frac{k \cdot O_2^{\bullet -}}{k_{app}} \approx \frac{k_{app} - k_{Tiron}}{k_{app}} \quad (3)$$

$$RC \cdot {}^1O_2 = \frac{k_{^1O_2}}{k_{app}} \approx \frac{k_{app} - k_{L-histidine}}{k_{app}} \quad (4)$$

$$RC \cdot H_2O_2 = \frac{k_{H_2O_2}}{k_{app}} \approx \frac{k_{app} - k_{Na2SO3}}{k_{app}} \quad (5)$$

In these equations, k_{app} is the apparent rate constant for 16S rRNA gene degradation in the control group (without scavenger), while $k_{tert\text{-}butanol}$, k_{Tiron}, $k_{L\text{-}histidine}$, and k_{Na2SO3} represent the rate constants in the presence of specific ROS scavengers targeting $OH^{\bullet}$, $O_2^{\bullet -}$, $^1O_2$, and H_2O_2, respectively.

4.2.3 Sampling and experimental setup

4.2.3.1 Experimental setup for CFU and qPCR comparison

To compare culture-based and molecular quantification methods, bacterial suspensions from the reference strains *P. aeruginosa* PA49 and *E. faecium* B7641 were prepared and processed as follows:

From the 11 mL bacterial suspension, 5.0 mL were aliquoted into 2.0 mL reaction tubes and centrifuged (BIOFUGE pico, Heraeus, Waltham, USA). The supernatant was discarded and the pellets were resuspended in 50 µL of PBS. The suspensions from the three reaction tubes were combined in a single 2.0 mL tube and stored at –18 °C. This constituted the initial sample (t_o) for subsequent DNA extraction. Additionally, 200 µL were transferred into a 1.5 mL tube for the t_o dilution series and cultivation. The same procedure was repeated following aBL treatment, representing the irradiated samples.

For aBL irradiation, 5.2 mL of bacterial suspension were placed in sterile 10 mL glass vials with sterilised magnetic stir bars (Ø 2 mm × 5 mm). In selected samples, TMPyP was added to a final concentration of 10^{-6} M, shown to effectively reduce ARB in aBL

applications (Cong et al., 2023). The photosensitizer in use, TMPYP was obtained from Sigma-Aldrich (Darmstadt, Germany).

5,10,15,20-Tetrakis(1-methyl-4-pyridinio)-porphyrin tetra (p-toluenesulfonate) (TMPyP) is a well-known PS used for aBL (Chaves et al., 2017). TMPyP has a planar tetracationic structure of porphyrin ring system (Figure SC1), which makes it to have a strong absorbance in the visible light and especially in Soret band (~400 nm), which is proper for photodynamic activation. A stock solution of TMPyP at 10^{-3} M is employed. 1×10^{-6} M, the more diluted sample, was taken for experimental purposes as well. Concentrations of TMPyP are selected based on empirical work that has shown them to be most effective in combatting antibiotic resistance (Cong et al., 2023). These samples were incubated in the dark for 30 minutes, and subsequent handling was performed under light-protected conditions to prevent unintended PS activation.

The static aBL photoreactor used in this experiment (Figure SC2) differed from the system applied for scavenger studies and oxidative stress gene expression analysis. It consisted of six LED lamps (L XS series, S/N 0281; Opsytec Dr. Gröbel GmbH, Ettlingen, Germany), each emitting at 420 nm with a total energy dose of 245 W/m^2 and 98.4% radiation intensity. Glass vials were placed on a magnetic stirrer (2Mag) mounted on a height-adjustable platform (Swiss Boy), both secured with adhesive foil, maintaining a 15.5 cm distance from the LEDs. The entire setup was housed in a temperature-controlled incubator (Memmert ICP 600) at 20 °C to prevent heat-induced effects. Irradiation conditions included: 2 h aBL, 4 h aBL, and 2 h aBL + TMPyP (10^{-6} M), each with n = 3 replicates.

4.2.3.2 Wastewater samples collection and experimental setup for scavenger studies and gene expression

To evaluate the role of ROS and bacterial oxidative stress responses under aBL treatment, wastewater samples were collected from the local WWTP influent located on the campus of the KIT in Karlsruhe, Germany. This facility primarily receives wastewater from scientific research institutes and serves a population of approximately 3,300 individuals, including international researchers and students during the academic week. The WWTP processes around 450 m^3 of wastewater daily using a combination of conventional physical and biological treatment methods. Influent samples from the WWTP were collected for further analysis.

The scavenger study primarily focused on aBL alone and aBL combined with TMPyP. Both scavenger-containing and control samples (without scavengers) were transferred into

sterile 20-mL glass vials, each containing a sterilized magnetic stir bar (Ø 2 mm × 5 mm) and subjected to aBL treatment in a static photoreactor setup. For each individual scavenger evaluated under both treatment conditions (aBL alone and aBL combined with TMPyP), three independent trials (n=3) were conducted for subsequent molecular analysis. Illumination was provided by four SolarStinger SunStrip DeepBlue LED bars (Econlux, Germany), each incorporating chips at 400, 420, 440, and 460 nm to deliver a broad-spectrum blue light source (Figure SC3). Further technical details are available in our previous study (Cong et al., 2023).

However, for the gene expression analysis of oxidative stress–responsive genes, all three treatment regimens were included: aBL alone, aBL + TMPyP (10^{-6} M), and aBL + H_2O_2 (1 mM). Oxidative agent H_2O_2 was tested at a final concentration of 1 mM and combined with aBL irradiation for its synergistic effect, as previous studies have also reported enhanced disinfection efficiency when aBL is used together with H_2O_2 (Ngo et al., 2023). The selected dose is within the reported range of ideal concentrations for ROS production without self-scavenging of $OH^{\bullet}$ (Truong et al., 2020). Control experiments showed that neither TMPyP (1×10^{-6} M) nor H_2O_2 (1 mM) were able to kill the bacteria in the dark without aBL irradiation. Enhanced bacterial inactivation was observed only when these agents were combined with blue light irradiation.

Scavenger assays were performed in triplicate (n=3), while gene expression experiments were conducted in four independent biological replicates (n=4). For both scavenger analysis and oxidative stress gene expression studies, a static aBL photoreactor (Figure SC3) was used, consistent with the setup previously applied by Cong et al. (2023). Following aBL treatment, 18 mL of sample, whether from the scavenger or gene expression experiments, was passed through a 47 mm, 0.2 µm polycarbonate membrane (Whatman Nucleopore Track-Etched, Sigma-Aldrich, Munich). Following filtration, membranes were treated with 20 µM PMA to differentiate live from dead bacteria. PMA selectively penetrates cells with compromised membranes and binds nucleic acids, thereby preventing amplification during qPCR. Samples were incubated in the dark for 10 min to avoid photodegradation, followed by photo-activation with the PhAST Blue system (GenIUL, Barcelona, Spain) at maximum intensity for 15 min to cross-link PMA to DNA (Cong et al., 2023; 2025). DNA extracted from these filters was used for qPCR in scavenger analysis, and RNA was isolated for gene expression analysis via RT-qPCR.

4.2.4 DNA extraction for Quantitative PCR (qPCR) analysis

DNA was extracted using the FastDNA™ Spin Kit for Soil (MP Biomedicals, Santa Ana, USA) in combination with the FASTPREP® homogenization system (MP Biomedicals, Santa Ana, USA). For mechanical cell disruption, the filtered biomass retained on the membranes was transferred into Lysing Matrix E tubes and processed according to the manufacturer's protocol. Proteins were removed by centrifugation and precipitation, and DNA was subsequently purified via binding to a silica matrix. The concentration of the extracted DNA was measured using both a NanoDrop spectrophotometer (ND-1000, PEQLAB Biotechnologie GmbH, Germany) and the Quant-iT™ PicoGreen® dsDNA Assay Kit (Thermo Fisher Scientific, Nidderau, Germany).

Quantitative real-time PCR (qPCR) assays using SYBR Green were performed with a Bio-Rad CFX96 Touch™ Deep Well Real-Time PCR Detection System (Bio-Rad, Munich, Germany), and data analysis was conducted using the Bio-Rad CFX Manager Software. Each reaction was carried out in a total volume of 20 µL, consisting of 10 µL Maxima SYBR Green/ROX qPCR Master Mix (2×) (Thermo Scientific, Nidderau, Germany), 7.4 µL nuclease-free water (Ambion, Life Technologies, Karlsbad, Germany), 0.8 µL forward primer (10 µM), 0.8 µL reverse primer (10 µM), and 1 µL of template DNA. Thermal cycling conditions included an initial denaturation step at 95 °C for 10 minutes, followed by 40 amplification cycles of 15 seconds at 95 °C and 60 seconds at 60 °C. Melting curve analysis was performed at the end of each run to verify amplification specificity. In this study, four genetic targets were analyzed to assess bacterial abundance and antibiotic resistance: *secE* (a taxonomic marker gene specific for *Acinetobacter baumannii*), *ermB* (a macrolide resistance gene), 16S rRNA gene (a universal marker for eubacterial abundance), and bla_{TEM} (a β-lactamase gene associated with resistance to penicillins). Primer sequences and related details are provided in Table SC2. DNA extraction has also been applied by KITs lab in related wastewater resistance studies (e.g., Hembach et al., 2019).

4.2.5 RNA extraction and RT-qPCR analysis

After the filtration steps, the filters were directly transferred into Lysing Matrix E Tubes (MP™ Biomedicals, USA) and 700 µL of RLT Buffer (QIAGEN, Netherlands) was added. The samples were homogenized for 40 seconds using a Fast-Prep R24 (MP™ Biomedicals, USA) and then vortexed for 15 seconds. The upper aqueous phase was carefully transferred to a new tube, mixed with 700 µL of 70% ethanol (prepared from

absolute ethanol, VWR™ Chemicals, USA), and loaded onto a RNeasy Mini Spin Column. The column was centrifuged at 11,000 rpm for 15 seconds, and the flow-through was discarded. Next, 350 µL of RW1 buffer was added to the column followed by centrifugation. To remove contaminating DNA, a digestion solution comprising 10 µL of DNase I stock and 70 µL of RDD buffer was applied directly to the column and incubated at room temperature for 15 minutes. Following incubation, 350 µL of RW1 buffer was added to the column. The column was then washed twice with 500 µL of RPE buffer, with centrifugation after each wash to discard the flow-through. Finally, the column was transferred to a new 1.5 mL collection tube, and 50 µL of RNase-free water was added. After centrifugation at 11,000 rpm for 1 minute, the RNA was eluted and collected. RNA concentration was determined using a NanoDrop 1000 Spectrophotometer (peqlab Biotechnologie GmbH, Germany), and the samples were used immediately for cDNA synthesis.

cDNA synthesis was performed using the SuperScript™ IV kit (Thermo Fisher Scientific, USA). For each sample, duplicate reactions were prepared. Thermal cycling was conducted on a C1000 Touch™ Thermal Cycler (Bio-Rad Laboratories, USA). For the annealing step, 1 µL of random hexamer primer, 1 µL of 10 mM dNTPs, and 50 ng of RNA template were combined, and nuclease-free water was added to bring the total volume to 13 µL. The mixtures were vortexed, briefly centrifuged, heated to 65 °C for 5 minutes, and then cooled to 2 °C for 2 minutes. For the elongation reaction, 4 µL of 5X SSIV buffer, 1 µL of 100 mM DTT, 1 µL of RNase inhibitor, and 1 µL of SuperScript IV polymerase were added to each reaction. After mixing and a brief centrifugation, the reactions were incubated at 50 °C for 10 minutes, followed by 80 °C for 10 minutes. Subsequently, 1 µL of RNase H was added, and the reactions were incubated at 37 °C for 20 minutes to remove residual RNA. The concentration of cDNA was determined using a NanoDrop 1000 Spectrophotometer (peqlab Biotechnologie GmbH, Germany), and the samples were stored at –20 °C. Additionally, quantitative PCR was performed on all cDNA samples (with the sequence described in Table SC2) using bacterial primers. Reactions were performed in volumes of 20 µL containing 10 µL Maxima SYBR Green/ROX qPCR Master Mix (2×) (Thermo Scientific Nidderau, Germany), 7.4 µL nuclease-free water (Ambion, Life technologies, Karlsbad, Germany), 0.8 µL primer forward (10 µM), 0.8 µL primer reverse (10 µM) and 1 µL template DNA. In the denaturation phase, double-stranded DNA was converted into single strands by heating at a high temperature (about 95 °C) for 10 min. This was followed by 40 cycles of 15 s at 95 °C and 60 s at 60 °C. The melting curves were recorded by increasing the temperature from 60 °C to 95 °C (1 °C every 10 s) to assess the specificity of the application. RT-qPCR assays were conducted following the MIQE guidelines for qPCR experiments (Bustin et al., 2009). 16s rRNA was used as a

reference gene to which the gene expression values were normalized (Smith & Osborn, 2009), and gene expression levels of stress-response genes were determined using the $2^{\wedge-\Delta\Delta Ct}$ method (Pfaffl et al., 2001; Livak & Schmittgen, 2001), with expression normalized to a housekeeping gene and relative to a control condition. Additionally, the standard curve of all oxidative stress response genes is provided in the supplementary information (Table SC4) and the corresponding primer details are listed in Table SC2.

4.2.6 Statistical Analysis

Gene expression data were analyzed in Graphpad Prism 10 (Graphpad software) using the two-tailed Mann-Whitney U test. Results with $p < 0.05$ were considered statistically significant, while $p < 0.10$ were regarded as trend-level and interpreted with caution (Schacksen et al., 2025). Results with $p < 0.1$ were highlighted in bold in Table 4.2. Scavenger assay data were compared by one-way ANOVA followed by Tukey's multiple comparison tests to evaluate differences between the control, aBL alone, and aBL combined with TMPyP or H_2O_2. The resulting *p*-values were used to determine statistical significance, which is indicated in the figures as follows: not significant (ns), $p \leq 0.0001$(****), $p \leq 0.001$ (***).

4.3 Results and discussion

4.3.1 Reduction effectiveness of aBL irradiation determined by cultivation and qPCR

The antimicrobial efficacy of aBL treatment was assessed by survival of the reference strains *P. aeruginosa* PA49 and *E. faecium* B7641 using culture based (CFU) and molecular methods (qPCR). The initial CFU counts of untreated cultures were 6.8×10^8 CFU/mL for *P. aeruginosa* and 9.2×10^7 CFU/mL for *E. faecium*. The corresponding error bars are shown in Figure 4.1.

Both strains showed a decrease in CFU mL^{-1} after aBL treatment, as depicted in Figure 4.1. In *P. aeruginosa*, 4.6 $\log_{10}$ unit reduction was obtained at 2 h after aBL (2.2×10^3 CFU mL^{-1}). Significantly, the CFU were not detected (n.d.) for both 4 h aBL and 2 h aBL + TMPyP treatments, with an at least 6.5 $\log_{10}$ unit reduction. *E. faecium*, on the other hand, was reduced below $\log_{10}$ 4 at 2 h aBL and below $\log_{10}$ 5 at 4 h aBL. Only for the combined treatment (2 h aBL + TMPyP) the CFU were not detected (≥6 $\log_{10}$ unit reduction).

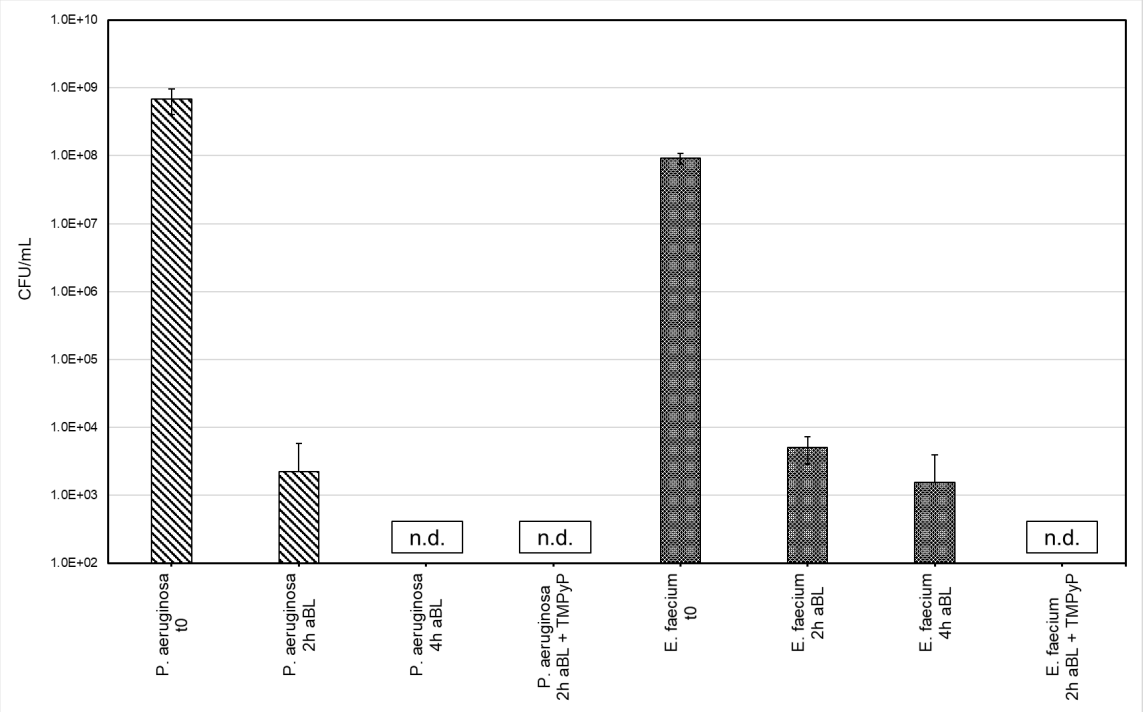

Figure 4.1: Logarithmic CFU/mL values, including standard deviations, are shown as light patter bars for *P. aeruginosa* and dark bars for *E. faecium*. Data are presented for untreated initial samples (t_o) and for samples following 2 h aBL, 4 h aBL, and 2 h aBL + TMPyP treatments (n=3). All aBL exposures were conducted using 420 nm LED lamps within a static photoreactor. In case of no colony detection these samples are indicated by n.d.: not detected.

Overall, the results demonstrate that *P. aeruginosa* can be inactivated more effectively by aBL than *E. faecium* as judged by cultivation results. Molecular analyses, however, allowed examination of this discrepancy in susceptibility further. The $\log_{10}$ unit reductions (measured by qPCR, Table 4.1) in cell equivalents/100 mL are presented in comparison to the initial numbers at t_0. It is worth noting that *in P. aeruginosa*, while the taxonomic marker gene (*ecf*X) and the resistance gene (bla_{VIM}) themselves were not completely depleted by aBL treatment, combined with TMPyP, respectively. Such a limited efficacy at the DNA level despite pronounced CFU loss could also explain that the highest observed drop was 1.17 $\log_{10}$ for *ecf*X and 1.42 $\log_{10}$ for bla_{VIM} for aBL plus TMPyP. These results are consistent with the previous study of Cong et al. (2025), indicating that culturability may be lost in *P. aeruginosa* under oxidative stress, while DNA is mostly preserved. In contrast, *E. faecium* showed only minimal gene copy number reduction after aBL exposure alone. Notably, at 2 h, we observed a small rise in cell equivalents. This transient increase does not indicate growth. One hypothesis is rapid repair of sublethal

oxidative lesions caused by aBL. This repair could resuscitate VBNC cells and restore culturability, which raises CFU relative to t_0 while qPCR targets remain stable. A second hypothesis is an analytical effect in qPCR. Inactivation treatments can disrupt envelopes and matrices, release intracellular DNA, and reduce PCR inhibition. These changes improve target recovery and lower Cq values, so gene copies per milliliter can appear to increase even as cellular activity declines. However, when aBL was combined with TMPyP, a marked decrease was observed, specifically, 5.61 $\log_{10}$ and 7.14 $\log_{10}$ unit reductions in the enterococci specific 23S rRNA gene and Vancomycin *van*A resistance gene in *Enterococcus faecium*, respectively. These results demonstrate the enhanced efficacy of aBL treatment when photoactivation is intensified by TMPyP and highlight *E. faecium*'s greater vulnerability to DNA-targeted oxidative damage under these conditions.

This discrepancy between CFU and qPCR is particularly pronounced in *P. aeruginosa*. While culture results indicate high susceptibility to aBL, qPCR suggests that the DNA of these cells remains largely intact. This observation is indicative of a “VBNC” state in which the bacteria are metabolically active but not culturable in the synthetic nutrient media. Consistent with this, DNA integrity in aBL-exposed *P. aeruginosa* was not affected and gene copy numbers were constant. For *E. faecium*, the correlation between CFU loss and qPCR data was better, especially upon aBL + TMPyP treatment. However, a minor discrepancy still suggests the presence of VBNC cells or sub-lethally damaged DNA.

These observations underscore the need of combining culture-based and molecular techniques when assessing antimicrobial interventions. Although CFU numbers only offer an estimation of viability, qPCR let us assess the presence of undamaged genetic material, thereby uncovering possible persistence mechanisms such as VBNC. Notably, the addition of TMPyP significantly enhanced aBL efficacy, especially against *E. faecium*, and may help overcome limitations related to sub-lethal or stress-tolerant bacterial states. These findings emphasize the necessity to carefully choose the analytical methodology in order to properly assess and optimize new disinfection procedures.

Table 4.1: The cell equivalents/100 mL are presented as mean values with standard deviation, along with the resulting log_{10} reductions, which are calculated relative to the average initial concentration at t_0 following 2 h aBL, 4 h aBL, and 2 h aBL + TMPyP treatments. The mean values of the cell equivalents/100 mL are calculated for t_0 (n = 9) and for the individual irradiation conditions (n = 3) for all four qPCR targets. These standard deviations represent the mean of the standard deviations of the cell equivalents/100 mL for each experiment. *ecf*X and *23S* represent taxonomic gene markers for *P. aeruginosa* and *E. faecium*, respectively, while *bla*$_{VIM}$ and *van*A denote their corresponding antibiotic resistance genes. Positive log_{10} values indicate a reduction in gene copy number, whereas negative values reflect an increase. Larger absolute values correspond to greater changes in concentration. The log_{10} reductions of 2h aBL + TMPyP for *ecf*X, *bla*$_{VIM}$, *23*S and *van*A are shown in bold to highlight the difference in the log_{10} reduction between *P. aeruginosa* and *E. faecium.*

Sample	Cell equivalents/100 mL	Log_{10} reduction
*ecf*X (*P. aeruginosa)*, reference t_0	$1.23 \times 10^{10} \pm 2.04 \times 10^{9}$	
*ecf*X (*P. aeruginosa)*, 2h aBL	$3.64 \times 10^{10} \pm 4.32 \times 10^{9}$	-0.47
*ecf*X (*P. aeruginosa)*, 4h aBL	$8.94 \times 10^{9} \pm 6.47 \times 10^{8}$	0.14
***ecf*X (*P. aeruginosa)*, 2h aBL + TMPyP**	**$8.33 \times 10^{8} \pm 9.03 \times 10^{7}$**	**1.17**
bla$_{VIM}$ (*P. aeruginosa)*, reference t_0	$4.46 \times 10^{10} \pm 6.14 \times 10^{9}$	
bla$_{VIM}$ (*P. aeruginosa)*, 2h aBL	$9.37 \times 10^{10} \pm 3.53 \times 10^{9}$	-0.32
bla$_{VIM}$ (*P. aeruginosa)*, 4h aBL	$1.50 \times 10^{10} \pm 7.73 \times 10^{9}$	0.47
***bla*$_{VIM}$ (*P. aeruginosa)*, 2h aBL + TMPyP**	**$1.69 \times 10^{9} \pm 1.38 \times 10^{9}$**	**1.42**
*23*S (*E. faecium*), reference t_0	$2.67 \times 10^{10} \pm 3.00 \times 10^{9}$	
*23*S (*E. faecium*), 2h aBL	$4.00 \times 10^{10} \pm 2.38 \times 10^{9}$	-0.17
*23*S (*E. faecium*), 4h aBL	$5.21 \times 10^{9} \pm 7.63 \times 10^{7}$	0.71
***23*S (*E. faecium*), 2h aBL + TMPyP**	**$6.58 \times 10^{4} \pm 4.19 \times 10^{3}$**	**5.61**
*van*A (*E. faecium*), reference t_0	$3.38 \times 10^{11} \pm 8.21 \times 10^{10}$	
*van*A (*E. faecium*), 2h aBL	$5.26 \times 10^{11} \pm 1.09 \times 10^{11}$	-0.19
*van*A (*E. faecium*), 4h aBL	$5.84 \times 10^{10} \pm 7.90 \times 10^{9}$	0.76
***van*A (*E. faecium*), 2h aBL + TMPyP**	**$2.46 \times 10^{4} \pm 2.41 \times 10^{3}$**	**7.14**

4.3.2 Identification of specific ROS responsible for the degradation of ARGs and FPB

Two aBL-treated groups (aBL, aBL/TMPyP) were analyzed for the efficacy of inactivation of the *A. baumannii*, and degradation of three selected genes (*erm*B, 16S rRNA, and *bla*$_{TEM}$) in this region. *A. baumannii* was selected because it is an ESKAPE pathogen and a WHO critical-priority organism (carbapenem-resistant lineages), is frequently detected in municipal wastewater and hospital effluents. 16S rRNA provides a broad proxy for total

bacterial DNA, *erm*B is a prevalent and often mobile macrolide resistance marker in wastewater, and bla_{TEM} represents a clinically important β-lactamase gene commonly found in WWTP ecosystems. Notably, our previous study employed a substantially broader suite of taxa and ARGs to establish the overall efficacy of aBL/aBL + photosensitizer; the present work builds on that foundation to resolve which ROS dominate under wastewater conditions and how strongly they affect representative genetic targets. The samples were collected from the influent of the WWTP at KIT. The static aBL photoreactor used in these experiments is illustrated in Figure SC3.

aBL combined with TMPyP appeared to be the optimal aBL tested for the killing of *A. baumannii* and the eradication of the three genes targeted (as presented in Figure 4.2). The individual cell equivalents obtained from qPCR for treatments with ROS scavengers were compared to those without scavengers. The results are presented as $\log_{10}$ fold changes, as shown in Figure 4.2. A value around 0 indicates that the addition of a scavenger had little to no effect on gene abundance, suggesting minimal interference with ROS activity. Positive $\log_{10}$ values reflect an increase in gene abundance relative to the treatment alone, indicating that the scavenger reduced the efficacy of photoinactivation, likely by quenching ROS. Higher values, therefore, suggest greater ROS involvement in the treatment effect. Notably, the aBL + TMPyP treatment group showed the most substantial decline in gene copy numbers, with a particularly stronger decrease in 16S rRNA gene abundance (as shown in Table SC3) and this effect was markedly diminished upon the addition of some ROS scavengers. This comes from that this combination was apparently most efficient in generating ROS, which we discussed above. The comparative analysis further demonstrated that the effectiveness of each treatment is directly influenced by the type and concentration of ROS generated, as well as by the susceptibility of specific bacterial strains and genetic targets. Particularly, $^1O_2$ and H_2O_2 have been identified as the major species contributing to the bacterial and gene degredation in the aBL + TMPyP regimen. In line with this, the addition of L-histidine and Na_2SO_3 (as quencher of $^1O_2$ and H_2O_2, respectively) resulted in a quantifiable reduction of the antimicrobial effect: for $^1O_2$ scavenging, gene copy numbers increased by approximately 2 $\log_{10}$ units for all investigated targets. Similarly, quenching H_2O_2 resulted in approximately 2 $\log_{10}$ increase for *sec*E, 16S, and around 1 $\log_{10}$ increase for bla_{TEM}, and a more pronounced 3.2 $\log_{10}$ increase for *erm*B after 4 hours of treatment. Such uniform pattern of all the genes quantified confirms the key role played by $^1O_2$ and H_2O_2 as main ROS inducing gene degradation and bacterial inactivation under aBL + TMPyP treatment (Figure 4.2B).

The relatively limited efficacy of aBL alone suggests that, while partially effective, this treatment may require optimization or combination with other agents to achieve maximal inactivation of bacteria and ARGs. This is also confirmed by the scavenger assay, since ROS inhibition in these treatments resulted in less than one $\log_{10}$ unit of higher gene copy numbers for all the targets detected (Figure 4.2A). As we did not directly quantify ROS, we do not draw conclusions about ROS yields. We interpret the small scavenger effects as evidence that, under our conditions, ROS made only a limited but detectable contribution to the measured molecular endpoint. We infer that ROS were not the principal drivers of gene degradation, or that their effects fell below our assay's sensitivity. These observations motivate tests that amplify ROS pathways.

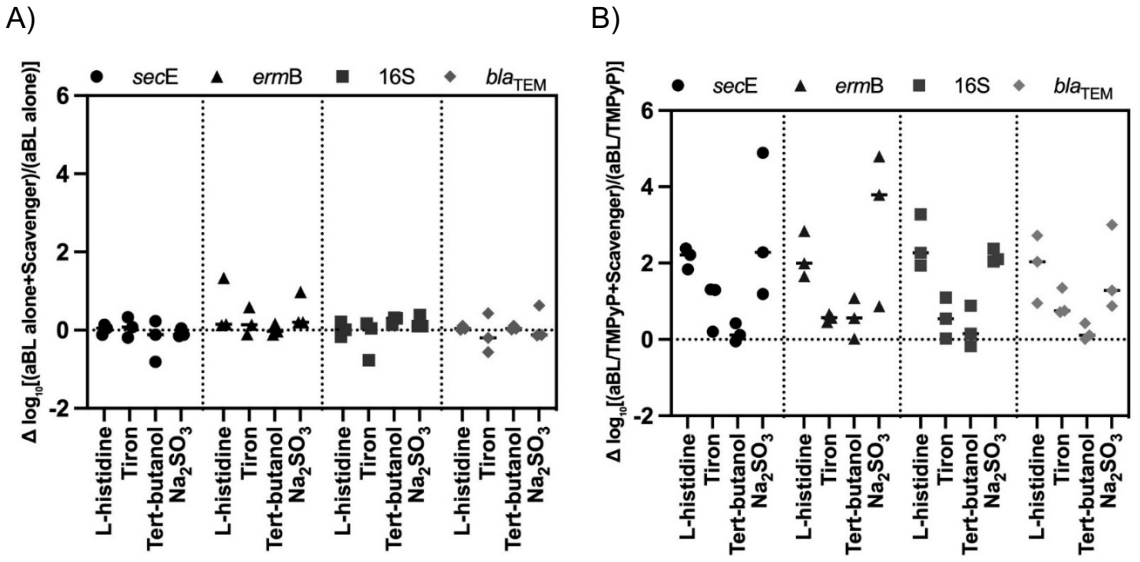

Figure 4.2: The plots show the relative abundance of bacterial genes after treatment with different ROS scavengers (L-histidine, Tiron, Tert-butanol, Na_2SO_3) combined with treatments either (A) aBL alone or (B) the photosensitizer TMPyP (n=3). The y-axis indicates the $\log_{10}$-transformed ratio of gene abundance in treated samples (treatments + scavenger) relative to control (treatments) after 4h irradiation time, measured in cell equivalents per 100 mL. Each data point represents a qPCR-based quantification of one of four bacterial gene targets: *sec*E, *erm*B, 16S rRNA gene, and bla_{TEM}. Dotted vertical lines separate different scavenger groups, and the same scavenger order is used across both panels. Mean value for each group are indicated by horizontal lines.

The measured attenuation of the aBL antimicrobial effect after removing ROS further verifies the criticality of ROS in aBL disinfection mechanism. These data highlight the importance of selecting optimized photosensitizers for ROS generation, if treatment

efficacy is to be enhanced, especially for decentralized wastewater disinfection applications. Indeed, TMPyP is a very efficient photosensitizer in this respect but more specific derivatives or even a more potent agent might be subject to future studies, including better definition of the irradiation conditions and potential synergism with other treatments. In addition, more deep mechanisms are required to understand how the individual ROS interacts with bacteria cells and ARGs at the molecular level. These findings will be critical to guide the rational design and application of future-generation light-activated antimicrobial strategies.

Four scavengers (tert-butanol, Tiron, L-histidine, Na_2SO_3) were used, as previously described, in order to selectively quench ROS species ($OH^{\bullet}$, $O_2^{\bullet-}$, $^1O_2$, and H_2O_2, respectively). This method facilitated the evaluation of the involvement of ROS in different treatment protocols. To assess the degradation kinetics of bacterial gene targets during different aBL treatment conditions, with or without the addition of ROS scavengers, a pseudo-first-order kinetic model was applied. Quantification was based on changes in 16S rRNA cell equivalents (Table SC3), comparing initial concentration (C_0) to those at time t (240 mins, C_t). Mean values from three independent trials were calculated and used for evaluation and comparison. It is evident that when aBL combined with TMPyP was applied, the corresponding rate constant (k) significantly decreased from 0.03 min^{-1} in the control experiment (without scavengers) to 0.006 min^{-1} and 0.009 min^{-1} in the presence of L-histidine and Na_2SO_3, respectively (as shown in Figure 4.3B). These results provide evidence that $^1O_2$ and H_2O_2 made the dominant contributions to the degradation of bacteria in this system. Calculated relative contributions (RC) of each ROS in aBL + TMPyP were the following: $^1O_2$ (78%) > H_2O_2 (68%) > $O_2^{\bullet-}$ (17%) > $OH^{\bullet}$ (9%). For aBL lone (As shown in Figure 4.3A), ROS played a less significant role in bacterial inactivation, as indicated by minimal changes in the degradation rate constant after the addition of specific scavengers. In the case of aBL-alone treatment, $^1O_2$ was the least useful ROS during bacterial inactivation process. On the contrary, contribution rates in $OH^{\bullet}$, $O_2^{\bullet-}$, and H_2O_2 demonstrated substantially higher relative contributions. Results suggest that while aBL on its own generates multiple ROS, their overall bactericidal impact is limited without an external photosensitizer. The presence of TMPyP is the major determinant that tips the balance toward ROS species, namely $^1O_2$ and H_2O_2, which are relevant for efficient inactivation of bacteria.

These results indicate that the major ROS for bacteria inactivation are quite different, depending on the treatment composition. In particular, $^1O_2$ and H_2O_2 were found to be the most abundant ROS involved in the bactericidal action with the combination of aBL and

TMPyP. Furthermore, in the case of aBL applied without specific substances, $OH^{\bullet}$, $O_2^{\bullet-}$, and H_2O_2 played an important role in bacterial inactivation, whereas $^1O_2$ had the lowest effect. These findings emphasize the need to optimize aBL based disinfection for the ROS differentially produced under different treatment circumstances. Strategic optimization, e.g., choosing the suitable photosensitizers and ROS enhancers, and maintaining small local variations in the wastewater microbial communities are needed to maximize the bacteria inactivation and ARGs degradation.

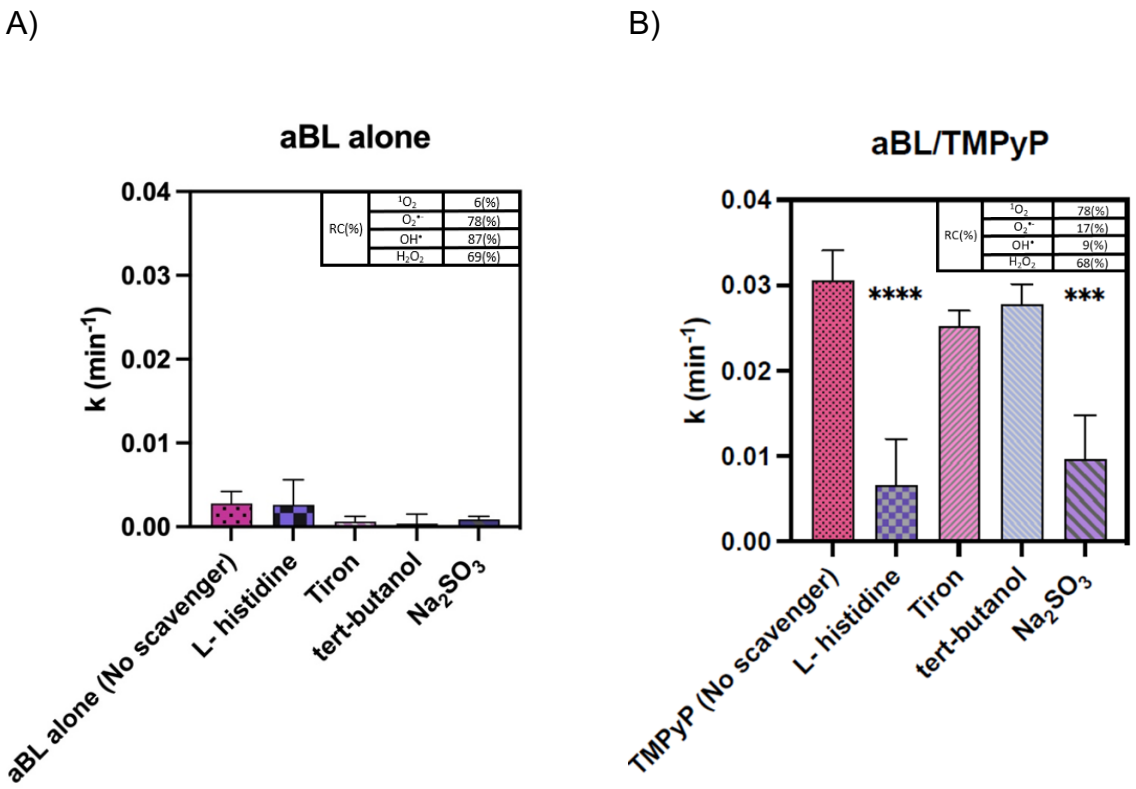

Figure 4.3: Comparative analysis of the degradation kinetics (k/min) of bacterial cells under (A) aBL alone and (B) aBL+TMPyP in the presence and absence of specific ROS scavengers. Each treatment was evaluated with four scavengers: L-histidine (targeting $^1O_2$), Tiron ($O_2^{\bullet-}$), tert-butanol ($OH^{\bullet}$), and Na_2SO_3 (H_2O_2). Bars represent the mean degradation rate constants (k) ± standard deviation (n=3), and statistical significance is indicated as $p \leq 0.0001$(****), $p \leq 0.001$ (***). Insets show the calculated relative contributions (RC%) of each ROS to bacterial inactivation for the respective treatment.

4.3.3 Quantification of ROS-responsive regulatory genes

RT-qPCR showed the different gene expression responses to various aBL treatments. The samples were collected from the influent of the WWTP at KIT. In the Table 4.2, we show the $2^{-\Delta\Delta Ct}$-derived expression fold changes of five core genes (i.e., *rec*A, *sod*A, *omp*F, *oxy*R, and *tol*C) to three treatment options (aBL alone, aBL + H_2O_2 and aBL + TMPyP). These treatment conditions were consistent with those used in our previous study (Cong et al., 2025).

All treatments resulted in significantly increased expression of *sod*A, *rec*A, *oxy*R and *tol*C, most notably by aBL combined with TMPyP, and a decrease in *omp*F. Excessive ROS can activate the processes of detoxification as well as culminate in the SOS response in bacterial cells. The gene product of *sod*A enzyme, which is a key enzyme for detoxification of oxidative stress, was significantly up-regulated under aBL treatment alone (>2-fold in the present study), being indicative of the strong oxidative stress response. This observation is supported by ROS scavenging assays and detected significant generation of $O_2^{\bullet-}$ in the existence of aBL. Also, the expression of *rec*A, which is a key regulator in the SOS response, was highly induced (>2-fold) when aBL was added to TMPyP, implying possible genotoxic damage and the induction of the subsequent DNA repair system. *Oxy*R, which is also involved in H_2O_2 detoxification, was the most strongly induced gene (>3-fold) following aBL+TMPyP treatment, emphasising the increased oxidative stress generated by this combined treatment.

Of all the outer membrane protein genes studied, *tol*C, which is associated with efflux pump systems, was significantly upregulated in all aBL-related treatments as compared to control conditions and this change was especially pronounced (>3-fold) under aBL+TMPyP, indicating increased efflux of toxic metabolites. In contrast, aBL changed the transcriptional expression of *omp*F in all the experiments, indicating that the *omp*F was down the control suggesting protective reduction in the permeability of the membrane that would result in prevention from entry of toxic substances (Bystritskaya et al., 2014).

Such findings emphasize the strong oxidative and genotoxic stress reaction induced by aBL, particularly after combination with a photosensitizer. The observed transcription profiles highlight the crosstalk between oxidative stress and bacterial defense mechanisms. It supports the involvement of ROS through the up-regulation of stress response genes, particularly under aBL plus TMPyP. Specifically, the upregulation of key genes, including those involved in antioxidant defense (*sod*A), DNA repair (*rec*A) and membrane stess

response (*tol*C), confirms that aBL-based treatments induce both DNA and membrane damage.

These molecular responses are correlated with the earlier discovery showed by ROS scavenger and gene degradation tests, supporting a conclusion that aBL-based disinfection induced a variety of stress pathways, such as antioxidant defence, DNA repair, and cell membrane adaption mechanisms. Overall, the evidence suggests that aBL treatments trigger a coordinated bacterial response encompassing oxidative detoxification, SOS-mediated DNA repair, and adaptive membrane regulation.

Table 4.2: Quantitative analysis of relative gene expression in wastewater from WWTP influent treated with aBL under three conditions: aBL alone, aBL+H_2O_2, aBL+TMPyP. Expression of five target genes (*rec*A, *sod*A, *omp*F, *oxy*R, *tol*C) was measured via RT-qPCR and calculated using the $2^{-\Delta\Delta Ct}$ method, normalized to 16S rRNA. Results are expressed as x-fold change relative to the untreated control, which is set to a value of 1. Data represent the mean ± standard deviation from four independent biological replicates (n=4). Statistical significance compared to the control was assessed using the Mann-Whitney U test; p values < 0.1 were considered significant and are indicated in bold.

Normalized to 16S rRNA expression				
		x-fold change	st.dev	p-value
***rec*A**	aBL alone	0.96	0.63	0.6
	aBL+H_2O_2	0.71	0.28	0.3429
	aBL+TMPyP	2.5	2.39	-
***sod*A**	aBL alone	2.48	2.14	0.8857
	aBL+H_2O_2	1.34	1.37	0.4857
	aBL+TMPyP	0.72	0.49	0.4857
***omp*F**	aBL alone	0.13	0.03	**0.0571**
	aBL+H_2O_2	0.21	0.25	**0.0571**
	aBL+TMPyP	1.12	0.68	0.8857
***oxy*R**	aBL alone	2.65	2.46	0.6857
	aBL+H_2O_2	2.82	4	0.8857
	aBL+TMPyP	3.11	1.81	0.2
***tol*C**	aBL alone	1.38	0.41	-
	aBL+H_2O_2	2.57	3.39	-
	aBL+TMPyP	4.29	2.93	0.3429

4.4 Conclusion and Perspectives

This work proves aBL, especially with the presence of the photosensitizer TMPyP or oxidative agent H_2O_2, is an efficiently emerging approach for inactivation of ARB and ARGs in wastewater. The relative values obtained from CFU enumeration and qPCR indicate that it was necessary to use culture-dependent and molecular methods in parallel to better examine the effectiveness of disinfection strategies, especially for organisms that may be able to enter into a VBNC state. Notably, understanding the mechanisms behind inactivation strategies requires insights into physiological and genetic responses that cultivation alone cannot provide. Therefore, in this study, molecular analyses, including gene degradation and expression profiling, were employed to elucidate the mechanisms underlying the antimicrobial effects of the innovative aBL technology.

Compared with other aBL treatments, aBL+TMPyP yielded the highest inactivation efficiency, mediated by ROS production, especially $^1O_2$ and H_2O_2, which were the primary ROS for gene and cell degradation. Upregulation of oxidative stress response genes (*oxy*R, *sod*A, *rec*A, and *tol*C) and downregulation of *omp*F which were confirmed by RT-qPCR, signified that the bacteria had successfully adapted to the ROS-induced damage. Collectively, our results establish a mechanistic basis for ROS-mediated disinfection and demonstrate the feasibility of aBL as a decentralized wastewater treatment option. The technology can support pilot-scale installation and on-site deployment. The approach offers a low-risk, mercury-free alternative to conventional UV systems, which is particularly suitable for high-risk effluents at AMR hotspots. The findings provide guidance for reactor design and operating conditions. Future work should optimize light parameters, photosensitizer selection, and combinatory treatments. These optimizations will increase efficacy and enable real-world application.

4.5 Supporting information C

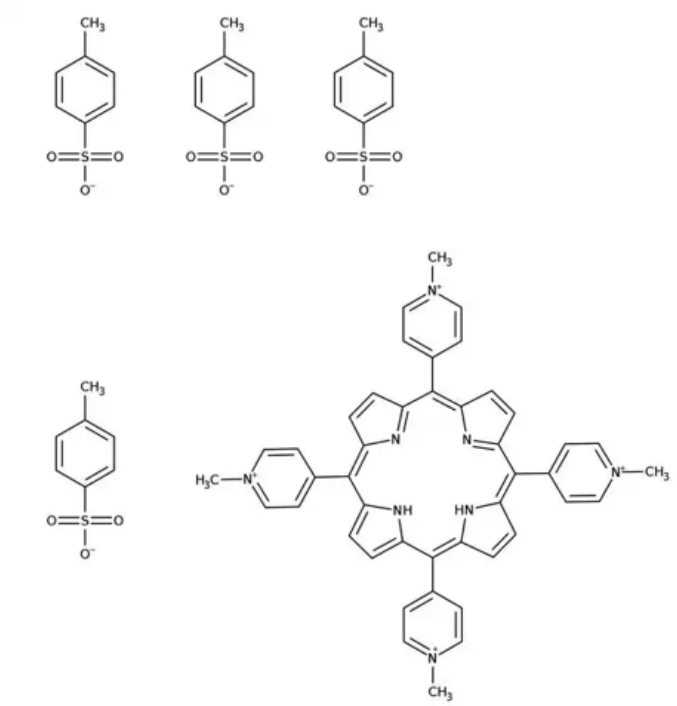

Figure SC 1: The structure of photosensitizer porphyrin TMPyP (5, 10, 15, 20-Tetrakis-(N-Methyl-4-pyridyl) 21, 23-porphyrin tetratosylate). The molecular formular is $C_{72}H_{66}N_8O_{12}S_4$. The central structure features a porphyrin core, a large, planar, and cyclic compound. The nitrogen-containing heterocycles form an integral part of the porphyrin ring. The sulfonic acid groups contribute to balancing the overall charge of the molecule while enhancing its stability.

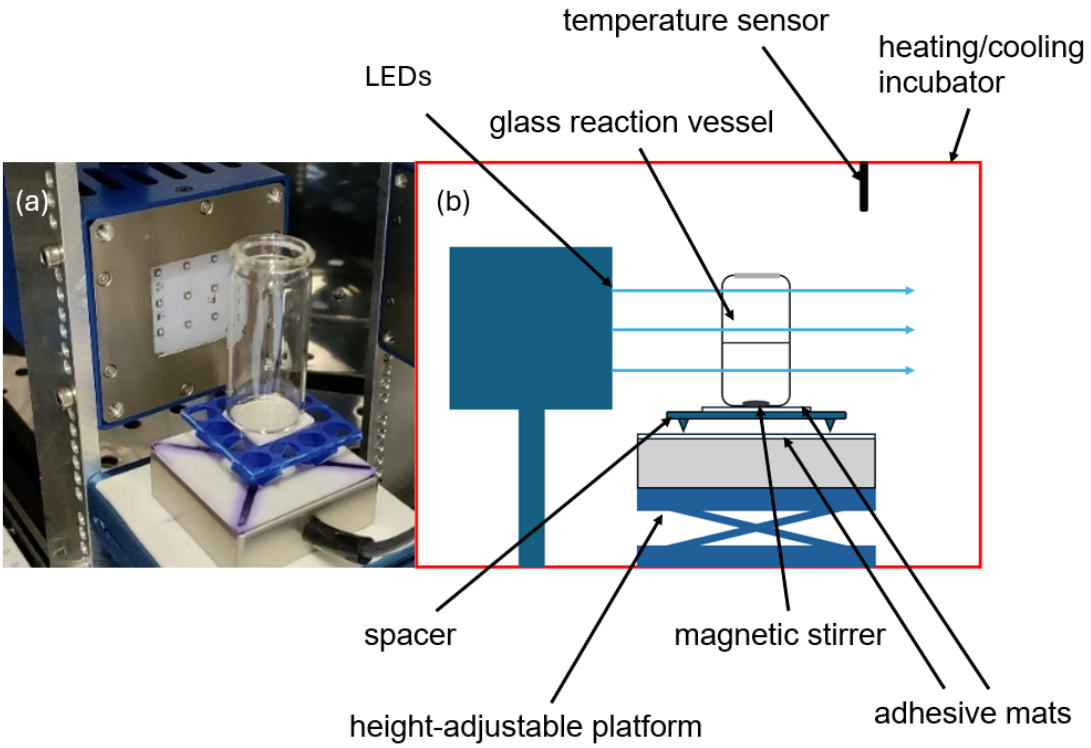

Figure SC 2: (a) Photograph of the experimental setup showing the static aBL reactor. (b) Schematic illustration of the reactor comprising six 420 nm LEDs, a glass reaction vessel, spacer, magnetic stirrer, height-adjustable platform, and two adhesive mats, all housed within a heating/cooling incubator equipped with a temperature sensor.

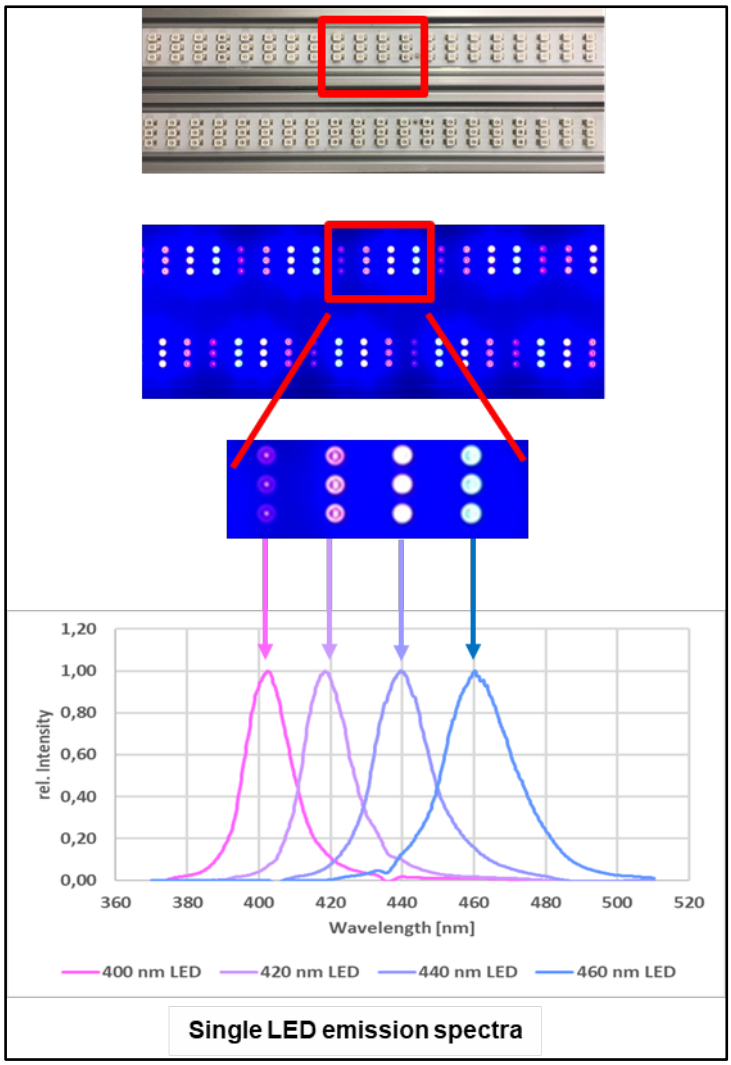

Figure SC 3: Exemplary: normalized entire emission spectrum of the LED bar (top); normalized emission spectra of each LED type on LED bar (bottom). A qualtitative characterization of the emitted spectrum was done with a spectrometer (FLAME-S-XR1-ES, OceanInsight, Ostfildern, Germany).

Table SC 1: The table summarizes primer sequences, amplicon sizes, and control strains with associated references. It groups the qPCR systems used for quantifying in taxonomic gene markers for *P. aeruginosa* (*ecf*X), *E. faecium* (23S), and antibiotic resistance genes for *P. aeruginosa* (*bla*$_{VIM}$), as well as *E. faecium* (*van*A).

Gene	Primer sequence	Amplicon size	Reference strain	Literature
*ecf*X	Fwd: AGCGTTCGTCCTGCACAAGT Rev: TCCACCATGCTCAGGGAGAT	81 bp	*P. aeruginosa* DSM1117	(Clifford et al. 2012)
*23*S	Fwd: AGAAATTCCAAACGAACTTG Rev: CAGTGCTCTACCTCCATCATT	93 bp	*E. faecium* DSM20477	(Frahm und Obst 2003)
bla$_{VIM}$	Fwd: GAGATTCCCACGCACTCTCTAGA Rev: AATGCGCAGCACCAGGATAG TaqMan Probe: ACGCAGTGCGCTTCGGTCCAGT	61 bp	*P. aeruginosa* PA49	(Van der Zee et al. 2014)
*van*A	Fwd: TCTGCAATAGAGATAGCCGC Rev: GGAGTAGCTATCCCAGCATT	376 bp	*E. faecium* B7641	(Klein et al, 1998)

Table SC 2: Target genes and primer details: forward (F) and reverse (R) sequences with corresponding literature references.

Genes	Primers (5'-3')	References
*rec*A	F: CCGGTAAAACCACGCTGAC	Kamruzzaman et al.,
	R: CGTGCGTAGATTGGGTCCAG	2019
*sod*A	F: CCGCTGAAGAGCTGATTACC	Najmuldeen et al.,
	R: TTGAAGTTCTCCACGGAACC	2019
*omp*F	F: GAACTTCGCTGTTCAGTACC	Viveiros et a., 2007
	R: CGTACTTCAGACCAGTAGCC	
*oxy*R	F: CGCGATCAGGCAATGG	Michan et al., 1999
	R: CAGCGCTGGCAGTAAAGTGAT	
*tol*C	F: AAGCCGAAAAACGCAACCT	Swick et al., 2011
	R: CAGAGTCGGTAAGTGACCATC	
*erm*B	F: TGAATCGAGACTTGAGTGTGCAA	Alexander et al., 2015
	R: GGATTCTACAAGCGTACCTT	
bla_{TEM}	F: TTCCTGTTTTTGCTCACCCAG	Rocha et al., 2018
	R: CTCAAGGATCTTACCGCTGTTG	
A. baumannii	F: GTTGTGGCTTTAGGTTTATTATACG	Clifford et al., 2012
	R: AAGTTACTCGACGCAATTCG	
16S rRNA	F: TCCTACGGGAGGCAGCAGT	Hembach et al. 2017
	R: ATTACCGCGGCTGCTGG	

Table SC 3: Quantification and normalization of 16S rRNA gene cell equivalents/ 100 mL under different ROS scavenger treatments with aBL alone and aBL/ TMPyP. Results of three independent trials are presented for each treatment condition (n=3).

Cell equivalents/ 100 mL			
16S			
t0	3.08E+11	2.21E+11	2.34E+11
aBL/TMPyP	5.16E+08	6.89E+07	1.29E+08
L-histidine	9.57E+10	1.30E+11	1.12E+10
Tiron	5.43E+08	8.59E+08	4.49E+08
tert-butanol	3.42E+08	5.30E+08	1.83E+08
Na_2SO_3	1.23E+11	8.71E+09	1.43E+10
aBL alone	2.09E+11	1.27E+11	8.14E+10
L-histidine	2.13E+11	2.06E+11	5.53E+10
Tiron	2.30E+11	1.89E+11	2.35E+11
tert-butanol	2.88E+11	2.62E+11	1.63E+11
Na_2SO_3	2.64E+11	1.62E+11	2.00E+11

Table SC 4: Standard curve equations, amplification efficiencies (E), and coefficients of determination (R^2) for genes involved in the oxidative stress response.

Target	Standard curve equations	R^2	E
*rec*A	y=-3.306x + 39.64	0.97	100.6%
*sod*A	y=-3.484x + 30.206	0.98	93.6%
*omp*F	y=-3.574x + 28.474	0.99	90.4%
*tol*C	y=-3.357x + 28.925	0.99	98.5%
*oxy*R	y=-3.413x + 28.881	0.99	96.3%

5 Summary and conclusion

The objective of this study is to develop innovative and effective methods for combating ARB and ARGs, particularly in WWTPs and other hotspots of dissemination, where conventional processes inadequately remove AMR. To address this, aBL enhanced by photosensitizers was evaluated. Looking forward, integrating upgraded aBL with AOPs may offer a promising solution to mitigate the impact of AMR.

Chapter 2 confirmed that wastewater from AMR hotspots (such as poultry and pig slaughterhouse wastewater) is characterized by high concentrations of clinically relevant ESKAPE group bacteria and critical kategories of ARGs. Conventional wastewater treatments showed partial but insufficient effectiveness against ARGs and FPB. A static aBL reactor was used to demonstrate the varying susceptibility of bacteria to aBL treatment, categorizing organisms as "highly sensitive," "sensitive," or "resistant/robust". The addition of the porphyrin-based photosensitizer TMPyP (10^{-6} M) notably improved bacterial inactivation, suggesting that combined treatments are essential for effectively safeguarding aquatic environments downstream from slaughterhouse effluents.

In chapter 3, the effectiveness of an innovative continuous-flow aBL irradiation at wavelengths of 405, 420, and 460 nm was examined to inactivate ARB, FPB, and ARGs in wastewater from AMR-contaminated WWTPs. The overarching goal is to progressively enhance aBL systems to mitigate the environmental threat posed by AMR. The study explored the impact of aBL alone and when combined with either TMPyP or the oxidative agent H_2O_2, achieving up to 4-5 log reductions in microbial and genetic contaminants. Among targeted FPBs, enterococci showed greater sensitivity to aBL than *A. baumannii*, *P. aeruginosa*, and *E. coli*. This suggests that Gram-positive bacterial are generally more susceptible to aBL-based treatments than Gram-negative counterparts. Additionally, ARGs such as *erm*B, *tet*M, *sul*1, and bla_{VIM} displayed substantial reductions under aBL treatment. The varying susceptibility of these ARGs indicates that the effectiveness of aBL is influenced not only by bacterial type but also by the specific resistance genes they harbor. In this chapter, DNA lesions were also quantified to assess the extent of molecular damage induced by the treatments. Detectable genomic DNA lesions being indicative for significant structural damage, support the long-standing assumption that photodynamic treatments compromise bacterial DNA integrity. Using the qPCR-based LORD-Q method, the combination of aBL and TMPyP induced the highest level of DNA damage, with up to 13 lesions per 10 kb of DNA.

Chapter 4 elucidated the mechanisms involved in aBL-related treatments, providing critical insights into how aBL inactivates ARGs and ARB. The relative values from CFU enumeration and qPCR highlight the need to combine culture-dependent and molecular methods to more accurately assess disinfection effectiveness, particularly for microorganisms in a VBNC state. Understanding inactivation mechanisms also requires insights into physiological and genetic responses that cultivation alone cannot reveal. The aBL treatment augmented with TMPyP demonstrated superior efficacy compared to static systems. This configuration enhances intracellular ROS generation, increasing microbial inactivation effectiveness. Mechanistic analyses revealed that ROS, particularly $^1O_2$ and H_2O_2, generated by aBL combined with TMPyP play a central role in driving bacterial cell death and gene degradation. aBL-related treatments were confirmed effective induce damages to bacterial cells and genetic elements. Furthermore, transcriptomic analysis indicated bacterial adaption to ROS-induced stress, evidenced by the upregulation of oxidative stress responsiv genes (*oxy*R, *sod*A, *rec*A, *tol*C) and downregulation of *omp*F. This suggests a shift in bacterial physiology towards oxidative stress adaptation, potentially affecting membrane permeability and DNA repair capacity. These adaptations may influence long-term treatment efficacy and resistance evolution.

The study suggests further optimization of aBL parameters, including intensities, irradiation durations, and wavelength combinations, alongside practical integration of photosensitizers and oxidants. Future research must explore scaling these systems. It should examine the feasibility of incorporating photosensitizers or oxidants in large-scale treatments. Additionally, long-term economic viability, environmental impact and regulatory considerations should be evaluated. Comparative analyses with existing disinfection technologies will support integrating aBL into broader wastewater management strategies, particularly for mitigating high-risk AMR contamination scenarios. In addition, studies should explore the combination of aBL with complementary technologies such as filtration, ozonation, or UV treatment could yield synergistic effects and help overcome matrix-related limitations, paving the way for hybrid and multi-barrier systems tailored to AMR hotspots.

Finally, long-term monitoring of microbial communities and resistance profiles following aBL-based treatment will be essential to assess ecological impacts and the potential for resistance re-emergence. As antibiotic resistance remains a pressing global health challenge, the continued refinement and responsible implementation of aBL-based disinfection technologies could play a pivotal role in next-generation, AMR-conscious wastewater management strategies.

6 Acknowledgements

I would like to express my deepest gratitude to Prof. Harald Horn for giving me the opportunity to pursue my PhD under his insigntful supervision. His support, guidance, and motivation have fundamentally shaped this work.

I am also deeply thankful to Prof. Thomas Schwartz for providing access to excellent laboratory infrastructure and for sharing his vast expertise, especially in the microbial resistance or environmental microbiology. His generosity in terms of both academic advice and resources greatly enriched this work, and I am grateful for the opportunity to conduct my research in his department. The core idea behind this project was his, and his enthusiasm for science has been a continuous source of inspiration. I am particularly grateful for his guidance in both academic and personal development, fostering a sense of independence and integrity.

I also want to sincerely thank Peter Krolla for his practical help in the laboratory and his support with microbiology experiments. His assistance was instrumental in completing many parts of this research, and I deeply appreciate his reliability and teamwork.

A special thank you to Dr. Norman Hembach who introduced me to the practical aspects of qPCR. His expertise in antibiotic resistance and his generous willingness to share knowledge made working together both productive and enjoyable.

Finally, I thank my family and friends for their constant presence in my life. Their support, love, and belief in me, even during the most difficult moments, have been the backbone of my journey.

7 List of abbreviations

$^1O_2$	Singlet Oxygen
8-OHdG	8-Hydroxy-Deoxyguanosine
aBL	Antimicrobial Blue Light
AMR	Antimicrobial Resistance
AOPs	Advanced Oxidation Processes
APE	AmpC producing Enterobacteriaceae
ARB	Antibiotic Resistant Bacteria
ARGs	Antibiotic Resistance Genes
BM2	Basal-Medium 2
CAMPs	Cationic Antimicrobial Peptides
CFUs	Colony Forming Units
COD	Chemical oxygen demand
CPDs	Cyclobutane Pyrimidine Dimers
CPE	Carbapenemase producing Enterobacteriaceae
Ct	Cycle Threshold
DDDs	Defined Daily Doses
dPCR	Digital Polymerase Chain Reaction
ESBL	Extended-Spectrum β-Lactamase
ETC	Electron Transfer Chain
EU	European Union
FPB	Facultative Pathogenic Bacteria
H_2O_2	Hydrogen Peroxide
HGT	Horizontal Gene Transfer
HPCIAs	Highest Priority Critically Important Antibiotics
HT-qPCR	High-throughput Quanitative Polymerase Chain Reaction
IRs	Inverted Repeats
IS	Insertion Sequences
KIT	Karlsruhe Institute for Technology
LB	Luria-Broth
LOD	Limit of Detection
LPS	Lipopolysaccharides
MAD	Median Absolute Deviation

MDR	Multidrug Resistance
MDRAB	Multidrug Resistant *Acinetobacter baumannii*
MF	Microfiltration
MGEs	Mobilizable Genetic Elements
MIC	Minimum Inhibitory Concentration
MRSA	Methicillin Resistant *Staphylococcus Aureus*
NF	Nanofiltration
$O_2^{\bullet-}$	Superoxide Anion
O_3	ozone
OD	Optical Density
$OH^{\bullet}$	Hydroxyl Radical
PABA	Para-aminobenzoic Acid
PBPs	Penicillin Binding Proteins
PC	Polycarbonate Membranes
PCO	Photocatalytic Oxidation
PCR	Polymerase Chain Reaction
PDT	Photo-dynamic Therapies
PMA	Propidium Monoazide
PS	Photosensitizers
qPCR	Quantitative Polymerase Chain Reaction
RCS	Reactive Chlorine Species
RO	Reverse Osmosis
ROS	Reactive Oxygen Species
RWW	Raw Wastewater
SnO_2	Tin Dioxide
$SO_4^{\bullet-}$	Sulfate radicals
SOD	Superoxide Dismutase
TiO_2	Titanium Dioxide
TMPyP	5, 10, 15, 20-Tetrakis-(N-Methyl-4-pyridyl) 21, 23-porphyrin tetratosylat
UF	Ultrafiltration
UV	Ultraviolet
VBNC	Viable but Non Culturable
VGT	Vertical Gene Transfer
VRE	Vancomycin Resistant *Enterococcus faecalis*
WHO	World Health Organisation

WO_3	Tungsten Trioxide
WWTP	Wastewater Treatment Plant
WWTPs	Wastewater Treatment Plants
ZnS	Zinc Sulfide

8 Appendix

8.1 List of publications

Cong, X., Hillert, J., Krolla, P., & Schwartz, T. (**2025**). Cellular insights into reactive oxidative species (ROS) and bacterial stress responses induced by antimicrobial blue light (aBL) for inactivating antibiotic resistant bacteria (ARB) in wastewater. Science of the Total Environment, 1005, 180878.

Cong, X., Schwermer, C. U., Krolla, P., & Schwartz, T. (**2025**). Inactivating facultative pathogen bacteria and antibiotic resistance genes in wastewater using blue light irradiation combined with a photosensitizer and hydrogen peroxide. Science of the Total Environment, 974, 179208.

Cong, X., Mazierski, P., Miodyńska, M., Zaleska-Medynska, A., Horn, H., Schwartz, T., & Gmurek, M. (**2024**). The role of TiO_2 and gC_3N_4 bimetallic catalysts in boosting antibiotic resistance gene removal through photocatalyst assisted peroxone process. Scientific Reports, 14(1), 22897.

Cong, X., Krolla, P., Khan, U. Z., Savin, M., & Schwartz, T. (**2023**). Antibiotic resistances from slaughterhouse effluents and enhanced antimicrobial blue light technology for wastewater decontamionation. Environmental Science and Pollution Research, 30(50), 109315-109330.

8.2 Verification of the contribution from the co-authors

Chapter 2

Title: Antibiotic resistances from slaughterhouse effluents and enhanced antimicrobial blue light technology for wastewater decontamination

Journal: Environmental Science and Pollution Research (2023) 30: 109315-109330

Authors: Xiaoyu Cong, Peter Krolla, Umer Zeb Khan, Mykhailo Savin, Thomas Schwartz

Position in the dissertation:

The content of this paper has been included in Chapter 2

Contribution of Xiaoyu Cong (first author) (80%)

- Formal analysis
- Visualization writing – original draft,
- Methodology
- Software

- Editing

Contribution of Peter Krolla (second author) (6%)

- Software
- Formal analysis
- Visualization writing
- Methodology
- Review-editing

Contribution of Umer Zeb Khan (third author) (6%)

- Formal analysis
- Data curation
- Methodology
- Visualization

Contribution of Mykhailo Savin (fourth author) (2%)

- Coordination of contact to food industry
- Sample preparation and transfer
- Editing

Contribution of Thomas Schwartz (corresponding author) (6%)

- Supervision
- Methodology
- Project administration
- Funding acquisition
- Review and editing

Signature of the authors:

Author	*Signature*
Xiaoyu Cong	
Peter Krolla	
Umer Zeb Khan	
Mykhailo Savin	
Thomas Schwartz	

Chapter 3

Title: Inactivating facultative pathogen bacteria and antibiotic resistance genes in wastewater using blue light irradiation combined with a photosensitizer and hydrogen peroxide

Journal: Science of the Total Environment 974 (2025) 179208

Authors: Xiaoyu Cong, Carsten Ulrich Schwermer, Peter Krolla, Thomas Schwartz

Position in the dissertation:

The content of this paper has been included in Chapter3

Contribution of Xiaoyu Cong (first author) (86%)

- Writing – original draft
- Visualization
- Validation
- Software
- Methodology
- Formal analysis

Contribution of Carsten Ulrich Schwermer (second author) (4%)

- Validation
- Project administration
- Writing – review & editing
- Data curation

Contribution of Peter Krolla (third author) (3%)

- Methodology
- Investigation
- Data curation

Contribution of Thomas Schwartz (corresponding author) (7%)

- Conceptualization
- Writing – review & editing
- Supervision
- Project administration
- Methodology
- Funding acquisition

Signature of the authors:

Author	*Signature*
Xiaoyu Cong	
Carsten Ulrich Schwermer	
Peter Krolla	
Thomas Schwartz	

Chapter 4

Title: Cellular insights into reactive oxidative species (ROS) and bacterial stress responses induced by antimicrobial blue light (aBL) for inactivating antibiotic resistant bacteria (ARB) in wastewater

Journal: Science of the Total Environment

Authors: Xiaoyu Cong, Jasna Hillert, Peter Krolla, Thomas Schwartz

Position in the dissertation:

The content of this paper has been included in Chapter 4

Contribution of Xiaoyu Cong (first author) (85%)

- Writing – original draft
- Visualization
- Validation
- Software
- Methodology
- Formal analysis

Contribution of Jasna Hillert (second author) (6%)

- Writing – review & editing
- Visualization
- Validation
- Data curation

Contribution of Peter Krolla (third author) (2%)

- Methodology
- Investigation
- Data curation

Contribution of Thomas Schwartz (corresponding author) (7%)

- Writing – review & editing
- Supervision
- Validation
- Project administration
- Methodology
- Funding acquisition

Signature of the authors:

Author	*Signature*
Xiaoyu Cong	
Jasna Hillert	
Peter Krolla	
Thomas Schwartz	

9 References

Abid, M. F., Zablouk, M. A., & Abid-Alameer, A. M. (2012). Experimental study of dye removal from industrial wastewater by membrane technologies of reverse osmosis and nanofiltration. *Iranian journal of environmental health science & engineering*, *9*, 1-9.

Acar Kirit, H., Bollback, J. P., & Lagator, M. (2022). The role of the environment in horizontal gene transfer. Molecular Biology and Evolution, 39(11), msac220.

Aghdassi SJ, Behnke M, Gastmeier P, Gropmann A, Hansen S, Pena Diaz LA, Piening B, Rosenbusch ML, Schröder C, Schwab F (2016) Deutsche nationale Punkt-Prävalenzerhebung zu nosokomialen infektionen und Antibiotikaanwendung, Nationales Referenzzentrum für Surveillance von nosokomialen Infektionen.

Ahmed, S. K., Hussein, S., Qurbani, K., Ibrahim, R. H., Fareeq, A., Mahmood, K. A., & Mohamed, M. G. (2024). Antimicrobial resistance: Impacts, challenges, and future prospects. Journal of Medicine, Surgery, and Public Health, 2, 100081.

Al Bayssari, C., Dabboussi, F., Hamze, M., & Rolain, J. M. (2015). Emergence of carbapenemase-producing Pseudomonas aeruginosa and Acinetobacter baumannii in livestock animals in Lebanon. Journal of Antimicrobial Chemotherapy, 70(3), 950-951.

Aldred, K. J., Kerns, R. J., & Osheroff, N. (2014). Mechanism of quinolone action and resistance. Biochemistry, 53(10), 1565-1574.

Alexander J, Bollmann A, Seitz W, Schwartz T (2015) Microbiological characterization of aquatic microbiomes targeting taxonomical marker genes and antibiotic resistance genes of opportunistic bacteria. Science of the Total Environment, 512, 316-325.

Alexander J, Hembach N, Schwartz T (2020) Evaluation of antibiotic resistance dissemination by wastewater treatment plant effluents with different catchment areas in Germany. Scientific Reports, 10:8952

Alexander J, Hembach N, Schwartz T (2022) Identification of critical control points for antibiotic resistance discharge in sewers. Science of the Total Environment 820 (2022) 153186

Alexander, J., Knopp, G., Dötsch, A., Wieland, A., & Schwartz, T. (2016). Ozone treatment of conditioned wastewater selects antibiotic resistance genes, opportunistic bacteria, and induce strong population shifts. Science of the Total Environment, 559, 103-112.

Allen, N. E. (2002). Effects of macrolide antibiotics on ribosome function. In Macrolide antibiotics (pp. 261-280). Basel: Birkhäuser Basel.

Amábile-Cuevas, C. F. (2021). Antibiotic resistance from, and to the environment. AIMS Environmental Science, 8(1), 18-35.

Amarasiri, M., Sano, D., & Suzuki, S. (2020). Understanding human health risks caused by antibiotic resistant bacteria (ARB) and antibiotic resistance genes (ARG) in water environments: Current knowledge and questions to be answered. Critical Reviews in Environmental Science and Technology, 50(19), 2016-2059.

Aminov, R. I. (2009). The role of antibiotics and antibiotic resistance in nature. Environmental microbiology, 11(12), 2970-2988.

Aminov, R. I. (2011). Horizontal gene exchange in environmental microbiota. Frontiers in microbiology, 2, 158.

Amos GC, Hawkey PM, Gaze WH, Wellington EM (2014a) Waste water effluent contributes to the dissemination of CTX-M-15 in the natural environment. Journal of Antimicrobial Chemotherapie, 2014 Jul;69(7):1785-91. doi: 10.1093/jac/dku079. Epub 2014 May 5

Amos GC, Zhang L, Hawkey PM, Gaze WH, Wellington EM (2014b) Functional metagenomic analysis reveals rivers are a reservoir for diverse antibiotic resistance genes. Journal of Veterinary Microbiology, 2014 Jul 16;171(3-4):441-7. doi: 10.1016/j.vetmic.2014.02.017. Epub 2014 Feb 16.

Anandabaskar, N. (2021). Protein synthesis inhibitors. In Introduction to basics of pharmacology and toxicology: volume 2: essentials of systemic pharmacology: from principles to practice (pp. 835-868). Singapore: Springer Nature Singapore.

Anastasi, E. M., Wohlsen, T. D., Stratton, H. M., & Katouli, M. (2013). Survival of *Escherichia coli* in two sewage treatment plants using UV irradiation and chlorination for disinfection. Water research, 47(17), 6670-6679.

Arbune, M., Gurau, G., Niculet, E., Iancu, A. V., Lupasteanu, G., Fotea, S., ... & Tatu, A. L. (2021). Prevalence of antibiotic resistance of ESKAPE pathogens over five years in an infectious diseases hospital from South-East of Romania. Infection and drug resistance, 2369-2378.

Arenz, S., & Wilson, D. N. (2016). Bacterial protein synthesis as a target for antibiotic inhibition. cold spring harbor perspectives in medicine, 6(9), a025361.

Awitor, K. O., Rafqah, S., Géranton, G., Sibaud, Y., Larson, P. R., Bokalawela, R. S. P., ... & Johnson, M. B. (2008). Photo-catalysis using titanium dioxide nanotube layers. Journal of Photochemistry and Photobiology A: Chemistry, 199(2-3), 250-254.

Ayrapetyan, M., Williams, T., & Oliver, J. D. (2018). Relationship between the viable but nonculturable state and antibiotic persister cells. Journal of bacteriology, 200(20), 10-1128.

Babakhani, S., & Oloomi, M. (2018). Transposons: the agents of antibiotic resistance in bacteria. Journal of basic microbiology, 58(11), 905-917.

Bang, Y. J., Lee, Z. W., Kim, D., Jo, I., Ha, N. C., & Choi, S. H. (2016). OxyR2 functions as a three-state redox switch to tightly regulate production of Prx2, a peroxiredoxin of Vibrio vulnificus. *Journal of Biological Chemistry*, *291*(31), 16038-16047.

Baptista, M. S., Cadet, J., Greer, A., & Thomas, A. H. (2021). Photosensitization reactions of biomolecules: definition, targets and mechanisms. Photochemistry and Photobiology, 97(6), 1456-1483.

Barber, J. L. (2015). Using Blue Light for Bacterial Inactivation (Master's thesis, Lancaster University (United Kingdom)).

Bauer, R., Hoenes, K., Meurle, T., Hessling, M., & Spellerberg, B. (2021). The effects of violet and blue light irradiation on ESKAPE pathogens and human cells in presence of cell culture media. Scientific Reports, 11(1), 24473.

Bengtsson-Palme, J., Kristiansson, E., & Larsson, D. J. (2018). Environmental factors influencing the development and spread of antibiotic resistance. FEMS microbiology reviews, 42(1), fux053.

Berditsch, M., Jäger, T., Strempel, N., Schwartz, T., Overhage, J., & Ulrich, A. S. (2015). Synergistic effect of membrane-active peptides polymyxin B and gramicidin S on multidrug-resistant strains and biofilms of Pseudomonas aeruginosa. *Antimicrobial agents and chemotherapy*, *59*(9), 5288-5296.

Beretsou, V. G., Michael-Kordatou, I., Michael, C., Santoro, D., El-Halwagy, M., Jäger, T., ... & Fatta-Kassinos, D. (2020). A chemical, microbiological and (eco) toxicological scheme to understand the efficiency of UV-C/H_2O_2 oxidation on antibiotic-related microcontaminants in treated urban wastewater. Science of The Total Environment, 744, 140835.

Bionda, N., Fleeman, R. M., Shaw, L. N., & Cudic, P. (2013). Effect of Ester to Amide or N-Methylamide Substitution on Bacterial Membrane Depolarization and Antibacterial Activity of Novel Cyclic Lipopeptides. ChemMedChem, 8(8), 1394-1402.

Biswal, B. K., Mazza, A., Masson, L., Gehr, R., & Frigon, D. (2014). Impact of wastewater treatment processes on genes and their co-occurrence with virulence genes in *Escherichia coli*. Water research, 50, 245-253.

Bouki, C., Venieri, D., & Diamadopoulos, E. (2013). Detection and fate of antibiotic resistant bacteria in wastewater treatment plants: a review. Ecotoxicology and environmental safety, 91, 1-9.

Broens, E. M., & van Geijlswijk, I. M. (2018). Prudent use of antimicrobials in exotic animal medicine. Veterinary Clinics: Exotic Animal Practice, 21(2), 341-353.

Bulit, F., Grad, I., Manoil, D., Simon, S., Wataha, J. C., Filieri, A., ... & Bouillaguet, S. (2014). Antimicrobial activity and cytotoxicity of 3 photosensitizers activated with blue light. Journal of endodontics, 40(3), 427-431.

Bundesamt für Verbraucherschutz und Lebensmittelsicherheit, and Paul-Ehrlich-Gesellschaft für Chemotherapie e. V. "GERMAP 2015–Bericht über den Antibiotikaverbrauch und die Verbreitung von Antibiotikaresistenzen in der Human-und Veterinärmedizin in Deutschland." (2016).

Bush, K., & Bradford, P. A. (2016). β-Lactams and β-lactamase inhibitors: an overview. Cold Spring Harbor perspectives in medicine, 6(8), a025247.

Bustin, S. A., Benes, V., Garson, J. A., Hellemans, J., Huggett, J., Kubista, M., ... & Wittwer, C. T. (2009). The MIQE Guidelines: M inimum I nformation for Publication of Q uantitative Real-Time PCR E xperiments.

Bystritskaya, E. P., Stenkova, A. M., Portnyagina, O. Y., Rakin, A. V., Rasskazov, V. A., & Isaeva, M. P. (2014). Regulation of Yersinia pseudotuberculosis major porin expression in response to antibiotic stress. Molecular Genetics, Microbiology and Virology, 29, 63-68.

Cacace D, Fatta-Kassinos D, Manaia CM, Cytryn E, Kreuzinger N, Rizzo L, Karaolia P, Schwartz T, Alexander J, Merlin C, Garelick H, Schmitt H, de Vries D, Schwermer CU, Meric S, Ozkal CB, Pons MN, Kneis D, Berendonk TU (2019) Antibiotic resistance genes in treated wastewater and in the receiving water bodies: A pan-European survey of urban settings, Water Research, 162 (2019) 320e330

Cerqueira, F., Matamoros, V., Bayona, J. M., Berendonk, T. U., Elsinga, G., Hornstra, L. M., & Piña, B. (2019). Antibiotic resistance gene distribution in agricultural fields and crops. A soil-to-food analysis. Environmental research, 177, 108608.

Chambers, H. F., & DeLeo, F. R. (2009). Waves of resistance: *Staphylococcus aureus* in the antibiotic era. Nature reviews microbiology, 7(9), 629-641.

Chaves, J. C. A., dos Santos, C. G., de Miranda, É. G. A., Junior, J. T. A., & Nantes, I. L. (2017). Free-Base and Metal Complexes of 5, 10, 15, 20-Tetrakis (NMethyl Pyridinium L) Porphyrin: Catalytic and Therapeutic Properties. In Phthalocyanines and Some Current Applications. IntechOpen.

Chen, H., & Zhang, M. (2013). Effects of advanced treatment systems on the removal of antibiotic resistance genes in wastewater treatment plants from Hangzhou, China. Environmental Science & Technology, 47(15), 8157-8163.

Chen, J., & Xie, S. (2018). Overview of sulfonamide biodegradation and the relevant pathways and microorganisms. Science of the Total Environment, 640, 1465-1477.

Chen, J., Quiles-Puchalt, N., Chiang, Y. N., Bacigalupe, R., Fillol-Salom, A., Chee, M. S. J., ... & Penadés, J. R. (2018). Genome hypermobility by lateral transduction. Science, 362(6411), 207-212.

Chen, Y. M., Holmes, E. C., Chen, X., Tian, J. H., Lin, X. D., Qin, X. C., ... & Zhang, Y. Z. (2020). Diverse and abundant resistome in terrestrial and aquatic vertebrates revealed by transcriptional analysis. Scientific Reports, 10(1), 18870.

Chiang, S. M., & Schellhorn, H. E. (2012). Regulators of oxidative stress response genes in *Escherichia coli* and their functional conservation in bacteria. Archives of biochemistry and biophysics, 525(2), 161-169.

Chu, Z., Hu, X., Wang, X., Wu, J., Dai, T., & Wang, X. (2019). Inactivation of Cronobacter sakazakii by blue light illumination and the resulting oxidative damage to fatty acids. Canadian Journal of Microbiology, 65(12), 922-929.

Clifford RJ, Milillo M, Prestwood J, Quintero R, Zurawski DV, Kwak Y I, Mc Gann P (2012) Detection of bacterial 16S rRNA and identification of four clinically important bacteria by real-time PCR. PloS One, 7(11), e48558.

Colwell, R. R. (2000). Viable but nonculturable bacteria: a survival strategy. *Journal of Infection and Chemotherapy*, *6*, 121-125.

Cong, X., Krolla, P., Khan, U. Z., Savin, M., & Schwartz, T. (2023). Antibiotic resistances from slaughterhouse effluents and enhanced antimicrobial blue light technology for wastewater decontamionation. Environmental Science and Pollution Research, 30(50), 109315-109330.

Cong, X., Mazierski, P., Miodyńska, M., Zaleska-Medynska, A., Horn, H., Schwartz, T., & Gmurek, M. (2024). The role of TiO_2 and gC_3N_4 bimetallic catalysts in boosting antibiotic resistance gene removal through photocatalyst assisted peroxone process. Scientific Reports, 14(1), 22897.

Cong, X., Schwermer, C. U., Krolla, P., & Schwartz, T. (2025). Inactivating facultative pathogen bacteria and antibiotic resistance genes in wastewater using blue light irradiation combined with a photosensitizer and hydrogen peroxide. Science of the Total Environment, 974, 179208.

Czatzkowska, M., Wolak, I., Harnisz, M., & Korzeniewska, E. (2022). Impact of anthropogenic activities on the dissemination of ARGs in the environment—A review. International journal of environmental research and public health, 19(19), 12853.

Dąbrowski, J. M. (2017). Reactive oxygen species in photodynamic therapy: mechanisms of their generation and potentiation. In Advances in inorganic chemistry (Vol. 70, pp. 343-394). Academic Press.

Dannenmann, B., Lehle, S., Lorscheid, S., Huber, S. M., Essmann, F., & Schulze-Osthoff, K. (2017). Simultaneous quantification of DNA damage and mitochondrial copy number by long-run DNA-damage quantification (LORD-Q). Oncotarget, 8(68), 112417.

Darby, E. M., Trampari, E., Siasat, P., Gaya, M. S., Alav, I., Webber, M. A., & Blair, J. M. (2023). Molecular mechanisms of antibiotic resistance revisited. Nature Reviews Microbiology, 21(5), 280-295.

Davis, C. (2014). Enumeration of probiotic strains: review of culture-dependent and alternative techniques to quantify viable bacteria. Journal of microbiological methods, 103, 9-17.

Davison, J. (1999). Genetic exchange between bacteria in the environment. Plasmid, 42(2), 73-91.

De Kraker MEA, Stewardson AJ, Harbarth S (2016) Will 10 Million people die a year due to antimicrobial resistance by 2050? PLoS Medicine, 13:e1002184. https://doi.org/10.1371/journal.pmed.1002184.

De Oliveira, D. M., Forde, B. M., Kidd, T. J., Harris, P. N., Schembri, M. A., Beatson, S. A., ... & Walker, M. J. (2020). Antimicrobial resistance in ESKAPE pathogens. Clinical microbiology reviews, 33(3), 10-1128.

Denissen, J., Reyneke, B., Waso-Reyneke, M., Havenga, B., Barnard, T., Khan, S., & Khan, W. (2022). Prevalence of ESKAPE pathogens in the environment: Antibiotic resistance status, community-acquired infection and risk to human health. International journal of hygiene and environmental health, 244, 114006.

Depardieu F, Perichon B, Courvalin P (2004) Detection of the van alphabet and identification of enterococci and *staphylococci* at the species level by multiplex PCR. Journal of Clinical Microbiology, 42(12), 5857-5860.

Ding, D., Wang, B., Zhang, X., Zhang, J., Zhang, H., Liu, X., ... & Yu, Z. (2023). The spread of antibiotic resistance to humans and potential protection strategies. Ecotoxicology and Environmental Safety, 254, 114734.

Dos Anjos C, Leanse LG, Ribero MS, Sellera FP, Dropa M, Arana-Chavez VE, Lincopan N, Baptista MS, Pogliana FC, Dai T, Sabino CP (2023) New insight into bacterial targets of antimicrobial blue light. Microbiol. Spectr. 21; 11 (2):e0283322. doi:10.1128/spectrum.02833-22.

Dowling, A., O'Dwyer, J., & Adley, C. (2017). Antibiotics: mode of action and mechanisms of resistance. Antimicrobial research: Novel bioknowledge and educational programs, 1, 536-545.

Drlica, K., & Zhao, X. (1997). DNA gyrase, topoisomerase IV, and the 4-quinolones. Microbiology and molecular biology reviews, 61(3), 377-392.

ECDC, E. (2009). The bacterial challenge: time to react European Centre for Disease Prevention and Control European Medicines Agency.

Eliopoulos, G. M., Cosgrove, S. E., & Carmeli, Y. (2003). The impact of antimicrobial resistance on health and economic outcomes. Clinical infectious diseases, 36(11), 1433-1437.

Enwemeka, C, Baker, T., Bumah, V. (2021). The role of UV and blue light in photo-eradication of microorganisms. Journal of Photochemistry and Photobiology 8,100064

Etebu, E., & Arikekpar, I. (2016). Antibiotics: Classification and mechanisms of action with emphasis on molecular perspectives. International journal of applied microbiology and biotechnology research, 4(2016), 90-101.

European Centre for Disease Prevention and Control. Antimicrobial resistance in the EU/EEA (EARS-Net) - Annual Epidemiological Report 2019. Stockholm: ECDC; 2020.

Ferrer-Espada R, Wang Y, Goh YS, Dai T (2020) Antimicrobial blue light inactivation of microbial isolates in biofilms. Lasers in Surgery and Medicine, 472-478 doi: 10.1002/lsm.23159. Epub 2019 Sep 19.

Ferrer-Espada, R, Liu X, Goh XS, Dai T (2019) Antimicrobial blue light inactivation of polymicrobial biofilms. Frontiers Microbiology, 10:721. doi: 10.3389/fmicb.2019.00721.

Ferro, G., Guarino, F., Cicatelli, A., & Rizzo, L. (2017). β-lactams resistance gene quantification in an antibiotic resistant Escherichia coli water suspension treated by advanced oxidation with UV/H_2O_2. Journal of Hazardous Materials, 323, 426-433.

Feuerstein, O., Ginsburg, I., Dayan, E., Veler, D., & Weiss, E. I. (2005). Mechanism of visible light phototoxicity on Porphyromonas gingivalis and Fusobacterium nucleatum. Photochemistry and Photobiology, 81(5), 1186-1189.

Foroughi, M., Khiadani, M., Kakhki, S., Kholghi, V., Naderi, K., & Yektay, S. (2022). Effect of ozonation-based disinfection methods on the removal of antibiotic resistant bacteria and resistance genes (ARB/ARGs) in water and wastewater treatment: A systematic review. Science of the Total Environment, 811, 151404.

Frahm, E., & Obst, U. (2003). Application of the fluorogenic probe technique (TaqMan PCR) to the detection of *Enterococcus spp.* and *Escherichia coli* in water samples. Journal of microbiological methods, 52(1), 123-131.

Gao, F. Z., Jia, W. L., Li, B., Zhang, M., He, L. Y., Bai, H., ... & Ying, G. G. (2025). Contaminant-degrading bacteria are super carriers of antibiotic resistance genes in municipal landfills: A metagenomics-based study. Environment International, 195, 109239.

Gao, P., Munir, M., & Xagoraraki, I. (2012). Correlation of tetracycline and sulfonamide antibiotics with corresponding resistance genes and resistant bacteria in a conventional municipal wastewater treatment plant. Science of the Total Environment, 421, 173-183.

Garcez, A. S., Núnez, S. C., Baptista, M. S., Daghastanli, N. A., Itri, R., Hamblin, M. R., & Ribeiro, M. S. (2011). Antimicrobial mechanisms behind photodynamic effect in the presence of hydrogen peroxide. Photochemical & Photobiological Sciences, 10, 483-490.

Gelband, H., Miller, Petrie, M., Pant, S., Gandra, S., Levinson, J., Barter, D., ... & Laxminarayan, R. (2015). The state of the world's antibiotics 2015. Wound healing southern africa, 8(2), 30-34.

Gillings, Michael R. "Class 1 integrons as invasive species." Current Opinion in Microbiology 38 (2017): 10-15.

Gmurek, M., Borowska, E., Schwartz, T., & Horn, H. (2022). Does light-based tertiary treatment prevent the spread of antibiotic resistance genes? Performance, regrowth and future direction. Science of The Total Environment, 817, 153001.

Greig, J., Rajić, A., Young, I., Mascarenhas, M., Waddell, L., & LeJeune, J. (2015). A scoping review of the role of wildlife in the transmission of bacterial pathogens and antimicrobial resistance to the food chain. Zoonoses and Public Health, 62(4), 269-284.

Guo, C., Wang, K., Hou, S., Wan, L., Lv, J., Zhang, Y., ... & Xu, J. (2017). H_2O_2 and/or TiO_2 photocatalysis under UV irradiation for the removal of antibiotic resistant bacteria and their antibiotic resistance genes. Journal of hazardous materials, 323, 710-718.

Guo, Y. (2021, June). Removal ability of antibiotic resistant Bacteria (arb) and antibiotic resistance genes (Args) by membrane filtration process. In IOP Conference Series: Earth and Environmental Science (Vol. 801, No. 1, p. 012004). IOP Publishing.

Haddad, M. F., Abdullah, B. A., AlObeidi, H. A., Saadi, A. M., & Haddad, M. F. (2024). Antibiotic classification, mechanisms, and indications: A review. International Journal of Medical and All Body Health Research, 5(3), 39-46.

Hadi J, Wu S, Brightwell G (2020) Antimicrobial blue light versus pathogenic bacteria: Mechanism, application in the food industry, hurdle technologies and potential resistance. Foods 9, 1895; doi:10.3390/foods9121895

Hamblin MR, Hasan T (2004) Photodynamic therapy: a new antimicrobial approach to infectious disease? Photochemical & Photobiological Sciences, 3:436-450.

Hameed, S., Xie, L., & Ying, Y. (2018). Conventional and emerging detection techniques for pathogenic bacteria in food science: A review. Trends in Food Science & Technology, 81, 61-73.

Han, J., Li, W., Yang, Y., Zhang, X., Bao, S., Zhang, X., ... & Leung, K. M. Y. (2024). UV-based advanced oxidation processes for antibiotic resistance control: Efficiency, influencing factors, and energy consumption. *Engineering*, *37*, 27-39.

Han, X. M., Hu, H. W., Chen, Q. L., Yang, L. Y., Li, H. L., Zhu, Y. G., ... & Ma, Y. B. (2018). Antibiotic resistance genes and associated bacterial communities in agricultural soils amended with different sources of animal manures. Soil Biology and Biochemistry, 126, 91-102.

Harnisz, M., Kiedrzyńska, E., Kiedrzyński, M., Korzeniewska, E., Czatzkowska, M., Koniuszewska, I., ... & Zalewski, M. (2020). The impact of WWTP size and sampling season on the prevalence of antibiotic resistance genes in wastewater and the river system. Science of the Total Environment, 741, 140466.

Hazra, M., & Durso, L. M. (2022). Performance Efficiency of Conventional Treatment Plants and Constructed Wetlands towards Reduction of Antibiotic Resistance. Antibiotics, 11(1), 114. https://doi.org/10.3390/antibiotics11010114

Hazra, M., Watts, J. E., Williams, J. B., & Joshi, H. (2024). An evaluation of conventional and nature-based technologies for controlling antibiotic-resistant bacteria and antibiotic-resistant genes in wastewater treatment plants. Science of The Total Environment, 917, 170433.

He, Y., Yuan, Q., Mathieu, J., Stadler, L., Senehi, N., Sun, R., & Alvarez, P. J. (2020). Antibiotic resistance genes from livestock waste: occurrence, dissemination, and treatment. NPJ Clean Water, 3(1), 4.

Heffron J, Bork M, Mayer BK, Skwor T (2021) A comparison of porphyrin photosentizisers in photodynamic inactivation of RNA and DNA bacteriophages. Viruses 13, 530; doi.org/10.3390/v13030530.

Hegstad, K., Mikalsen, T., Coque, T. M., Werner, G., & Sundsfjord, A. (2010). Mobile genetic elements and their contribution to the emergence of antimicrobial resistant *Enterococcus faecalis* and *Enterococcus faecium*. Clinical microbiology and infection, 16(6), 541-554.

Helinski, D. R. (2022). A brief history of plasmids. EcoSal Plus, 10(1), eESP-0028.

Hembach N, Bierbaum G, Schreiber C, Schwartz T (2022) Facultative pathogenic bacteria and antibiotic resistance genes in swine livestock manure and clinical wastewater: A molecular biology comparison. Environmental Pollution, 313 (2022) 120128

Hembach N, Schmid F, Alexander J, Hiller C, Rogall ET, Schwartz T (2017) Occurrence of the mcr-1 colistin resistance gene and other clinically relevant antibiotic resistance genes in microbial populations at different municipal wastewater treatment plants in Germany. Frontiers Microbiology, 8, 1282.

Hembach, N., Alexander, J., Hiller, C., Wieland, A., & Schwartz, T. (2019). Dissemination prevention of antibiotic resistant and facultative pathogenic bacteria by ultrafiltration and ozone treatment at an urban wastewater treatment plant. Scientific Reports, 9(1), 12843.

Herigstad, B., Hamilton, M., & Heersink, J. (2001). How to optimize the drop plate method for enumerating bacteria. *Journal of microbiological methods*, *44*(2), 121-129.

Herraiz-Carboné, M., Cotillas, S., Lacasa, E., de Baranda, C. S., Riquelme, E., Cañizares, P., ... & Sáez, C. (2021). A review on disinfection technologies for controlling the antibiotic resistance spread. Science of the Total Environment, 797, 149150.

Hessling M, Spellerberg, B, Hoenes K (2017) Photoinactivation of bacteria by endogenous phtosensitizers and exposure to visible-light of different wavelengths – a review on existing data. FEMS Microbiology Letters. 364:fnw270. doi: 10.1093/femsle/fnw270

Hickman, A. B., & Dyda, F. (2015). Mechanisms of DNA transposition. Mobile DNA III, 529-553.

Hiller, C. X., Schwaller, C., Wurzbacher, C., & Drewes, J. E. (2022). Removal of antibiotic microbial resistance by micro-and ultrafiltration of secondary wastewater effluents at pilot scale. Science of The Total Environment, 838, 156052.

Hoenes K, Bauer R, Meurie T, Spellerberg B, Hessing M (2021) Inactivation effect of violet and blue light on ESKAPE pathogens and closely related non-pathogenic bacterial species – a pormising tool against antibiotic-sensitive and antibiotic-resistant microorganisms. Frontiers Microbiololgy, 11, 612367; doi: 10.3389/fmicb.2020.612367

Hoenes K, Wenzel U, Spellerberg B, Hessling M (2019) Photoinactivation sensitivity of *Staphylococcus carnosus* to visible-light irradiation as afunction of wavelength. Photobiology, 96, 156-169. doi: 10.1111/php.13168

Hu, H. W., Han, X. M., Shi, X. Z., Wang, J. T., Han, L. L., Chen, D., & He, J. Z. (2016). Temporal changes of antibiotic-resistance genes and bacterial communities in two contrasting soils treated with cattle manure. FEMS microbiology ecology, 92(2), fiv169.

Hu, X., Huang, Y. Y., Wang, Y., Wang, X., & Hamblin, M. R. (2018). Antimicrobial photodynamic therapy to control clinically relevant biofilm infections. Frontiers in microbiology, 9, 1299.

Huang, E., & Yousef, A. E. (2014). The lipopeptide antibiotic paenibacterin binds to the bacterial outer membrane and exerts bactericidal activity through cytoplasmic membrane damage. Applied and environmental microbiology, 80(9), 2700-2704.

Huang, H., Yang, Z. L., Wu, X. M., Wang, Y., Liu, Y. J., Luo, H., ... & Gao, F. (2012). Complete genome sequence of *Acinetobacter baumannii* MDR-TJ and insights into its mechanism of antibiotic resistance. Journal of antimicrobial chemotherapy, 67(12), 2825-2832.

Huang, J. J., Hu, H. Y., Tang, F., Li, Y., Lu, S. Q., & Lu, Y. (2011). Inactivation and reactivation of antibiotic-resistant bacteria by chlorination in secondary effluents of a municipal wastewater treatment plant. Water research, 45(9), 2775-2781.

Huang, S., Lin, S., Qin, H., Jiang, H., & Liu, M. (2023). The parameters affecting antimicrobial efficiency of antimicrobial blue light therapy: A review and prospect. Biomedicines, 11(4), 1197.

Idil, O., Darcan, C., & Ozkanca, R. (2011). The effect of UV-A and different wavelengths of visible lights on survival of *Salmonella typhimurium* in seawater microcosms. Journal of Pure and Applied Microbiology, 5(2), 581-592.

Jäger, T., Hembach, N., Elpers, C., Wieland, A., Alexander, J., Hiller, C., ... & Schwartz, T. (2018). Reduction of antibiotic resistant bacteria during conventional and advanced wastewater treatment, and the disseminated loads released to the environment. Frontiers in microbiology, 9, 2599.

Jungfer, C., Schwartz, T., & Obst, U. (2007). UV-induced dark repair mechanisms in bacteria associated with drinking water. Water Research, 41(1), 188-196.

Kalli, M., Noutsopoulos, C., & Mamais, D. (2023). The fate and occurrence of antibiotic-resistant bacteria and antibiotic resistance genes during advanced wastewater treatment and disinfection: a review. Water, 15(11), 2084.

Kamruzzaman, M., & Iredell, J. (2019). A ParDE-family toxin antitoxin system in major resistance plasmids of Enterobacteriaceae confers antibiotic and heat tolerance. Scientific reports, 9(1), 9872.

Karumathil, D. P., Yin, H. B., Kollanoor-Johny, A., & Venkitanarayanan, K. (2014). Effect of chlorine exposure on the survival and antibiotic gene expression of multidrug resistant Acinetobacter baumannii in water. International journal of environmental research and public health, 11(2), 1844-1854.

Katz, L., & Ashley, G. W. (2005). Translation and protein synthesis: macrolides. Chemical reviews, 105(2), 499-528.

Kim, S., Park, H., & Chandran, K. (2010). Propensity of activated sludge to amplify or attenuate tetracycline resistance genes and tetracycline resistant bacteria: a mathematical modeling approach. Chemosphere, 78(9), 1071-1077.

Klein G, Pack A, Reuter G (1998) Antibiotic resistance patterns of enterococci and occurrence of vancomycin-resistant enterococci in raw minced beef and pork in Germany. Applied and Environmental Microbiology, 64(5), 1825-1830.

Klein, E. Y., Van Boeckel, T. P., Martinez, E. M., Pant, S., Gandra, S., Levin, S. A., ... & Laxminarayan, R. (2018). Global increase and geographic convergence in antibiotic consumption between 2000 and 2015. Proceedings of the National Academy of Sciences, 115(15), E3463-E3470.

Klein, E. Y., Impalli, I., Poleon, S., Denoel, P., Cipriano, M., Van Boeckel, T. P., ... & Nandi, A. (2024). Global trends in antibiotic consumption during 2016–2023 and future projections through 2030. *Proceedings of the National Academy of Sciences*, *121*(49), e2411919121.

Korzeniewska, E., Korzeniewska, A., & Harnisz, M. (2013). Antibiotic resistant *Escherichia coli* in hospital and municipal sewage and their emission to the environment. Ecotoxicology and environmental safety, 91, 96-102.

Kralik, P., & Ricchi, M. (2017). A basic guide to real time PCR in microbial diagnostics: definitions, parameters, and everything. Frontiers in microbiology, 8, 108.

Kruszewska-Naczk, B., Grinholc, M., Waleron, K., Bandow, J. E., & Rapacka-Zdończyk, A. (2024). Can antimicrobial blue light contribute to resistance development? Genome-wide analysis revealed aBL-protective genes in *Escherichia coli*. Microbiology spectrum, 12(1), e02490-23.

Kumar, A., & Pal, D. (2018). Antibiotic resistance and wastewater: Correlation, impact and critical human health challenges. Journal of environmental chemical engineering, 6(1), 52-58.

Kurpiel PM, Hanson ND (2012) Point mutations in the inc antisense RNA gene are associated with increased plasmid copy number, expression of *bla*$_{CMY-2}$ and resistance to piperacillin/tazobactam in *Escherichia coli*. Journal of Antimicrobial Chemotherapy, 67(2), 339-345.

Kutuzova, A., Dontsova, T., & Kwapinski, W. (2021). Application of TiO_2-based photocatalysts to antibiotics degradation: cases of sulfamethoxazole, trimethoprim and ciprofloxacin. Catalysts, 11(6), 728.

Laht, M., Karkman, A., Voolaid, V., Ritz, C., Tenson, T., Virta, M., & Kisand, V. (2014). Abundances of tetracycline, sulphonamide and beta-lactam antibiotic resistance genes in conventional wastewater treatment plants (WWTPs) with different waste load. PloS one, 9(8), e103705.

Lane, D. J. (1991). Nucleic acid techniques in bacterial systematics.

Larsson, D. J., & Flach, C. F. (2022). Antibiotic resistance in the environment. Nature Reviews Microbiology, 20(5), 257-269.

Lawrence, K. P., Douki, T., Sarkany, R. P., Acker, S., Herzog, B., & Young, A. R. (2018). The UV/visible radiation boundary region (385–405 nm) damages skin cells and induces “dark” cyclobutane pyrimidine dimers in human skin in vivo. Scientific Reports, 8(1), 12722.

Leanse, L. G., Dos Anjos, C., Mushtaq, S., & Dai, T. (2022). Antimicrobial blue light: A ‘Magic Bullet’ for the 21st century and beyond?. Advanced Drug Delivery Reviews, 180, 114057.

Lei, L., Chen, N., Chen, Z., Zhao, Y., Lin, H., Li, X., ... & Luo, Y. (2024). Dissemination of antibiotic resistance genes from aboveground sources to groundwater in livestock farms. Water Research, 256, 121584.

Lewis, K. (2020). The science of antibiotic discovery. Cell, 181(1), 29-45

Li, L., Wang, Q., Bi, W., Hou, J., Xue, Y., Mao, D., ... & Li, X. (2020). Municipal solid waste treatment system increases ambient airborne bacteria and antibiotic resistance genes. Environmental science & technology, 54(7), 3900-3908.

Li, S., Ondon, B. S., Ho, S. H., Zhou, Q., & Li, F. (2023). Drinking water sources as hotspots of antibiotic-resistant bacteria (ARB) and antibiotic resistance genes (ARGs): Occurrence, spread, and mitigation strategies. Journal of Water Process Engineering, 53, 103907.

Li, S., Zhang, C., Li, F., Hua, T., Zhou, Q., & Ho, S. H. (2021). Technologies towards antibiotic resistance genes (ARGs) removal from aquatic environment: a critical review. Journal of Hazardous Materials, 411, 125148.

Li, W., & Zhang, G. (2022). Detection and various environmental factors of antibiotic resistance gene horizontal transfer. Environmental Research, 212, 113267.

Liu, X., Guo, X., Liu, Y., Lu, S., Xi, B., Zhang, J., ... & Bi, B. (2019). A review on removing antibiotics and antibiotic resistance genes from wastewater by constructed wetlands: performance and microbial response. Environmental Pollution, 254, 112996.

Liu, Y., & Breukink, E. (2016). The membrane steps of bacterial cell wall synthesis as antibiotic targets. Antibiotics, 5(3), 28.

Livak, K. J., & Schmittgen, T. D. (2001). Analysis of relative gene expression data using real-time quantitative PCR and the $2^{-\Delta\Delta CT}$ method. *methods*, *25*(4), 402-408.

Lu, J., Zhang, Y., Wu, J., Wang, J., & Cai, Y. (2020). Fate of antibiotic resistance genes in reclaimed water reuse system with integrated membrane process. Journal of hazardous materials, 382, 121025.

MacIsaac, S. A., Reid, B., Ontiveros, C., Linden, K. G., Stoddart, A. K., & Gagnon, G. A. (2024). UV LED Wastewater Disinfection: the future is upon us. Water Research X, 24, 100236.

Mackie, R. I., Koike, S., Krapac, I., Chee-Sanford, J., Maxwell, S., & Aminov, R. I. (2006). Tetracycline residues and tetracycline resistance genes in groundwater impacted by swine production facilities. Animal biotechnology, 17(2), 157-176.

Maclean M, MacGregor J, Anderson J, Woolsey G (2009) Inactivation of bacterial pathogens following exposure to light from a 405-nanometer light-emitting diode array. Applied and Environmental Microbiology, 1932-1937.

Maclean, M., Macgregor, S. J., Anderson, J. G., & Woolsey, G. A. (2008). The role of oxygen in the visible-light inactivation of *Staphylococcus aureus*. *Journal of photochemistry and photobiology B: Biology*, *92*(3), 180-184.

Maldonado-Carmona, N., Ouk, T. S., & Leroy-Lhez, S. (2022). Latest trends on photodynamic disinfection of Gram-negative bacteria: Photosensitizer's structure and delivery systems. Photochemical & Photobiological Sciences, 1-33.

Manaia, C. M., Macedo, G., Fatta-Kassinos, D., & Nunes, O. C. (2016). Antibiotic resistance in urban aquatic environments: can it be controlled?. Applied microbiology and biotechnology, 100, 1543-1557.

Mandal, T. K. (2024). Nanomaterial-Enhanced Hybrid Disinfection: A Solution to Combat Multidrug-Resistant Bacteria and Antibiotic Resistance Genes in Wastewater. Nanomaterials, 14(22), 1847.

Marano, R. B., Fernandes, T., Manaia, C. M., Nunes, O., Morrison, D., Berendonk, T. U., ... & Cytryn, E. (2020). A global multinational survey of cefotaxime-resistant coliforms in urban wastewater treatment plants. *Environment international*, *144*, 106035.

Marchesi, J. R., Sato, T., Weightman, A. J., Martin, T. A., Fry, J. C., Hiom, S. J., & Wade, W. G. (1998). Design and evaluation of useful bacterium-specific PCR primers that amplify genes coding for bacterial 16S rRNA. Applied and environmental microbiology, 64(2), 795-799.

Marraffini, L. A., & Sontheimer, E. J. (2008). CRISPR interference limits horizontal gene transfer in staphylococci by targeting DNA. science, 322(5909), 1843-1845.

Marti, E., Variatza, E. and Balcazar, J.L., 2014. The role of aquatic ecosystems as reservoirs of antibiotic resistance. Trends in microbiology, 22(1), pp.36-41.

Martin, M. J., Thottathil, S. E., & Newman, T. B. (2015). Antibiotics overuse in animal agriculture: a call to action for health care providers. American journal of public health, 105(12), 2409-2410.

Martiny, A. C., Martiny, J. B., Weihe, C., Field, A., & Ellis, J. C. (2011). Functional metagenomics reveals previously unrecognized diversity of antibiotic resistance genes in gulls. Frontiers in microbiology, 2, 238.

Mathers, A. J., Cox, H. L., Kitchel, B., Bonatti, H., Brassinga, A. K. C., Carroll, J., ... & Sifri, C. D. (2011). Molecular dissection of an outbreak of carbapenem-resistant Enterobacteriaceae reveals intergenus KPC carbapenemase transmission through a promiscuous plasmid. MBio, 2(6), 10-1128.

Mathur, A., Parihar, A. S., Modi, S., & Kalra, A. (2023). Photodynamic therapy for ESKAPE pathogens: An emerging approach to combat antimicrobial resistance (AMR). Microbial Pathogenesis, 106307.

McCall, M. N., McMurray, H. R., Land, H., & Almudevar, A. (2014). On non-detects in qPCR data. Bioinformatics, 30(16), 2310-2316.

McLain, J. E., Cytryn, E., Durso, L. M., & Young, S. (2016). Culture-based methods for detection of antibiotic resistance in agroecosystems: Advantages, challenges, and gaps in knowledge. Journal of environmental quality, 45(2), 432-440.

Melzer, M., & Petersen, I. (2007). Mortality following bacteraemic infection caused by extended spectrum beta-lactamase (ESBL) producing *E. coli* compared to non-ESBL producing *E. coli*. Journal of Infection, 55(3), 254-259.

Méndez-Hurtado, J., López, R., Suárez, D., & Menéndez, M. I. (2012). Theoretical study of the oxidation of histidine by singlet oxygen. Chemistry–A European Journal, 18(27), 8437-8447.

Michael, I., Rizzo, L., McArdell, C. S., Manaia, C. M., Merlin, C., Schwartz, T., ... & Fatta-Kassinos, D. J. W. R. (2013). Urban wastewater treatment plants as hotspots for the release of antibiotics in the environment: a review. Water research, 47(3), 957-995.

Michán, C., Manchado, M., Dorado, G., & Pueyo, C. (1999). In vivo transcription of the Escherichia coli oxyR regulon as a function of growth phase and in response to oxidative stress. *Journal of bacteriology*, *181*(9), 2759-2764.

Mishra, S., & Imlay, J. (2012) Why do bacteria use so many enzymes to scavenge hydrogen peroxide? Arch Biochem Biophys 52(2),145-160.

Monteiro J, Widen RH, Pignatari AC, Kubasek C, Silbert S (2012) Rapid detection of carbapenemase genes by multiplex real-time PCR. Journal of Antimicrobial Chemotherapy, 67(4), 906-909.

Mulani MS, Kample BE, Kumkar SM, Tawre MS, Pardesi KA (2019) Emerging strategies to combat ESKLAPE pathogens in the era of antimicrobial resistance: a review. Frontiers Microbiology, 10:539. Doi: 10.3389/fmicb.2019.00539

Mulchandani, R., Wang, Y., Gilbert, M., & Van Boeckel, T. P. (2023). Global trends in antimicrobial use in food-producing animals: 2020 to 2030. PLOS Global Public Health, 3(2), e0001305.

Murugaiyan, J., Kumar, P. A., Rao, G. S., Iskandar, K., Hawser, S., Hays, J. P., ... & van Dongen, M. B. (2022). Progress in alternative strategies to combat antimicrobial resistance: focus on antibiotics. Antibiotics, 11(2), 200.

Mušković, M., Planinić, M., Crepulja, A., Lušić, M., Glad, M., Lončarić, M., & Gobin, I. (2023). Photodynamic inactivation of multidrug-resistant strains of Klebsiella pneumoniae and Pseudomonas aeruginosa in municipal wastewater by tetracationic porphyrin and violet-blue light: The impact of wastewater constituents. PLoS One, 18(8), e0290080.

Muyzer, G., De Waal, E. C., & Uitterlinden, A. (1993). Profiling of complex microbial populations by denaturing gradient gel electrophoresis analysis of polymerase chain reaction-amplified genes coding for 16S rRNA. Applied and environmental microbiology, 59(3), 695-700.

Najmuldeen, H., Alghamdi, R., Alghofaili, F., & Yesilkaya, H. (2019). Functional assessment of microbial superoxide dismutase isozymes suggests a differential role for each isozyme. Free radical biology and medicine, 134, 215-228.

Ngo, V. N., Truong, T. N. T., Tran, T. T., Nguyen, L. T., Mach, N. B., Vu, V. V., & Vu, T. M. (2023). A combination of blue light at 460 nm and H_2O_2 for the safe and effective eradication of *Staphylococcus aureus* in an infected mouse skin abrasion model. Microorganisms, 11(12), 2946.

Nguyen, A. Q., Vu, H. P., Nguyen, L. N., Wang, Q., Djordjevic, S. P., Donner, E., ... & Nghiem, L. D. (2021). Monitoring antibiotic resistance genes in wastewater treatment: Current strategies and future challenges. Science of the Total Environment, 783, 146964.

Niestępski, S., Harnisz, M., Ciesielski, S., Korzeniewska, E., & Osińska, A. (2020). Environmental fate of Bacteroidetes, with particular emphasis on Bacteroides fragilis group bacteria

and their specific antibiotic resistance genes, in activated sludge wastewater treatment plants. Journal of hazardous materials, 394, 122544.

Nikaido, H. (1994). Prevention of drug access to bacterial targets: permeability barriers and active efflux. Science, 264(5157), 382-388.

Nishiyama, M., Praise, S., Tsurumaki, K., Baba, H., Kanamori, H., & Watanabe, T. (2021). Prevalence of antibiotic-resistant bacteria ESKAPE among healthy people estimated by monitoring of municipal wastewater. Antibiotics, 10(5), 495.

Nnorom, M. A., Saroj, D., Avery, L., Hough, R., & Guo, B. (2023). A review of the impact of conductive materials on antibiotic resistance genes during the anaerobic digestion of sewage sludge and animal manure. Journal of Hazardous Materials, 446, 130628.

Nocker A, Sossa-Fernandez P, Burr MD, Camper AK (2007a). Use of propidium monoazide for live/dead distinction in microbial ecology. Applied and Environmental Microbiology, 73(16), 5111-5117.

Nocker A, Sossa KE, Camper AK (2007b) Molecular monitoring of disinfection efficacy using propidium monoazide in combination with quantitative PCR. Journal of Microbiological Methods, 70(2), 252-260.

Nocker, A., Shah, M., Dannenmann, B., Schulze-Osthoff, K., Wingender, J., & Probst, A. J. (2018). Assessment of UV-C-induced water disinfection by differential PCR-based quantification of bacterial DNA damage. Journal of microbiological methods, 149, 89-95.

Noel, H. R., Petrey, J. R., & Palmer, L. D. (2022). Mobile genetic elements in Acinetobacter antibiotic-resistance acquisition and dissemination. Annals of the New York Academy of Sciences, 1518(1), 166-182.

O'Neil, J. (2014). Review on antibiotic resistance: Tackling a crisis for the health and wealth of nations. Heal Wealth Nations.

Ondon, B. S., Li, S., Zhou, Q., & Li, F. (2021). Sources of antibiotic resistant bacteria (ARB) and antibiotic resistance genes (ARGs) in the soil: a review of the spreading mechanism and human health risks. Reviews of Environmental Contamination and Toxicology Volume 256, 121-153.

O'Neill, J. (2016). Tackling drug-resistant infections globally: final report and recommendations.

Patel, R., Uhl, J. R., Kohner, P., Hopkins, M. K., & Cockerill 3rd, F. R. (1997). Multiplex PCR detection of vanA, vanB, vanC-1, and vanC-2/3 genes in enterococci. *Journal of clinical microbiology*, *35*(3), 703-707.

Pärnänen, K. M., Narciso-da-Rocha, C., Kneis, D., Berendonk, T. U., Cacace, D., Do, T. T., ... & Manaia, C. M. (2019). Antibiotic resistance in European wastewater treatment plants mirrors the pattern of clinical antibiotic resistance prevalence. Science advances, 5(3), eaau9124.

Partridge, S. R., Kwong, S. M., Firth, N., & Jensen, S. O. (2018). Mobile genetic elements associated with antimicrobial resistance. Clinical microbiology reviews, 31(4), 10-1128.

Paulus G K, Hornstra LM, Alygizakis N, Slobodnik J, Thomaidis N, Medema G (2019) The impact of on-site hospital wastewater treatment on the downstream communal wastewater system in terms of antibiotics and antibiotic resistance genes. Int. Journal of Hygiene and Environmental Health, 222, 4, 2019, 635-644

Peak N, Knapp CW, Yang RK, Hanfelt MM, Smith MS, Aga DS, Graham DW (2007) Abundance of six tetracycline resistance genes in wastewater lagoons at cattle feedlots with different antibiotic use strategies. Environmental Microbiology, 9(1), 143-151.

Pei, M., Zhang, B., He, Y., Su, J., Gin, K., Lev, O., ... & Hu, S. (2019). State of the art of tertiary treatment technologies for controlling antibiotic resistance in wastewater treatment plants. Environment international, 131, 105026.

Percival, S. L., Yates, M. V., Williams, D., Chalmers, R., & Gray, N. (2014). Ultraviolet disinfection. Microbiology of waterborne diseases: microbiological aspects and risks.

Pfaffl, M. W. (2001). A new mathematical model for relative quantification in real-time RT–PCR. *Nucleic acids research*, *29*(9), e45-e45.

Piddock, L. J. (2006). Multidrug-resistance efflux pumps? not just for resistance. Nature Reviews Microbiology, 4(8), 629-636.

Piechowski, M. V., Thelen, M. A., Hoigné, J., & Bühler, R. E. (1992). tert-Butanol as an OH-Scavenger in the Pulse Radiolysis of Oxygenated Aqueous Systems. Berichte der Bunsengesellschaft für physikalische Chemie, 96(10), 1448-1454.

Plavskii VY, Mikulich AV, Tretyakova AI, Leusenka LA, Plaskaya LG, Kazyuchits OA et al. (2018) Porphyrins and flavins as endogenous acceptors of optical radiation of blue spectral regions determining photoinactivativation of microbial cell. Journal of Photochemistryand Photobiology B, 183, 172-183. Doi: 10.1016/j.jphotobiol.2018.04.021

Popa, L. I., Barbu, I. C., & Chifiriuc, M. C. (2018). Mobile genetic elements involved in the horizontal transfer of antibiotic resistance genes. Romanian Archives of Microbiology & Immunology, 77(4).

Prescott, J. F., & Hardefeldt, L. Y. (2024). Other Beta-lactam Antibiotics: Beta-lactamase Inhibitors, Carbapenems, and Monobactams. Antimicrobial therapy in veterinary medicine, 169-186.

Qi, W., Jonker, M. J., de Leeuw, W., Brul, S., & Ter Kuile, B. H. (2023). Reactive oxygen species accelerate de novo acquisition of antibiotic resistance in E. coli. *Iscience*, *26*(12).

Randall, C. P., Mariner, K. R., Chopra, I., & O'Neill, A. J. (2013). The target of daptomycin is absent from *Escherichia coli* and other gram-negative pathogens. Antimicrobial agents and chemotherapy, 57(1), 637-639.

Rapacka-Zdonczyk, A., Wozniak, A., Kruszewska, B., Waleron. K., & Grinholc, M. (2021). Can Gram-negative bacteria develop resistance to antimicrobial blue light treatment? Int. J. Mol. Sci. 22, 11579.

Regulation (EU) 2019/6 of the European Parliament and of the Council of 11 December 2018 on Veterinary Medicinal Products and Repealing Directive 2001/82/EC (Text with EEA Relevance). Available online: https://www.legislation.gov.uk/eur/2019/6/contents (accessed on 29 December 2022).

Rizzo, L., Manaia, C., Merlin, C., Schwartz, T., Dagot, C., Ploy, M. C., ... & Fatta-Kassinos, D. (2013a). Urban wastewater treatment plants as hotspots for antibiotic resistant bacteria and genes spread into the environment: a review. Science of the total environment, 447, 345-360.

Rizzo, L., Fiorentino, A., & Anselmo, A. (2013b). Advanced treatment of urban wastewater by UV radiation: Effect on antibiotics and antibiotic-resistant E. coli strains. Chemosphere, 92(2), 171-176.

Rocha J, Cacace D, Kampouris I, Guilloteau H, Jäger T, Marano RB, Schwartz T (2018) Inter-laboratory calibration of quantitative analyses of antibiotic resistance genes. Journal of Environmental Chemical Engineering, 8(1), 102214.

Rocha, D. J., Santos, C. S., & Pacheco, L. G. (2015). Bacterial reference genes for gene expression studies by RT-qPCR: survey and analysis. Antonie Van Leeuwenhoek, 108, 685-693.

Rodloff, A., Bauer, T., Ewig, S., Kujath, P., & Muller, E. (2008). MEDIZIN-Ubersichtsarbeit-Sensibel, intermediar und resistent--Wirkintensitat von Antibiotika. Deutsches Arzteblatt-Arztliche Mitteilungen-Ausgabe B, 105(39), 657.

Rowe-Magnus, D. A., & Mazel, D. (2002). The role of integrons in antibiotic resistance gene capture. International Journal of Medical Microbiology, 292(2), 115-125.

Rozman, U., Duh, D., Cimerman, M., & Turk, S. Š. (2020). Hospital wastewater effluent: hot spot for antibiotic resistant bacteria. Journal of Water, Sanitation and Hygiene for Development, 10(2), 171-178.

Safitri, E. (2025). More Than Just Resistance: Understanding Bacterial Defense Mechanisms as a Source of Future Antibiotics-A Literature Review. RADINKA JOURNAL OF HEALTH SCIENCE, 2(4), 385-390.

Sah, S. K., & Hemalatha, S. (2015). Extended spectrum Beta lactamase (ESBL) Mechanism of antibiotic resistance and Epidemiology. Int J pharmtech Res, 7(2), 303-9.

Sanchez-Alberola, N., Campoy, S., Barbé, J., & Erill, I. (2012). Analysis of the SOS response of Vibrio and other bacteria with multiple chromosomes. BMC genomics, 13, 1-12.

Santajit, S., & Indrawattana, N. (2016). Mechanisms of antimicrobial resistance in ESKAPE pathogens. BioMed research international, 2016(1), 2475067.

Savin M, Bierbaum G, Hammerl JA, Heinemann C, Parcina M, Sib E, Kreyenschmidt J (2020) ESKAPE bacteria and extended-spectrum-β-lactamase-producing *Escherichia coli* isolated from wastewater and process water from German poultry slaughterhouses. Applied and Environmental Microbiology, 86(8), e02748-19.

Savin, M., Alexander, J., Bierbaum, G., Hammerl, J. A., Hembach, N., Schwartz, T.,& Kreyenschmidt, J. (2021). Antibiotic-resistant bacteria, antibiotic resistance genes, and antibiotic residues in wastewater from a poultry slaughterhouse after conventional and advanced treatments. Scientific Reports, 11(1), 16622.

Saxena, D., Maitra, R., Bormon, R., Czekanska, M., Meiers, J., Titz, A., ... & Chopra, S. (2023). Tackling the outer membrane: facilitating compound entry into Gram-negative bacterial pathogens. npj Antimicrobials and Resistance, 1(1), 17.

Schacksen, P. S., Macêdo, W. V., Rellegadla, S., Vergeynst, L., & Nielsen, J. L. (2025) Dynamics of nitrogen-transforming microbial populations in wastewater treatment during recirculation of hydrothermal liquefaction process-water. Water Research, 276, 123254.

Schwaiger K, Huther S, Hölzel C, Kämpf P, Bauer J (2012) Prevalence of antibiotic-resistant enterobacteriaceae isolated from chicken and pork meat purchased at the slaughterhouse and at retail in Bavaria, Germany. International Journal of Food Microbiology, 15;154(3):206-11. doi: 10.1016/j.ijfoodmicro.2011.12.014. Epub 2011 Dec 19.

Schwarz S, Chaslus-Dancla E (2001) Use of antimicrobials in veterinary medicine and mechanisms of resistance. Veterinary Research, 32(3-4), 201-225.

Schwermer CU, Krzeminski P, Wennberg AC, Vogelsang C, Uhl W (2018) Removal of antibiotic resistant *E. coli* in two Norwegian wastewater treatment plants and by nano- and ultra-filtration processes. Water Science Technology, 77(3-4):1115-1126. doi: 10.2166/wst.2017.642.

Servais, P., & Passerat, J. (2009). Antimicrobial resistance of fecal bacteria in waters of the Seine river watershed (France). Science of the Total Environment, 408(2), 365-372.

Shao, S., Hu, Y., Cheng, J., & Chen, Y. (2018). Research progress on distribution, migration, transformation of antibiotics and antibiotic resistance genes (ARGs) in aquatic environment. Critical reviews in biotechnology, 38(8), 1195-1208.

Shi, P., Jia, S., Zhang, X. X., Zhang, T., Cheng, S., & Li, A. (2013). Metagenomic insights into chlorination effects on microbial antibiotic resistance in drinking water. Water research, 47(1), 111-120.

Sib, E., Lenz-Plet, F., Barabasch, V., Klanke, U., Savin, M., Hembach, N., & Bierbaum, G. (2020). Bacteria isolated from hospital, municipal and slaughterhouse wastewaters show characteristic, different resistance profiles. Science of The Total Environment, 746, 140894.

Sib, E., Voigt, A. M., Wilbring, G., Schreiber, C., Faerber, H. A., Skutlarek, D.,& Schmithausen, R. M. (2019). Antibiotic resistant bacteria and resistance genes in biofilms in clinical wastewater networks. International Journal of Hygiene and Environmental Health, 222(4), 655-662.

Sinha RP, Hader D-P (2002) UV-induced DNA damage and repair: a review. Photochem. Photobiol. Sci. 1, 225–236.

Slipko, K., Reif, D., Schaar, H., Saracevic, E., Klinger, A., Wallmann, L., ... & Kreuzinger, N. (2022). Advanced wastewater treatment with ozonation and granular activated carbon filtration: inactivation of antibiotic resistance targets in a long-term pilot study. Journal of Hazardous Materials, 438, 129396.

Smith, C. J., & Osborn, A. M. (2009). Advantages and limitations of quantitative PCR (Q-PCR)-based approaches in microbial ecology. *FEMS microbiology ecology*, *67*(1), 6-20.

Sorn, S., Sabar, M. A., Hara-Yamamura, H., Matsuura, N., Watanabe, T., Yamamoto-Ikemoto, R., & Honda, R. Unravelling Antibiotic Resistance Mechanisms in Wastewater Treatment: Transcription of Args and the Role of Stress Conditions.

Sousa, J. M., Macedo, G., Pedrosa, M., Becerra-Castro, C., Castro-Silva, S., Pereira, M. F. R., ... & Manaia, C. M. (2017). Ozonation and UV254 nm radiation for the removal of microorganisms and antibiotic resistance genes from urban wastewater. Journal of Hazardous Materials, 323, 434-441.

Spencer, A. C., & Panda, S. S. (2023). DNA Gyrase as a Target for Quinolones. Biomedicines, 11(2), 371.

Stoll, C., Sidhu, J. P., Tiehm, A., & Toze, S. (2012). Prevalence of clinically relevant antibiotic resistance genes in surface water samples collected from Germany and Australia. Environmental science & technology, 46(17), 9716-9726.

Su, H. C., Liu, Y. S., Pan, C. G., Chen, J., He, L. Y., & Ying, G. G. (2018). Persistence of antibiotic resistance genes and bacterial community changes in drinking water treatment system: from drinking water source to tap water. Science of the Total Environment, 616, 453-461.

Süß, J., Volz, S., Obst, U., & Schwartz, T. (2009). Application of a molecular biology concept for the detection of DNA damage and repair during UV disinfection. Water Research, 43(15), 3705-3716.

Swick, M. C., Morgan-Linnell, S. K., Carlson, K. M., & Zechiedrich, L. (2011). Expression of multidrug efflux pump genes acrAB-tolC, mdfA, and norE in Escherichia coli clinical isolates as a function of fluoroquinolone and multidrug resistance. Antimicrobial agents and chemotherapy, 55(2), 921-924.

Tacconelli, E., Carrara, E., Savoldi, A., Harbarth, S., Mendelson, M., Monnet, D. L., ... & Zorzet, A. (2018). Discovery, research, and development of new antibiotics: the WHO priority list of antibiotic-resistant bacteria and tuberculosis. The Lancet infectious diseases, 18(3), 318-327.

Taiwo, F. A. (2008). Mechanism of tiron as scavenger of superoxide ions and free electrons. Journal of spectroscopy, 22(6), 491-498.

Tang, K. W. K., Millar, B. C., & Moore, J. E. (2023). Antimicrobial resistance (AMR). British journal of biomedical science, 80, 11387.

Taylor, J. C., Gu Liu, C., Chang, J. D., Thompson, B. E., & Maresso, A. W. (2024). Gene discovery from microbial gene libraries I: protection against reactive oxygen species-driven DNA damage. *Microbiology Spectrum*, *12*(11), e00365-24.

Tomb RG, White TA, Coia JE, Anderson JG, MacGregor SJ, Maclean M (2018) Review of the comparative susceptibility of microbial species to photoinactivation using 380-480 nm violet-blue light. Jpurnal of Photochemistry and Photobiology, 94,445-458. doi: 10.1111/php.12883

Top, J., Willems, R., van der Velden, S., Asbroek, M., & Bonten, M. (2008). Emergence of clonal complex 17 *Enterococcus faecium* in The Netherlands. Journal of Clinical Microbiology, 46(1), 214-219.

Truong, H. B., Huy, B. T., Ray, S. K., Lee, Y. I., Cho, J., & Hur, J. (2020). H_2O_2-assisted photocatalysis for removal of natural organic matter using nanosheet C_3N_4-WO_3 composite under visible light and the hybrid system with ultrafiltration. Chemical Engineering Journal, 399, 125733.

Tsai, T. M., Chang, H. H., Chang, K. C., Liu, Y. L., & Tseng, C. C. (2010). A comparative study of the bactericidal effect of photocatalytic oxidation by TiO_2 on antibiotic-resistant and antibiotic-sensitive bacteria. Journal of Chemical Technology & Biotechnology, 85(12), 1642-1653.

Tzouvelekis, L. S., Markogiannakis, A., Psichogiou, M., Tassios, P. T., & Daikos, G. L. (2012). Carbapenemases in Klebsiella pneumoniae and other Enterobacteriaceae: an evolving crisis of global dimensions. Clinical microbiology reviews, 25(4), 682-707.

Urban-Chmiel, R., Marek, A., Stępień-Pyśniak, D., Wieczorek, K., Dec, M., Nowaczek, A., & Osek, J. (2022). Antibiotic resistance in bacteria—A review. Antibiotics, 11(8), 1079.

Valenzuela, J. K., Thomas, L., Partridge, S. R., van der Reijden, T., Dijkshoorn, L., & Iredell, J. (2007). Horizontal gene transfer in a polyclonal outbreak of carbapenem-resistant Acinetobacter baumannii. Journal of clinical microbiology, 45(2), 453-460.

Van Bambeke, F., Balzi, E., & Tulkens, P. M. (2000). Antibiotic efflux pumps. Biochemical pharmacology, 60(4), 457-470.

Van Boeckel, Thomas P., et al. "Global antibiotic consumption 2000 to 2010: an analysis of national pharmaceutical sales data." The Lancet infectious diseases 14.8 (2014): 742-750.

Van der Zee A. Roorda L, Bosman G, Fluit AC, Hermans M, Smits PH, Ossewaarde JM (2014) Multi-centre evaluation of real-time multiplex PCR for detection of carbapenemase genes OXA-48, VIM, IMP, NDM and KPC. BMC Infectious Diseases, 14(1), 1-5.

Van Hoek, A. H., Mevius, D., Guerra, B., Mullany, P., Roberts, A. P., & Aarts, H. J. (2011). Acquired antibiotic resistance genes: an overview. Frontiers in microbiology, 2, 203.

Vila, J., Martí, S., & Sanchez-Céspedes, J. (2007). Porins, efflux pumps and multidrug resistance in *Acinetobacter baumannii*. Journal of antimicrobial chemotherapy, 59(6), 1210-1215.

Vilvanathan, S. (2021). Penicillins, Cephalosporins, and Other b-Lactam Antibiotics. Abialbon Paul Nishanthi Anandabaskar Jayanthi Mathaiyan, 821.

Viveiros, M., Dupont, M., Rodrigues, L., Couto, I., Davin-Regli, A., Martins, M., ... & Amaral, L. (2007). Antibiotic stress, genetic response and altered permeability of E. coli. PloS one, 2(4), e365.

Voigt AM, Zacharias N, Timm C, Wasser F, Sib E, Skutlarek D, Parcina M, Schmithausen RM, Schwartz T, Hembach N, Tiehm A, Stange C, Engelhart S, Bierbaum G, Kistemann T, Exner M, Faerber HA, Schreiber C (2020) Association between antibiotic residues, antibiotic resistant bacteria and antibiotic resistance genes in anthropogenic wastewater - An evaluation of clinical influences. Chemosphere, 241 125032

Volkmann H, Schwartz T, Bischoff P, Kirchen S, Obst U (2004) Detection of clinically relevant antibiotic-resistance genes in municipal wastewater using real-time PCR (TaqMan). Journal of Microbiological Methods, 56(2), 277-286.

von Sonntag, C. (2006). Free-radical-induced DNA damage and its repair (Vol. 13). Berlin: Springer.

Wagner, A. O., Malin, C., Knapp, B. A., & Illmer, P. (2008). Removal of free extracellular DNA from environmental samples by ethidium monoazide and propidium monoazide. Applied and Environmental Microbiology, 74(8), 2537-2539.

Wainwright M (1998) Photodynamic antimicrobial chemotherapy (PACT). J. Antimicrobial. Chemotherapy, 42:13-28.

Wang Y, Wang Y, Wang Y, Murray CK, Hamblin MR, Hooper DC, Dai T. Antimicrobial blue light inactivation of pathogenic microbes: State of the art. Drug Resist Updat. 2017 Nov;33-35:1-22. doi: 10.1016/j.drup.2017.10.002. Epub 2017 Oct 13. PMID: 29145971; PMCID: PMC5699711.

Wang, J. Y., An, X. L., Huang, F. Y., & Su, J. Q. (2020a). Antibiotic resistome in a landfill leachate treatment plant and effluent-receiving river. Chemosphere, 242, 125207.

Wang, J., & Chen, X. (2022). Removal of antibiotic resistance genes (ARGs) in various wastewater treatment processes: An overview. Critical Reviews in Environmental Science and Technology, 52(4), 571-630.

Wang, J., & Zhuan, R. (2020). Degradation of antibiotics by advanced oxidation processes: An overview. Science of the Total Environment, 701, 135023.

Wang, J., Chu, L., Wojnárovits, L., & Takács, E. (2020b). Occurrence and fate of antibiotics, antibiotic resistant genes (ARGs) and antibiotic resistant bacteria (ARB) in municipal wastewater treatment plant: An overview. Science of the Total Environment, 744, 140997.

Wang, Y., Ferrer-Espada, R., Baglo, Y., Gu, Y., & Dai, T. (2019). Antimicrobial blue light inactivation of Neisseria gonorrhoeae: roles of wavelength, endogenous photosensitizer, oxygen, and reactive oxygen species. Lasers in surgery and medicine, 51(9), 815-823.

Wang, Y., Han, Y., Li, L., Liu, J., & Yan, X. (2022). Distribution, sources, and potential risks of antibiotic resistance genes in wastewater treatment plant: a review. Environmental Pollution, 310, 119870.

Wang, Y., Li, W., & Irini, A. (2013). A novel and quick method to avoid H_2O_2 interference on COD measurement in Fenton system by Na_2SO_3 reduction and O_2 oxidation. Water science and technology, 68(7), 1529-1535.

Wang, Y., Wang, Y., Wang, Y., Murray, C. K., Hamblin, M. R., Hooper, D. C., & Dai, T. (2017). Antimicrobial blue light inactivation of pathogenic microbes: State of the art. Drug Resistance Updates, 33, 1-22.

Wang, Y., Yang, J., Zhao, R., Zhang, S., Guo, J., & Wang, J. (2024). Nonantibiotic pharmaceuticals exhibit antibacterial activity and enhance bacterial evolution toward antibiotic resistance. ACS ES&T Water, 4(4), 1701-1710.

Wen, Q., Yang, L., Duan, R., & Chen, Z. (2016). Monitoring and evaluation of antibiotic resistance genes in four municipal wastewater treatment plants in Harbin, Northeast China. Environmental Pollution, 212, 34-40.

White, D., & Cox, E. (2016). Fighting the impact of antibiotic-resistance. FDA Consumer Health Information. www. fda. gov/downloads/.../UCM350090. pdf. Accessed, 4.

WHO (2017) Global priority list of antibiotic-resistant bacteria to guide research, discovery, and development of new antibiotics. Cadernos de Pesquisa, 43(148), 348–365.

WHO (2019a) New report calls for urgent action to avert antimicrobial resistance crisis 2019. https://www.who.int/news/item/29-04-2019-new-report-calls-for-urgent-action-to-avert-antimicribial-resistance-crisis Accessed 29 April 2019

WHO (2019b) No time to wait: Securing the future from drug-resistant infections. Artforum International, 54(April), 113–114.

WHO (2020) Technical Brief on Water, Sanitation, Hygiene and Wastewater Management to Prevent Infections and Reduce the Spread of Antimicrobial Resistance.

https://www.who.int/water_sanitation_health/publications/wash-wastewater-management-to-prevent-infections-and-reduce-amr/en/

WHO, 2019. No time to wait: Securing the future from drug-resistant infections. Artforum Int. 54, 113–114.

Woolhouse, M. E., & Ward, M. J. (2013). Sources of antimicrobial resistance. Science, 341(6153), 1460-1461.

Woźniak, A., & Grinholc, M. (2022). Combined antimicrobial blue light and antibiotics as a tool for eradication of multidrug-resistant isolates of Pseudomonas aeruginosa and *Staphylococcus aureus*: in vitro and in vivo studies. Antioxidants, 11(9), 1660.

Xi, C., Zhang, Y., Marrs, C. F., Ye, W., Simon, C., Foxman, B., & Nriagu, J. (2009). Prevalence of antibiotic resistance in drinking water treatment and distribution systems. Applied and environmental microbiology, 75(17), 5714-5718.

Xiao, R., Bai, L., Liu, K., Shi, Y., Minakata, D., Huang, C. H., ... & Sun, P. (2020). Elucidating sulfate radical-mediated disinfection profiles and mechanisms of *Escherichia coli* and *Enterococcus faecalis* in municipal wastewater. Water research, 173, 115552.

Yamin, D., Uskoković, V., Wakil, A. M., Goni, M. D., Shamsuddin, S. H., Mustafa, F. H., ... & Yusof, N. Y. (2023). Current and future technologies for the detection of antibiotic-resistant bacteria. Diagnostics, 13(20), 3246.

Yao, S., Ye, J., Yang, Q., Hu, Y., Zhang, T., Jiang, L., ... & Cui, C. (2021). Occurrence and removal of antibiotics, antibiotic resistance genes, and bacterial communities in hospital wastewater. Environmental Science and Pollution Research, 28(40), 57321-57333.

Yoon, H., Kim, H. C., Kim, J., You, K., Cho, Y., & Kim, S. (2022). Toxicity impact of hydrogen peroxide on the fate of zebrafish and antibiotic resistant bacteria. Journal of Environmental Management, 302, 114072

Yoon, Y., Chung, H. J., Di, D. Y. W., Dodd, M. C., Hur, H. G., & Lee, Y. (2017). Inactivation efficiency of plasmid-encoded antibiotic resistance genes during water treatment with chlorine, UV, and UV/H2O2. *Water Research*, *123*, 783-793.

Yoshida, A., Sasaki, H., Toyama, T., Araki, M., Fujioka, J., Tsukiyama, K., & Yoshino, F. (2017). Antimicrobial effect of blue light using Porphyromonas gingivalis pigment. Scientific Reports, 7(1), 5225.

Yuan, Q. B., Guo, M. T., & Yang, J. (2015). Fate of antibiotic resistant bacteria and genes during wastewater chlorination: implication for antibiotic resistance control. PloS one, 10(3), e0119403.

Zhang, A., Call, D. R., Besser, T. E., Liu, J., Jones, L., Wang, H., & Davis, M. A. (2019a). β-lactam resistance genes in bacteriophage and bacterial DNA from wastewater, river water, and irrigation water in Washington State. Water research, 161, 335-340.

Zhang, R., Yang, S., An, Y., Wang, Y., Lei, Y., & Song, L. (2022). Antibiotics and antibiotic resistance genes in landfills: a review. Science of the Total Environment, 806, 150647.

Zhang, T., Hu, Y., Jiang, L., Yao, S., Lin, K., Zhou, Y., & Cui, C. (2019b). Removal of antibiotic resistance genes and control of horizontal transfer risk by UV, chlorination and UV/chlorination treatments of drinking water. Chemical Engineering Journal, 358, 589-597.

Zhang, Y., Zhao, Y. G., Maqbool, F., & Hu, Y. (2022). Removal of antibiotics pollutants in wastewater by UV-based advanced oxidation processes: Influence of water matrix components, processes optimization and application: A review. Journal of Water Process Engineering, 45, 102496.

Zhang, Y., Zhuang, Y., Geng, J., Ren, H., Xu, K., & Ding, L. (2016). Reduction of antibiotic resistance genes in municipal wastewater effluent by advanced oxidation processes. Science of the Total Environment, 550, 184-191.

Zhang, Y., Zhuang, Y., Geng, J., Ren, H., Zhang, Y., Ding, L., & Xu, K. (2015). Inactivation of antibiotic resistance genes in municipal wastewater effluent by chlorination and sequential UV/chlorination disinfection. Science of the total environment, 512, 125-132.

Zhang, Y., Zuo, S., Zheng, Q., Yu, G., & Wang, Y. (2024). Removal of antibiotic resistant bacteria and antibiotic resistance genes by an electrochemically driven UV/chlorine process for decentralized water treatment. Water Research, 265, 122298.

Zheng, J., Su, C., Zhou, J., Xu, L., Qian, Y., & Chen, H. (2017). Effects and mechanisms of ultraviolet, chlorination, and ozone disinfection on antibiotic resistance genes in secondary effluents of municipal wastewater treatment plants. Chemical Engineering Journal, 317, 309-316.

Zhu, S., & Coffman, J. A. (2017). Simple and fast quantification of DNA damage by real-time PCR, and its application to nuclear and mitochondrial DNA from multiple tissues of aging zebrafish. BMC Research Notes, 10, 1-6.

ZMP (2003) Fleischverzehr pro Kopf der Bevölkerung in Deutschland 2003. Marktbilanz/Gemüse. Central Market and Price Report Office, Bonn.